Taras Shevchenko National University of Kyiv
Astronomical Observatory

Astronomy and Space Physics in the Kyiv University

Book of Abstracts

International Conference
in part of the Science Day in Ukraine

May 23 – May 26, 2023

Kyiv, Ukraine

Scientific organizing committee (SOC)

Chair Vasyl' Ivchenko (Ukraine)
Co-chair: Volodymyr Efimenko (Ukraine)

Conference Secretary I. Lyk'yanyk (Ukraine)

SOC Members
Artem Bohdan (Germany), Bohdan Hnatyk (Ukraine), Olexandra Ivanova (Slovakia), Liliya Kazantseva (Ukraine), Vsevolod Lozitsky (Ukraine), Gennadi Milinevsky (Ukraine), Sergiy Parnovsky (Ukraine), Oleh Petruk (Italy), Vira Rosenbush (Ukraine), Sergiy Silich (Mexico), Valentyna Zharkova (UK), Valery Zhdanov (Ukraine), Yaroslav Yatskiv (Ukraine), Vasyl' Yurchyshyn (USA).

Local organizing committee (LOC)

Chair: Vasyl' Ponomarenko (Ukraine)
Secretary: Alena Mozgova (Ukraine)

LOC Members
Asen Grytsai, Liliya Kazantseva, Ivan Yakovkin

E-mail: aoconf@ukr.net

Place of the meeting
Astronomical observatory of the Taras Shevchenko National University of Kyiv, Observatorna str., 3

CONTENTS

ПЛЕНАРНІ ЗАСІДАННЯ

PLENARY SESSIONS

Self-consistent equilibrium of a helical magnetic flux rope

Oleg K. Cheremnykh[1], Victor Fedun[2], Volodymyr M. Lashkin[3]

[1]Space Research Institute, Pr. Glushkova 40 k.4/1, Kyiv 03187, Ukraine
[2]Solar Physics and Space Plasma Research Centre, University of Sheffield, Hounsfield Road, Hicks Building, Sheffield, S3 7RH, UK
[3]Institute for Nuclear Research, Pr. Nauki 47, Kyiv 03028, Ukraine

We present a model of self-consistent equilibrium of a magnetic flux rope in cylindrical coordinates. A nonlinear equation for the current density is obtained and its analytical solution is found. The remaining equilibrium quantities, namely, the azimuthal magnetic field and plasma pressure are determined in a self-consistent way through the found current density. By minimizing the energy functional, we show that the found equilibrium state is stable. The obtained results are compared with the results obtained in the model of a cylindrical tokamak. It is shown that the analytically predicted radial plasma pressure profile is in good agreement with the experimental data for a number of tokamaks.

New results in investigation of Ionospheric and magnetic disturbances caused by the Tonga volcano explosion of January 15, 2022

L. F. Chernogor

V. N. Karazin Kharkiv National University, Kharkiv, Ukraine

New results in investigation of Ionospheric and magnetic disturbances caused by the Tonga volcano explosion are presented. The capability of volcanoes to generate powerful explosive eruptions influencing the state of the ionosphere became known back in the 1980s. The Hunga-Tonga-Hunga-Ha'apai (Tonga for short) volcano explosion of January 15, 2022, has shown a surge of a renewed interest in investigating effects in the Earth–atmosphere–ionosphere–magnetosphere system, since this volcano can be rightfully classified as unique. A number of papers have already dealt with the ionospheric effects from Tonga volcano. The temporal variations in the total electron content (TEC) were used to determine the number of volcano explosions to be five. The second and third explosions were the strongest,

with the second being the most intense. The response of the ionosphere to the Tonga volcano explosion has been studied on a local and global scales by making use of the Global Positioning System satellite constellation and measurements onboard the Swarm satellite network. In the vicinity of the volcano explosion, disturbances in TEC attained 5–10 TECU. In addition to the local effect, traveling ionospheric disturbances, which were due to the generation and propagation of atmospheric gravity waves with speeds of 180 m/s to 1,050 m/s, were observed to propagate. Of particular importance to global-scale perturbations is the Lamb wave, which propagated with a speed of 315 m/s. At nighttime, plasma depletions of the equatorial ionosphere were revealed over the tropical Pacific Ocean when the electron density at 400–500 km altitude showed a decrease by 2–3 orders of magnitude. The length of these formations in longitude exceeded ~10 Mm, and they were observed in excess of 4–5 h.

The scientific objective of this study is an analysis of aperiodic and quasi-sinusoidal perturbations in the ionosphere and the geomagnetic field, which were caused by the Tonga volcano explosion, in a wide range of distances from the source of disturbance (from ~0.1 Mm to 5 Mm).

Ionospheric disturbances. To reveal the ionospheric response to the Tonga volcano explosion, the records of signals from Global Positioning System satellites have been analyzed. The intercomparison of temporal variations in TEC observed on the reference days and on the day when the volcano explosion occurred has resulted in the determination of basic principles of the generation of ionospheric perturbations and the estimation of numerical magnitudes of the parameters of the perturbations. Four groups of disturbances have been detected, each of which arrived at different time delays with respect to the moment of the volcano explosion. It is important to note that the time delay increases with increasing distance from the volcano to the observational instruments. The first group of speeds included the disturbances traveling with a speed close to 1,000 m/s and having an *N*-shaped profile. This perturbation was generated by a blast wave whose speed depended on the excess pressure and a priori exceeded the speed of sound. In the second group, the speed varied in the 336 m/s to 500 m/s range, within which the speeds of atmospheric gravity waves are found. The speeds in the third group exhibited variability within the 260–318 m/s limits, within which the Lamb wave propagates. The speed in the fourth group was estimated to be 190–220 m/s, which is a characteristic speed of the tsunami that was caused directly by the volcano explosion. The period of quasi-sinusoidal perturbations varied from ~10 min to 20 min, while their amplitude from 0.5 TECU to 1 TECU. The observed ionospheric «hole» was proved to be

produced by the volcano explosion directly, with the modules of the absolute and relative magnitudes of disturbances showing a tendency for decreasing with increasing distance from the explosion epicenter, from ~10 TECU to 2 TECU and from 37 % to 7 %, respectively. Contrary to the amplitude, the «hole» time delay and its duration exhibited an increase with distance from the volcano to the observational sensors, from 35 min to 100 min and from ~30–40 min to 120–150 min, respectively. A mechanism for generating the ionospheric «hole» has been advanced, which is based on both the electric and non-electric processes (cracking, friction of particles, condensation of water vapor, coagulation of water droplets, attachment of electrons, gravity segregation, etc.). The ionospheric «hole» is formed as a result of perturbing the global electric circuit, arising external electric currents, an increase in the electric field strengths by orders of magnitude in the atmosphere and the ionosphere, diffusion of the ionospheric plasma down to lower altitudes where the recombination processes become fast. The basic numerical characteristics have been established of the disturbances, whose fluctuations account for local time, the dusk terminator, sensor geographic locations, the location of subionospheric points on the satellite to receiver ray paths with respect to the equatorial anomaly, etc.

Magnetic disturbances. To analyze the variations of the *X*-, *Y*-, and *Z*-components of the geomagnetic field, registrations at 12 stations of the worldwide INTERMAGNET network were used. When processing the time series, the trend calculated over an interval of 60 min with a step of 1 min was first subtracted, and then a system spectral analysis was applied. An analysis of the state of space weather made it possible to choose January 13 and 17, 2022 as reference days. An analysis of time variations in the level of all components of the geomagnetic field showed the following. On the day of the volcano explosion, approximately after 04:21, there were significant variations in the level of all components, but the largest variations were observed in the level of the *Y*-component. The shortest time delay was 6 min. At the same time, quasi-periodic variations of the geomagnetic field with a period of 4–4.5 min and an amplitude of ~2 nT were caused by acoustic resonance in the field of a standing acoustic wave generated by the explosion of the volcano. In addition, six groups of possible disturbances stimulated by the volcano explosion were found. It is important that in each group, the time delay of disturbances increased with increasing distance between the volcano and the station. The disturbances were transported at speeds close to 4, 1.5, 1 km/s and 500, 313, and 200 m/s. Such velocities are characteristic of slow MHD waves, a blast wave, atmospheric gravity wave, Lamb wave, and an ionospheric tsunami wave.

With the time delay, which varied depending on the distance to the volcano from several tens to 100–200 min, bay-disturbances of all components of the geomagnetic field were observed. The magnitude of the effect varied from ~10 to ~60 nT. The greatest disturbances occurred in the *Y* component. The delay time and duration of disturbances increased with increasing distance from the volcano, while their amplitude, on the contrary, decreased. The propagation speed of bay-disturbances was close to the speed of the blast wave. Bay-disturbances were weakly expressed or completely absent on the night side of the planet. It is substantiated that bay-disturbances are closely related to the occurrence of an ionospheric «hole» under the action of a blast wave from the volcano. The results of estimates of the bay-disturbance are in good agreement with the observation results.

Work by L. F. Chernogor was supported by the National Research Foundation of Ukraine for financial support (project 2020.02/0015, "Theoretical and experimental studies of global perturbations of natural and man-made origin in the Earth–Atmosphere–Ionosphere system"). Work by L. F. Chernogor also was supported by Ukraine state research project #0121U109881 and #0122U001476.

Creator of the catalogs of star positions and the history of the Astronomical Observatory

(to the centenary of Mykola Yakimovich Chernega)

V. Efimenko, L. Kazantseva

Astronomical Observatory of the Taras Shevchenko National University of Kyiv, Kyiv, Ukraine

In the post-war history of the Astronomical Observatory, a special role rightfully belongs to Mykola Yakymovych Chernega for his contribution to the scientific work and research of the history of the observatory. When the term "astrometrist" is used in professional circles, at least in Kyiv, the image of M. Chernega, who will be 100 years old in 2023, immediately comes to mind. And not only because he headed the astrometry department at the Astronomical Observatory of the Taras Shevchenko Kyiv University for several decades. And also because he embodied all the main qualities of the profession – the ability to consistently conduct many observations of the same type for years, carefully perform large amounts of calculations, analyze and

summarize them, and obtain appropriate star catalogs so that in the future they could be used unconditionally by others.

Mykola Chernega was born on July 29, 1923 in the village of Berezivka, Zhulyna district of Vinnytsia region. His parents died early, his mother, Chernega Hanna Lukinichna, who ran the household, died in 1937, and his father, Chernega Yakym Mitrofanovych, worked as an elementary school teacher, he died in 1947.

After graduating from the Ternov secondary school in 1941, he was evacuated to the Voroshilovograd region (now Luhansk), and from there he was drafted into the army in August 1941, and already in October 1941 he was sent to study at the 2nd Tomsk Artillery School. After graduating from school in May 1942, he was sent to the South-Western Front. He fought as a platoon commander on the Stalingrad, Voronezh and Steppe fronts.

In August 1943, in the battles for Kharkiv, he received multiple shrapnel wounds to his left shoulder and forearm, was treated in a hospital, and in March 1944 he was demobilized with a discharge of "restricted fitness of the 2nd degree". For his participation in hostilities, he had the status of a war veteran and was awarded the Order of the Patriotic War 1st degree, the Order of the Red Star and 10 medals, the first of which he received back in 1944 for the defense of Stalingrad.

In 1945, he entered the physics faculty of the Kyiv State University, which he graduated in 1950 and received a referral to work at the Astronomical Observatory, which stated that Chernega M. received the specialty of astronomer. He was enrolled on July 11, 1950, immediately to the vacant position of senior researcher of the astrometric department. At that time, many observational programs worked at the Observatory, every night astronomers went out to observe on several instruments at once. Mykola Chernega mainly observed with the meridian circle. Right here, in the Observatory, he lived with his family for the first time in one of the rooms of the Professor's wing. In 1961, M. Chernega headed the department of astrometry - one of the oldest departments of the Kyiv University Observatory, continuing active observational work.

During his leadership in the department, several important topics were completed. In particular, the observation and creation of a catalog of the positions of bright stars has been completed, and studies of the meridian circle have been carried out. In accordance with the decisions of the 16th Congress of the IAS, the Astronomical Observatory was entrusted with compiling a consolidated catalog of bright stars based on observations in various observatories around the world, which was led by M. Chernega.

In the 1970s, M. Chernega became interested in the history of the Observatory, worked a lot in the archives of Kyiv and Leningrad, and together with O.F. Bogorodskyi published a number of studies on the history of the formation and development of astronomical research at the Astronomical Observatory of Kyiv University. During his work at the Astronomical Observatory, he published 59 scientific works, 4 of which were monographs.

Mykola Yakymovych Chernega died on May 22, 2012.

Waves and oscillations generated by magnetic reconnection in solar flares

M. Gordovskyy[1], P.K. Browning[2], J. Stewart[2] and C. Smith[2]

[1]University of Hertfordshire, Hatfield AL10 9AB, UK
[2]University of Manchester, Manchester M13 9PL, UK

Magnetic reconnection is believed to be the key mechanism responsible for fast release of magnetic energy in solar flares. This energy is converted in kinetic energy of non-thermal particles and fast plasma flows, radiation, and waves. Waves play very important role in flares, can trigger magnetic reconnection and, on the other hand, can be generated by the reconnection process. I will discuss the second type of wave: those generated during magnetic reconnection and energy release. I will show that this effect is ubiquitous, and can be observed during the reconnection in laboratory and space plasmas. Two specific examples will be discussed in detail: small-scales waves propagating in the immediate vicinity of the reconnection region, and global intrinsic oscillations of magnetic field in the flaring corona. The latter is likely to be responsible for quasi-periodic pulsations observed in different spectral domains following some solar flares.

My talk will be based on several recent publications including

- Stewart, J., Browning, P.K. & Gordovskyy, M. 2022, MNRAS, 513, 5224
- Smith, C., Gordovskyy, M. & Browning, P.K., 2022, MNRAS, 511, 2880

Peculiarities of gas and dust distribution in the inner coma of comet 67P/Churyumov–Gerasimenko

V.V. Kleshchonok[1,2], H. Sierks[1], C. Güttler[1]

[1]Max-Planck Institut für Sonnensystemforschung, Göttingen, Germany
[2]AO of Taras Shevchenko National University, Kyiv, Ukraine

The OSIRIS Wide-Angle Camera on the Rosetta spacecraft observed the gas and dust distribution in the inner coma of comet 67P/Churyumov–Gerasimenko (67P) using several narrow-band filters. These filters were tuned to the emission lines and bands of the main comet species, allowing the spatial distribution of the gas and dust in the inner coma of comet 67P to be determined. The observations were made near the perihelion, covering three dates before and three dates after the perihelion.

The WAC camera frames undergo several steps of preliminary processing before they can be used for analysis. These steps include: bias subtraction, coherent noise removal, dark current removal, flat fielding, bad pixels removal, stray light correction, radiance factor calibration, and geometric distortion and boresight correction.

The images of the coma for individual emissions were obtained by applying the appropriate continuum subtraction method at the first stage of the analysis. The continuum frames in the 375 nm filter, which were closest in time to the observations, were used to subtract the continuum. The distribution of the flux density in the solar analog spectrum and the reddening of the continuum in the comet's coma were also considered.

The frames obtained in this way were used to construct spatial profiles of surface brightness, determine the azimuthal distribution of surface brightness, as well as variations in gas and dust production during the nucleus rotation period for individual emissions. The emissions of OH, NH and NH_2 have the highest surface brightness in the direction of the Sun, while the emissions of OI and CN have the highest surface brightness in the region of the illuminated pole of the comet's nucleus. The spatial distribution of NH and NH_2 as well as OH and OI shows their significant difference, which indicates the presence of other types of parent molecules for NH and OI.

The characteristics of the coma on August 22-23, 2015 indicate that an active process was observed, which was possibly accompanied by the release of ice particles into the near nuclear region of the coma. During this period, there was also an increased density of dust particles, which led to the

appearance of a visible shadow from the nucleus. We used a novel technique to measure the dust spatial distribution in the shadowed area. We found two kinds of regions: a dense region close to the nucleus and a free expansion region. The dust spatial distribution in the free expansion region reveals the fast evolution of dust particles at short distances from the nucleus.

Astronomical research at the Shevchenko Scientific Society. To the 150th anniversary of the establishment of the SSS (NTSh)

R. Kushnir[1], R. Plyatsko[1], V. Pelykh[1], O. Petruk[1], B. Hnatyk[2], B. Novosyadlyi[3]

[1]Pidstryhach Institute for Applied Problems in Mechanics and Mathematics of NAS of Ukraine, Lviv, Ukraine
[2]Astronomical Observatory of Taras Shevchenko National University of Kyiv, Kyiv, Ukraine
[3]Ivan Franko National University of Lviv, Lviv, Ukraine,

The Scientific Society named after Shevchenko is the first Ukrainian National Academy of Sciences created in 1873 in Lviv. After updating the statute in 1892 the Shevchenko Scientific Society turned into a genuine multidisciplinary academy of sciences. In the conditions of Ukrainian statelessness the activities of the Society from the first years of work had a clearly defined nation-building and national-defense direction.The structure of Society was determined by three sections: Historical-Philosophical, Philological, and Mathematical-Natural Sciences-Medical.

Already in the period before the First World War, the Society achieved significant success in the development of scientific research with the significant of such outstanding personalities as Mykhailo Hrushevskyi (the chairman in 1897-1913, author of the multi-volume "History of Ukraine-Rus"), Ivan Franko (the head of the Philological Section), Volodymyr Hnatyuk (folklorist, ethnographer).

In the twentieth century, especially during the Second World War and Soviet occupation the Society survived the tragic pages of history together with its people and in 1989 resumed active work in Ukraine, which restored its statehood. And now, in independent Ukraine, the Shevchenko Scientific Society as the All-Ukrainian Academy of Sciences acts as an important factor in building a free, independent, democratic Ukraine in the community of European nations.

Important scientific achievements were obtained by Society scientists working in the field of natural sciences, in particular mathematician Volodymyr Levytsky, famous experimental physicist and electrical engineer Ivan Puluj, the world-famous biochemist Ivan Horbachevsky. A number of famous European scientists were members of Mathematical-Natural Sciences-Medical Section of the Shevchenko Scientific Society. Namely, Max Plank, Albert Einstein, Felix Klein, David Hilbert to name the few.

In the report, we present the past and modern astronomical research carried out under the auspices of the Shevchenko Scientific Society.

Periods of solar activity and orbital asymmetry of solar radiation deposition into the terrestrial atmosphere

V.V. Zharkova[1,2], I. Vasilieva[2,3], S.J. Shepherd[2,4] and E. Popova[5]

[1]MPEE, Northumbria University, Newcastle upon Tyne, UK
[2]ZVS Research Enterprise Ltd., London, UK
[3]Solar Physics Department, Main Astronomical Observatory, Ukraine
[4]PRIMAL Research Group, Sorbonne University, Paris, France
[5]Centro de Investigaci´on en Astronom´ıa, Universidad Bernardo O'Higgins, Santiago, Chile

In this paper, a spectral analysis of the averaged sunspot numbers, solar irradiance, and the summary curve of eigenvectors of SBMF was carried out using Morlet wavelet and Fourier transforms. We confirm a 10.7-year cycle derived from the sunspots and modulus summary curve of eigenvectors as well a 22 years cycle and the grand solar cycle of 342-350-years from the summary curve of eigen- vectors. The Gleissberg centennial cycle is only detected on the full set of averaged sunspot numbers for 400 years or by adding a quadruple component to the summary curve of eigen- vectors. Another period of 2200-2300 years is detected in the Holocene data of solar irradiance measured from the abundance of ^{14}C isotope. This period was also confirmed with the period of about 2100 years derived from a baseline of the so- lar background magnetic field, supposedly, caused by the solar inertial motion (SIM) induced by the gravitation of large planets. We also report the implication of solar inertial motion on different magnitudes of solar radiation deposited into the northern and southern hemispheres of the Earth caused by

the combined effects of the solar activity and solar inertial motion on the terrestrial atmosphere.

Reference:

Zharkova et al, 2023, Natural Science, Vol.15 No.3, March 2023 https://www.scirp.org/journal/paperinformation.aspx?paperid=124007

АСТРОФІЗИКА, ГРАВІТАЦІЯ І КОСМОЛОГІЯ

ASTROPARTICLE PHYSICS, GRAVITATION AND COSMOLOGY

Multimessenger Research of Shapley Supercluster

V. M. Babur[1], B.I. Hnatyk[2], V.V. Voitsekhovskyi[2]

[1]Taras Shevchenko National University of Kyiv, Kyiv, Ukraine
[2]Astronomical Observatory of Taras Shevchenko National University of Kyiv, Kyiv, Ukraine

The Shapley Supercluster is one of the largest and most massive structures in the nearby Universe at the distance of about 200 Mpc, consisting of thousands of galaxies. Multimessenger research has been a powerful tool in understanding the properties and evolution of this structure. The use of multiple messengers, such as electromagnetic radiation, high energy cosmic rays and neutrino, has allowed for a more complete understanding of the physics of the Shapley Supercluster, including its dynamics and morphology. It is known that galaxy clusters are some of the most massive structures in the universe, where high-energy processes such as mergers occur. As a result of this process, shock waves and turbulent movements are formed, which effectively accelerate particles of intergalactic plasma. Thus, galactic clusters are potential sources of ultra-high-energy cosmic rays. Also a significant issue in modern astrophysics is the absence of detection of gamma-ray emission, which is a predicted result of collisions of relativistic protons.

We present predicted spectra obtained using the MINOT software for the diffuse gamma-ray emission and neutrinos caused by hadronic interactions in the Shapley Supercluster. Using the obtained results, the possibility of detecting gamma-ray emission and neutrinos by the existing and future observatories, IceCube and Cherenkov Telescope Array (CTA), was analyzed.

Catastrophic dark matter particle capture

R. Durrer[1], S.L. Parnovsky[2]

[1]Département de Physique Théorique and Centre for Astroparticle Physics, Université de Genève, Genève, Switzerland
[2]Taras Shevchenko National University of Kyiv, Astronomical observatory, Kyiv, Ukraine

The report is based on results published in two articles: Durrer, Ruth; Parnovsky, Serge Catastrophic dark matter particle capture. Physical Review D, V. 107, id.063528 (2023) and Durrer, Ruth; Parnovsky, Serge; Parnowski, Aleksei Capture of Dark Matter Particles by a Galaxy in the Case of a Bimodal Distribution of Their Velocities Letters in High Energy Physic V. 2023, 331, (2023).

Dark matter (DM) particle velocities increase as they enter from intergalactic space into the halo of the galaxy and decrease as they leave. If during the flight the mass of the galaxy has increased, then slow DM particles are captured by the galaxy, further increasing its mass, while faster particles slow down, transferring part of their energy to the galaxy. A simple model describes this process. It allows one to estimate the minimum initial velocity of a particle required for a passage without capture through the center of the galaxy and the rate of galaxy mass increase. An analysis carried out using the ideas of the theory of catastrophes shows that for intensive capture of dark matter, an increase in the mass of galactic baryonic matter is necessary, exceeding a certain threshold value in the present or past. It may be associated with the accretion of matter or the merger of galaxies. Additionally, the density of intergalactic DM must exceed the threshold value. Then the rate of increase in the mass of DM can be many times higher than one for the baryonic matter. The capture rate sharply decreases after the DM density decreases below the threshold value due to expansion.

Extrapolation of IllustrisTNG galaxy sample with neural networks

O. Gugnin[1], A. Tugay[1]

[1]Taras Shevchenko National University of Kyiv, Kyiv, Ukraine

The widespread usage of neural networks in astrophysical research is today's reality, which has already been faced by a large number of scientists from completely different fields. From already familiar problems of classification and regression to technical problems of adaptive optics and improving the quality of astronomical images - deep learning algorithms are applicable everywhere. And therefore, the relevance of research related to them is thorough. As part of this work, we investigated the ability of machine learning methods to extrapolate a simulated sample using the example of dark matter halos distributions of the IllustrisTNG project. This included getting acquainted with the theory of neural networks, building a large number of different models, choosing the most optimal ones according to a set of parameters, testing them, and actually analysing the results obtained by various methods. Based on the results of the work, a pair of architectures was obtained, one of which is able to extrapolate the dark matter halos in time, imitating the original simulation, and the second - to increase the sampling resolution by the method of successive convolutions and transposed convolutions. The practical application of this work is reducing the time required to run large physical simulations.

Search for the sources of extremely-high energy cosmic rays

O. Gugnin[1], V. Voitsekhovskyi[2], B. Hnatyk[3]

[1]Taras Shevchenko National University of Kyiv, Kyiv, Ukraine
[2]University of Geneva, Geneva, Switzerland
[3]Astronomical Observatory of Taras Shevchenko National University of Kyiv, Kyiv, Ukraine

Search for sources of ultra-high energy cosmic rays (UHECRs, $E>5\cdot10^{19}$ eV) remains one of the main unsolved problems in modern high energy astrophysics. High degree of isotropy in observed arrival directions of UHECRs caused mainly by deflections of charged particles in Galactic and

extragalactic magnetic fields. Such deflections significantly complicate the process of linking UHECR directions to their potential sources. One of the ways for solving problem of searching UHECR sources is calculating backtracking trajectories of charged particles in known models of magnetic fields. To reduce impact of magnetic field, we considered UHECRs only with highest detected yet energies - extremely-high energy cosmic rays (EHECRs, $E>10^{20}$ eV). In this work we calculate backtracking trajectories using CRPropa software for the EHECRs from the latest publicly available data by Pierre Auger Observatory. We use the obtained recovered trajectories in Galactic random and regular magnetic fields as a proxy to positions of potential Galactic (magnetars) and extragalactic (starburst galaxies, galaxy clusters) sources.

The radial distribution of chemical compositions in Crab Nebula filaments

N.V. Havrylova[1], B.Ya. Melekh[1], V.V. Holovatyy

[1]Department of Astrophysics of Ivan Franko National University, Lviv, Ukraine

The chemical compositions of the filaments in the Crab Nebula are determined using a 3-stage method based on optimized photoionization modeling of the nebular gas. This method uses diagnostic ratios between emission line intensities. In the first stage, the ionization structure of the nebula is determined by reproducing the observed diagnostic ratios between line intensities. In the second stage, the chemical element abundances are corrected based on the ionization structure obtained in the previous stage. In the final third stage, all free parameters are simultaneously optimized to avoid potential biases resulting from the assumptions made in dividing the optimization process into the first two stages. The optimized photoionization modeling of the Crab Nebula employs several free parameters: hydrogen density, covering factor, energy distribution in ionizing spectra, and chemical abundances (He/H and O/H in Stage I, all available chemical elements in Stage II and Stage III). The chemical composition of elements is initialized using data obtained through diagnostic methods. The modeling results are compared with observations using the model emission line spectra, the flux in the H_β line, the nebular outer radius, and diagnostic ratios. The ionizing Lyman continuum spectrum is also varied during the optimization process,

allowing for the reproduction of the optimal energy distribution in the ionizing radiation spectrum within the modeled region. Consequently, a detailed consideration of the ionizing radiation transfer from the pulsar to the modeled part of the nebula is not required. The optimized photoionization modeling of the nebular gas in filaments employs Gary Ferland's code Cloudy 08.00, which we have upgraded to include the ionizing spectrum shape as a free parameter and to compare model diagnostic ratios with observed ones.

We analyze the radial distribution of chemical compositions in the filaments of the Crab Nebula using results obtained for seven parts of the filaments. Our findings do not confirm an increase in abundances outward from the nebula.

Identifying Ring Galaxies in the SDSS Dataset through Augmented Training Samples and Deep Learning

Oleksandr Hetmantsev[1], Daria Dobrycheva[2]

[1]Taras Shevchenko National University of Kyiv
[2]Main Astronomical Observatory of NAS of Ukraine

This study focuses on the development of a training sample of galaxies with polar rings. Given the limited number of objects available in the current sample (only 114), we propose to augment it using different Python packages. By leveraging deep learning techniques, we aim to identify galaxies with polar rings in the SDSS dataset. We hope that our findings hold significant potential for advancing the understanding of galaxy formation and evolution.

Non-Parametric Morphology in the Age of Modern Surveys and High-Quality Data

I. Kolesnikov[1], V. M. Sampaio[2], R. R. de Carvalho[2], C. Conselice[3], R. R. Rosa[1]

[1]Instituto Nacional de Pesquisas Espaciais - COPDT, São Paulo, Brazil
[2]NAT - Universidade Cruzeiro do Sul / Universidade Cidade de São Paulo, São Paulo, Brazil
[3]Jodrell Bank Centre for Astrophysics, University of Manchester, Manchester, UK

Morphology has been at the forefront of modern astronomy since the time of Hubble, serving as one of the primary tools to infer galactic properties and uncover the secrets of the construction and evolution of the universe. Morphological metrics are relatively straightforward numerical descriptors that capture specific aspects of a galaxy's appearance, such as its size, shape, and structural features. These parameters allow researchers to objectively classify galaxies and investigate the relationships between their morphologies and other astrophysical properties. One widely-used set of morphological parameters is the Concentration-Asymmetry-Smoothness (CAS) system.

However, the advent of contemporary surveys like JWST, and upcoming ones like Euclid and LSST, brings a new set of challenges that need to be addressed in order to overcome some inherent limitations of the current approach. These limitations include issues with high-resolution images, high-redshift galaxies, and simply the sheer volume of data. For example, as the resolution of galaxy images increases, the complexity of the observed structures grows, revealing intricate details such as star-forming regions, dust lanes, and other small-scale features that may not have been discernible in lower-resolution images. Additionally, by observing galaxies at different redshifts, astronomers can effectively look back in time and study the evolution of galaxy morphology over cosmic history. Understanding how galaxy morphology changes with redshift is essential for constraining models of galaxy formation and evolution, as well as for investigating the role of environmental factors, such as dark matter and dark energy, in shaping galactic structures.

Furthermore, machine learning methods, both supervised and unsupervised, are increasingly coming into the spotlight due to their speed, lower sensitivity to input data, and superior performance. Therefore, it is

essential to invest time into the development of new implementations of morphological metrics and additional image manipulation techniques to enhance the performance of non-parametric morphology.

Analytical solutions of the transport equation for steady-state 2D case for different problems CR modulation

Yu. L. Kolesnyk

Main Astronomical Observatory of the NAS of Ukraine, Kyiv

The goal of the last research is to derive the analytical solution of the transport equation (TPE) for steady-state 2D case with take account the drift of the particles ($\kappa_{r\theta} \neq 0$, $\kappa_{\theta r} \neq 0$) and when diffusion coefficients κ_{rr}, $\kappa_{\theta\theta}$ have dependence on heliospheric magnetic field (HMF).

It should be noted that TPE (as and for any dimensional case) has not purely analytical solution but may be solved by analytically iterative method which was initially proposed by [Shakhov B. A., and Kolesnyk Yu. L., 2006] and analyzed in detail in [Kolesnyk Yu. L.,et. all, 2017] that applied in [Kolesnyk Yu. L.,et. all, 2018]. The method for steady-state 2D case was adapted to obtain the force-field approximation (FFS). LIS spectrum was chosen by the power-law spectrum with the slope of the initial spectrum α, namely $LIS = p^{-\alpha}$. The effective radial diffusion coefficient κ_{rr} and generally its value depends on the momentum of the particle, p the particle speed, v and value of heliospheric magnetic field, B.

The proposed problem was considered in three stages. At first stage, there was investigated case when $\kappa_{rr} = const$, no the diffusion of particles along the heliolatitude ($\kappa_{\theta\theta} = 0$) and without considering the drift of the particles ($\kappa_{r\theta} = 0$, $\kappa_{\theta r} = 0$). At second one, to solve when κ_{rr} has dependence on HMF, there is the diffusion of particles along the heliolatitude ($\kappa_{\theta\theta} \neq 0$) but the drift of the particles absence. And finally, for real physical conditions of CR modulation in heliosphere, i.e. as in the second stage, but with considering of the drift of the particles.

General X-ray properties of 2MIG isolated AGN at z < 0.05

O. Kompaniiets

Main Astronomical Observatory of the NAS of Ukraine, Kyiv, Ukraine

Isolated galaxies in particular offer a unique opportunity to study the interplay between different astrophysical processes without the complicating factors of interactions with other galaxies or the effects of a dense cluster environment. Here we present general information in the X-ray band for 2MIG isolated AGNs. We have checked all available archival databases and only for 20 galaxies from our sample were observed in X-ray band, 13 of them are in the hard X-ray which was detected by SWIFT. The small number of isolated AGNs in X-ray is the first limitation on the possibilities for statistical analysis.

Photoionization modeling of nebular environments in dwarf galaxies with detailed calculation of diffuse ionizing radiation fluxes

I.O. Koshmak[1], B.Ya. Melekh[1], O.S. Buhajenko[1]

[1]Ivan Franko National University of Lviv, Lviv, Ukraine

Photoionization modeling allows to determine the ionization structure of nebular plasmas surrounding active star-forming region in dwarf galaxy using spatial distributions of density, chemical abundances and temperature provided by chemo-dynamical simulations (ChDS) of such objects. We perform multicomponent photoionization modeling (MPhM) of the ionized gas with detailed calculation of the diffuse ionizing radiation (DCDIR) transfer using 2-D ChDSs of dwarf galaxies. In our paper (see Melekh et al. 2015) we calculated ionization structure of nebular plasmas and, correspondingly, the emissivity maps for important nebular emission lines using MPhM in outward only (OUTW) approximation. To reproduce the relative intensity of these lines the thin dense shell (TDS) was artificially added between superwind region and outer part of the nebular environment. Obtained in such way emissivities and opacities of emission lines and continuum are used on the following iterations for calculations of the diffuse ionizing radiation fluxes in detailed way with adaptive selection of the

integration steps. After convergence of ionization structure (spatial distributions of density and temperature which defines the ionization fractions of chemical elements and the emissivities) it is shown that in some sectors (mainly in equatorial ones) in outer part of nebular environment appears large difference between obtained results and ones calculated in OUTW approximation: so-called shadow regions from MPhM results calculated in OUTW approximation disappear in MPhM+DCDIR results because of ionizing radiation transfer in non-radial directions. Obtained from MPhM+DCDIR emission lines are used to derive the chemical abundance of oxygen by the so-called T_e– and R_{23}–methods that is in good agreement with one obtained as results of ChDSs. Also we have analyzed the escape fraction of ionizing photons and tested the Kennicutt's calibration to determine the SFR using H_α luminosity.

Dark Ages global signal in the rovibrational lines of the first molecules

Yu. Kulinich, B. Novosyadlyj,

Astronomical Observatory of Ivan Franko National University of Lviv, Lviv, Ukraine

The only sources of signals in the Dark Ages before the appearance of the first stars were neutral hydrogen atoms and the first molecules, which give rise to the CMB spectral distortions by emitting, absorbing and scattering in the 21 cm line and in the lines of rovibrational transitions, respectively. Signals from the first molecules are important sources of information about the ionization and thermal history of the post-recombination Universe. In our research, we aim to find out whether it will be possible to detect the CMB spectral distortions caused by the first molecules during the implementation of the proposed spectrometer concepts for space-based (PIXIE, PRISM, PRISTINE, SuperPIXIE and Voyage2050), balloon-based (BISOU) or ground-based (APSERa and Cosmo at Dome-C, TMS at Teide Observatory) missions in the near future. To do this, we calculate the contents of the first molecules by integrating the equations of the kinetics of chemical reactions in the weakly ionized plasma of the early Universe, as well as the population of rovibrational levels of these molecules for standard cosmology, as well as for cosmology with decaying dark matter particles or primordial magnetic fields that are additional sources of ionization and heating. We show that in

standard cosmology the signal from the first molecules has the character of an absorption profile against the background of relic radiation, while the presence of the additional sources of ionization and heating lead to the emission of the first molecules (mainly H_2). The calculated signal from the first molecules is several orders of magnitude smaller than other sources of relic spectrum distortion (e.g., μ and y distortions), but its detection is still possible due to the different angular distribution.

Dark Ages global signal in the redshifted 21-cm line as a cosmology test

B. Novosyadlyj, Yu. Kulinich

Astronomical Observatory of Ivan Franko National University of Lviv, Lviv, Ukraine

We analyze the formation of the redshifted hyperfine structure line 21-cm of hydrogen atoms from the Dark Ages ($30<z<150$) in different cosmologies. To study its dependence on the values of cosmological parameters and physical conditions in the intergalactic medium, the evolution of the sky-averaged (or global) differential brightness temperature in this line was computed in standard and non-standard cosmological models with different parameters. The standard ΛCDM model with post-Planck parameters predicts a value of the differential brightness temperature in the center of the absorption line ~30 mK at z~90. The variations of the depth of the Dark Ages absorption line at z~90 (ν~16 MHz) with variations of the cosmological parameters Ω_b , Ω_{cdm} , Ω_Λ, Ω_K and H_0 in the ΛCDM model are studied. It is shown that the ten percents variations of each of them result into ~25%, 4%, 0%, 0% and 10% variations of the line depth accordingly. In the non-standard cosmological models with annihilating or decaying dark matter, primordial stochastic magnetic field etc. the profile of this line can be quite another including an emission bump instead absorption trough in the standard model. So, the detection of the redshifted 21-cm absorption/emission line of neutral hydrogen at frequencies 10-30 MHz from the Dark Ages could be a powerful new cosmological test. The projects for realization will be mentioned also.

N-body simulations: advantages and problems

S.L. Parnovsky

Astronomical observatory of Taras Shevchenko National University of Kyiv, Kyiv, Ukraine

The N-body simulations method is widely used in astrophysics and cosmology. The article briefly lists its advantages, disadvantages and possible errors. The main source of the differences between the results of applying this method and the processes occurring in the real Universe are the huge difference in the number of particles and the strong simplification of the calculation algorithms, especially for baryonic matter. The best N-body simulations have a resolution of 10^{-11} M_{Sun} to 10^{12} M_{Sun}, depending on the size of the region they want to simulate and on computational resources. Even 10^{-11} M_{Sun} is much larger than the mass of dark matter particles which have typically masses of elementary particles, m~100 Gev ~$10^{-45}M_{Sun}$.This is not quite true in the case of primordial black holes which have a window of possible masses between 10^{-16} $M_{Sun}<m<10^{-11}$ M_{Sun}. Additionally, might it be that due to the much smaller effect from dynamical friction, elementary particles might behave significantly different from 'chunks of phase space' with a mass of 10^6 M_{Sun}?

It is concluded that the results of computer simulation not only cannot replace the data of astronomical observations, but also are not a sufficient reason to reject new hypotheses that do not have other drawbacks, other than the discrepancy between their conclusions and the results of N-body simulations.

Cosmic distance ladder and related problems

S.L. Parnovsky

Astronomical observatory of Taras Shevchenko National University of Kyiv, Kyiv, Ukraine

A brief description of the methods of determining the distances to celestial bodies in the Solar System, the Galaxy and beyond is given; the concept of the "distance ladder" is described. The problems that arise when moving from

one level to another are shown. A bias in the determination of distances and a systematic error in the Hubble constant occur if we use distances estimated using statistical dependencies to calibrate ones obtained by another method. This is a consequence of statistical data processing when approximating any dependence based on a set of measurement data. Random errors in the values of the ordinate lead to random errors in the parameters of the dependence. However, random errors in the values of the abscissa lead additionally to systematic errors in the dependence parameters. This gives a systematic error when estimating the value based on the obtained dependence.

When astronomers calibrate distances to the stars in the Galaxy estimated by Cepheid or main-sequence star luminosities, the abscissa is the distance to nearby stars determined by parallaxes, which have small errors that can be reduced as measurement accuracy improves. A spread in ordinate for fixed abscissa is related to the statistical nature of dependence. When moving to the next rung of the ladder, astronomers compare the distances obtained for a sample of nearby galaxies by other methods (Tully-Fisher-type dependencies, surface brightness fluctuations, etc.), which are ordinate, and the ones obtained from Cepheid, etc, which are the abscissa. It is the errors in the abscissas that lead to the appearance of the bias of the calibration and all the distances estimated by the obtained dependence. This bias increases when moving to the next rungs of the distance ladder. The consequences of it and ways to reduce the bias impact are discussed. Appropriate corrections could be done using the error estimations obtained from the Monte Carlo simulations. This bias can be the source of the Hubble tension.

Comparing the real Universe with the Kasner's space-time

S.L. Parnovsky

Astronomical observatory of Taras Shevchenko National University of Kyiv, Kyiv, Ukraine

We investigate possible astronomical manifestations of space-time anisotropy. The homogeneous vacuum Kasner solution was chosen as a reference anisotropic cosmological model. The study of its geodesic structure made it possible to clarify the properties of this space-time. It showed that the degree of manifestation of anisotropy varies significantly depending on the time after which the light from the observed object reaches the observer. For

nearby objects, for which it does not exceed half the age of the universe, the manifestations of anisotropy are very small.

Distant objects show more pronounced manifestations, for example, in the distribution of objects over the sky and over photometric distances. These effects for each of the individual objects decrease with time, but in general, the manifestations of anisotropy in the Kasner space-time remain constant due to the fact that new sources emerging from beyond the cosmological horizon. These effects were not found in astronomical observations, including the study of the CMB. We can assume that the Universe has always been isotropic or almost isotropic since the recombination era. This does not exclude the possibility of its significant anisotropy at the moment of the Big Bang followed by rapid isotropization during the inflationary epoch.

New approach to measuring a black hole spin

V.O. Pelykh, Y.V. Taistra

Pidstryhach Institute for Applied Problems in Mechanics and Mathematics, Lviv, Ukraine

Currently, there are two approaches to measuring black hole spins under the assumption of Kerr background: the study of the thermal spectrum of thin disks (continuum-fitting method) and the analysis of the relativistically measured reflection spectrum of thin disks (the iron line method).

We propose a method for defining an angular momentum density of the Kerr black hole, which is based on our obtained exact solution of the Maxwell equations in the form of a one-way null field. The expression for angular momentum density is obtained from the expression for ellipticity angle of electromagnetic radiation, emitted from the vicinity of the black hole and measured for two different frequencies

$$a = \frac{2\mathrm{arsh}\left(\frac{1}{2}(-Z-1)\left(\frac{\sin\theta}{1-\cos\theta}\right)^{m} - \ln Z\right)}{4(\omega_1-\omega_2)\cos\theta},$$

a is the Kerr black hole angular momentum, Z is an ellipticity angle ratio for two different frequencies ω_1, ω_2, m – azimuthal number of a wave, θ – polar angle.

Remnant of SN1006: in expectation for the X-ray polarization data

O. Petruk[1,2], R. Bandiera[3]

[1]Institute for Applied Problems in Mechanics and Mathematics, Lviv, Ukraine
[2]INAF-Astronomical observatory of Palermo, Italy
[3]INAF-Arcetri Astrophysical observatory, Florence, Italy

The space observatory Imaging X-ray Polarimetry Explorer (IXPE) was launched on 9 December 2021. It is a product of cooperation between the Italian Space Agency and NASA. It works in the X-ray photon energy range (2-8 keV) and is the first instrument able to produce the polarization images of astronomical sources in X-rays. We will briefly outline its characteristics and highlight a few recent results which demonstrate the power of observations in a new 'X-ray polarization' window. One of the results which is highly expected to be reported in the next few months is the X-ray polarization observations of the famous remnant of the supernova SN1006. In our talk, we discuss properties of its radio polarization and make some theoretical predictions for the X-ray polarization.

On circular orbits in a Schwarzschild field: from S. Kaplan's article onwards

R.M. Plyatsko, M.T. Fenyk

Pidstryhach Institute for Applied Problems in Mechanics and Mathematics, Lviv, Ukraine

In short article [1], the results on regions of existing both stable and unstable circular orbits according to the geodesic equations in Schwarzschild's field were presented, and later were described in known books on general relativity, where possible types of orbits of a simple test body\particle are analyzed. In this context it is important to generalize these results for a particle with inner structure, first of all, with inner rotation or spin. For this purpose the Mathisson-Papapetrou equations are used as a clear generalization of the geodesic equations. It follows from these equations that for a spinning particle with the orbital velocity which is not very close to the

speed of light its orbits are very close the corresponding orbits of a spinless particle. Other situations arise for a highly relativistic spinning particle orbiting a zits is much wider then for a highly relativistic spinless particle [2-4]: it is known that according to the geodesic equations the highly circular orbits exist only in the small neighborhood of the value $r=3M$, with $r>3M$, where r and M are the radial coordinate and Schwarzschild's mass, respectively.

Now we present more detailed analysis of possible highly relativistic circular orbits of a spinning particle in Schwarzschild's field, determine the physical reason of the essential deviation of the spinning particle motion from geodesic, estimate binding energy due to the spin-gravity coupling.

1. Каплан С.А. О круговых орбитах в теории тяготения Эйнштейна (Письмо в ред.) // Журн. эксп. теор. физ. - 1949. - Т. 19, №10. - С. 951-952 (English translation: On circular orbits in Einstein's theory of gravitation, arXiv: 2201.07971).

2. Plyatsko R. Ultrarelativistic circular orbits of spinning particles in a Schwarzschild field // Class. Quant. Grav. – 2005. – V. 22. – 1545-1551.

3. Plyatsko R., Fenyk M. Highly relativistic spinning particle in the Schwarzschild field: Circular and other orbits // Phys. Rev. D. - 2012.- V. 85. – 104023.

4. Plyatsko R., Fenyk M. Energy and radiation of a highly relativistic spinning particle in Schwarzschild's field // Acta Phys. Pol. B. – 2021. – V. 52. – 323-339.

Photometric variability of AGN PKS 1222+216 and Markarian 501 in the optical range

V.O. Ponomarenko[1], A.O. Simon[2], V.V. Vasylenko[2], K.V. Kulish[3], I.O. Izviekova[4]

[1]Taras Shevchenko National University of Kyiv, Kyiv, Ukraine
[2]National Center Junior academy of sciences of Ukraine, Kyiv, Ukraine
[3]Comenius University in Bratislava, Bratislava, Slovakia
[4]Main Astronomical Observatory of NAS of Ukraine, Kyiv, Ukraine

We present the results of photometric observations and research of AGN PKS 1222+216 and Markarian 501 with high temporal resolution (30–60 s) in BVRI filters of Johnson/Bessel system. The most observations for these

objects were obtained during 2018-2020 with the CCD camera FLI PL4710-1-BB-E2V (1027x1048 pixels, 13x13 μm/pixel, the scale is 0.95″/pixel, the field of view is 16.2′) and the telescope AZT-8 (D = 0.7 m; F = 2.8 m) of the observation station Lisnyky of Astronomical Observatory of Taras Shevchenko National University of Kyiv.

The substrate (bias), dark current, and flat-field were taken into account during processing. The fluxes of energy from the objects of research have been turned into visible stellar magnitudes with the help of standard stars. Light curves for PKS 1222+216 and Mrk 501 were plotted and they were examined for the apparent magnitude variations over the observation period. Intraday variability and the variability of color indexes for AGN were also investigated. The search for mechanisms of brightness variation and the correlation between the optical and gamma ranges were also carried out.

In 2020, for PKS 1222+216, we registered a long burst of brightness in all our filters. During the burst, we detected significant changes in color indexes, and the correlation between changes in brightness in optical and gamma ranges was detected in addition.

Transient and multimessenger astrophysics with CTA

O. Sergijenko

Astronomical Observatory of Taras Shevchenko National University of Kyiv, Kyiv, Ukraine

The Cherenkov Telescope Array (CTA), a next generation ground-based very-high-energy gamma-ray observatory, will be a key instrument for time-domain astrophysics in the very-high-energy (VHE, > 100 GeV) range, owing to its unprecedented sensitivity, rapid response, and capability to monitor a large sky area via a scanning mode of operation. The detection of electromagnetic (EM) emission following the gravitational wave (GW) event GW170817 provided the first direct evidence that at least a fraction of binary neutron star (BNS) mergers are progenitors of short Gamma-Ray Bursts (GRBs). GRBs also emit VHE photons, as proven by the recent MAGIC and H.E.S.S. detections. The spatially and temporally correlated observations of the flaring gamma-ray blazar TXS 0506+056 and a high-energy neutrino detected by IceCube as well as the detection of high-energy neutrinos from the active galaxy NGC 1068 by IceCube are the most compelling evidence for a high-energy neutrino point source so far. These discoveries have shown

the importance of coordinated observational campaigns. One of the challenges for future multimessenger observations will be the detection of VHE emission from GRBs in association with GWs and from steady or flaring sources in association with high-energy neutrinos. We present the transient program which is one of the Key Science Projects of the CTA Observatory and includes a wide range of sources at VHE from GRBs and multimessenger events to core-collapse supernovae and Galactic transients.

Radio-γ-ray response in blazars: an evidence of adiabatic blob expansion in the jet

V.M. Sliusar

Department of Astronomy, University of Geneva, Geneva, Switzerland

Geometrical constraints, specifically alignment of relativistic jet with observer's light of sight, make blazars the most rare and powerful active galactic nuclei observed from the Earth. They show extreme variability on all time-scales and on all wavelengths. Flares last from typical sub/few-hours in X-rays and TeVs, to months or years in the radio. Numerous teams carry out multi-wavelength long-term campaigns to investigate individual flaring events, or spectral evolution in general, focusing on spectral energy distribution (SED) fitting assuming different emission process in the jet. For the current study we employ γ-ray and radio light curves taken during 5 years by Fermi LAT and OVRO to find an inter-band connection between the bands. We perform such analysis for already well-studies blazars Mrk 501, Mrk 421 and 3C 273. We find that the radio emission for those three sources lags behind the γ-rays and generally resembles γ-rays variability, but with longer lasting (weeks-months vs days) flares. This behaviour is compatible with an assumption that γ-rays originate from upstream jet, while radio radiation being released later when jet becomes transparent enough. We propose a model of adiabatic expansion of the jet, which can explain these delays. We find a response profile between the bands, which when convolved with γ-ray light curve can reproduce the variability in the radio. Such response profile includes the delay, rising and decaying time-scales, which constrain expansion velocity and properties of the blob environment.

Betti curves of evolving Cosmic web

M. Tsizh[1,2], V. Tymchyshyn[3,4], F. Vazza[1,5]

[1]Dipartimento di Fisica e Astronomia, Universitá di Bologna, Bologna, Italy
[2]Ivan Franko National University of Lviv, Lviv, Ukraine
[3]Bogolyubov Institute for Theoretical Physics, Kyiv, Ukraine
[4]Kyiv Academic University, Kyiv, Ukraine
[5]Institute of Radioastronomy - INAF, Bologna, Italy

We elaborate and develop probing of Cosmic web with newly emergent approach of studying large scale structure of the Universe, the topological data analysis. As we have already shown, the topological analysis, and persistent homologies in particular, can be useful in the problem of discriminating Cosmic webs of different cosmologies [1]. In this work, we explore the behavior of Betti curves of such homologies with cosmological evolution. Betti curves which are nothing else but Betti numbers dependent on the filtration radius of the simplex complex of Cosmic web, also have been already introduced into large scale analysis as an instrument, which can distinguish two Cosmic webs generated by different cosmologies. In our study we concentrate on the evolution of Betti curves themselves: as the the Cosmic web changes under impact self-gravitation and of Hubble expansion, Betti curves change their shapes, radii of maxima, and other characteristics. We examine the evolution of Betti curves of several N-body cosmological simulations and point out their similarities. We also analyze how the usage of weighted complexes, in particular, DMT-filtered Cech complexes alternates the evolution of curves, and find that it introduces minor changes.

We also pay attention to homology features of dimension 2 and their Betti curves, as they can be in a certain way related to cosmic voids. Cosmic voids spark special interest among cosmologists, as it was shown earlier, they can serve as probes of the nature of dark energy [2], and, in general, can be used for cosmological tests. We note the tendency of growth of 2-dimensional homology features with cosmic time, which is common also to cosmic voids. With development of such studies, one can eventually come up with Betti curves and persistent diagram “portraits” of Cosmic webs as a new cosmological test.

[1] M. Tsizh, V. Tymchyshyn, F. Vazza, *Wasserstein distance as a new tool for discriminating cosmologies through the topology of large scale structure*. Monthly Notices of the Royal Astronomical Society, Volume 522, Issue 2, June 2023, Pages 2697-2706

[2] B. Novosyadlyj, M. Tsizh,*Voids in the Cosmic Web as a probe of dark energy*. Condens. Matter Phys., 2017, vol. 20, No. 1, 13901

Spectral energy distribution of radiation from star-like sources in the expanding Universe at reionization epoch

A. Yang

International Center of Future Science, College of Physics, Jilin University, Changchun, China

The study of radiation's spectral energy distribution in our galaxy Milky Way and other galaxies is a significant problem of current astrophysics. Knowledge of this distribution makes it possible to estimate interstellar gas and dust's ionization and thermal states, luminescence, line absorption, and electromagnetic radiation ranges. I study the mean spectral energy density of radiation from thermal sources with varying temperatures in the early Universe when the first stars and galaxies appeared in Cosmic Dawn and Reionization epochs. The cosmological redshift and equation of propagation of signals in the expanding Universe are taken into account. The computations illustrate how integrated redshifted radiation of far sources affects radiation's averaged spectral energy distribution at any point in the inter-galaxy medium. We assume that hydrogen is completely reionized at redshift z=6. We have estimated the number density of star-like sources with a given effective temperature. We also obtained the graphical dependence of the product of the effective number density of sources and their squared effective radius and ratio of fractions of neutral to ionized hydrogen atoms in the inter-galaxy medium with given temperature on the effective temperature, and contrary, the dependence of the same production on the temperature of medium for sources with given temperatures. It provides a possibility to estimate the number density of sources with any set of effective radius and temperature, which is necessary to ionize the medium at z=6 with some value of hydrogen ionized fraction. All computations are done in the framework of Einstein - de Sitter and Lemaitre cosmological models with concordance parameters.

Radioactive elements in stellar atmospheres. Promethim

V. Yushchenko[2,1], V. Gopka[1], A. Shavrina[2], Ja. Pavlenko[2], A. Shereta[1], A. Yushchenko[3]

[1]Astronomical Observatory, Odessa National University, Odessa, Ukraine
[2]Main Astronomical Observatory of National Academy of Science of Ukraine, Kyiv, Ukraine
[3]Astrocamp Contents Research Institute, Goyang, Republic of Korea

All known 34 promethium isotopes are radioactive with short half-life times. The longest half-life is 17.3 years for 145 Pm. The studies of the absorption lines of promethium in the spectra of certain stars showed that the detection of promethium lines in the spectra is possible for late type stars and for magnetic peculiar stars. The detection of promethium in late type stars that have undergone a certain evolutionary path has been explained. We identified promethium lines in several spectra of Magellanic Clouds supergiants and calculated the abundances of this unstable element.

Gravitational microlensing of ring-like sources

V.I. Zhdanov

Taras Shevchenko National University of Kyiv, Kyiv, Ukraine

Ring-like structures may appear in some images of accretion disks around relativistic compact objects, which represent a possible alternative to conventional black holes. We present a qualitative treatment of photometric microlensing effects in case of such structures. Amplification curves are constructed for simple models of a thin accretion disk which is the source in the gravitational lens system. Two models of a source consisting of two unconnected regions are considered: (i) a circular area in the center and a ring, (ii) two rings with comparable integral brightness. We use the linear caustic approximation. The simulation was carried out for a number of radii and thicknesses of the ring, observed in full face. The graphs show amplification curves giving the increase of the microlensed radiation flux

when the caustic moves in the direction of its "tail" (the region, where there is an amplification). In the presence of ring regions, characteristic features of the light curves appear, which can serve as an indication of the possible existence of these regions.

Quasi-normal modes from naked singularities with non-linear scalar fields

O.S. Stashko[1], O.V. Savchuk[2], V.I. Zhdanov[3],

[1] Goethe Universitat, Frankfurt am Main, Germany
[2] Facility for Rare Isotope Beams, Michigan State University, East Lansing, USA
[3] Taras Shevchenko National University of Kyiv, Kyiv, Ukraine

We study the quasi-normal modes (QNM) of linear perturbations against a static spherically symmetric background in General Relativity having a non-linear scalar field (SF) that has a power-law self-interaction potential. The background metric describes a static spherically symmetric isolated configuration with a naked singularity at the center. We investigate axial perturbations of this system in the Regge-Wheeler gauge and reduce the problem to wave equations with positive potentials that demonstrate stability with respect to this type of perturbation. By solving these equations numerically, we identified the fundamental QNM frequencies for various sets of background solution parameters. Our analysis shows significant differences when compared to the cases of the Schwarzschild background and the Fisher-Janis-Newman-Winicour solution for the massless linear SF.

Naked singularities in spherically symmetric configurations in the quadratic f(R) gravity

V.I. Zhdanov[1], Yu.V. Shtanov[1,2], O.S. Stashko[3]

[1] Taras Shevchenko National University of Kyiv, Kyiv, Ukraine
[2] Bogolyubov Institute for Theoretical Physics, Kyiv, Ukraine
[3] Goethe Universitat, Frankfurt am Main, Germany

We study isolated compact configurations in the quadratic f(R) gravity with the scalaron mass corresponding to astrophysically small lengths scale L, which has been proposed earlier to explain the origin of the dark matter. The equations of the f(R) gravity are reduced, using the conformal transformation, to usual Einstein equations with scalar field (SF). In case of a static spherically symmetric configuration with a non-trivial SF, there is a naked singularity at the center. We obtain an approximate and numerical solutions including the region of strong gravitational and scalar field near the singularity to look for effects that can be used to deny or confirm the existence of such a structure. In case of small L, we show that the space-time metric is practically unaffected by SF outside the Schwarzschild sphere. However, the singularity drastically changes the space-time properties in the interior region that is permeable to the external signals moving to the singularity.

АСТРОМЕТРІЯ І МАЛІ ТІЛА СОНЯЧНОЇ СИСТЕМИ

ASTROMETRY AND SMALL BODIES OF THE SOLAR SYSTEM

Phase-angle dependence of polarization for the Galilean satellites of Jupiter: Io, Europa, and Ganymede

V. Rosenbush[1,2], N. Kiselev[3], K. Muinonen[4], L. Kolokolova[5], A. Savushkin[3], N. Karpov[6]

[1]Astronomical Observatory of Taras Shevchenko National University of Kyiv, Kyiv, Ukraine
[2]Main Astronomical Observatory of the National Academy of Sciences of Ukraine, Kyiv, Ukraine
[3]Crimean Astrophysical Observatory, Nauchny, Crimea
[4]University of Helsinki, Helsinki, Finland
[5]University of Maryland, USA
[6]ICAMER, Peak Terskol Observatory, Ukraine

Polarimetry is a powerful technique to study the surfaces of Solar System objects, especially at small phase angles where the so-called negative polarization branch (NPB) is observed. The NPB can have different shape and polarization degree for different composition of the surfaces. It has a parabolic shape for rocky surfaces with a minimum of around 10° and an inversion point (the angle where the polarization changes from negative to positive) of around 20°. However, for icy surfaces (satellites of outer planets, cometary nuclei, and Trans-Neptunian objects), the NPB becomes very asymmetric, and its minimum shifts to smaller phase angles. The cause of this has been attributed to the Coherent Backscattering Mechanism (CBM), which is known to be very sensitive to the size of particles and porosity of the medium.

During 2018–2023, we have been able to make extensive observations and accurately determine the NPB for Jovian satellites Io, Europa, and Ganymede (Fig. 1). The NPBs for Europa and Ganymede are very similar (despite the difference in their geometric albedo, 0.67 for Europa and 0.44 for Ganymede). Unlike Ganymede and Europa, Io has a more extended, although still asymmetric, NPB, despite a similarity of Io's albedo (0.63) to Europa's albedo. Their NPB is evidently formed by CBM. To find the properties of the regolith particles, we accomplished computer modeling of the polarimetric curves using the radiative-transfer coherent-backscattering (RT-CB) method (e.g., Muinonen et al. 2015). The best fit for Europa, shown in (Kiselev et al. 2022), was achieved for a regolith layer of single-scattering

albedo ~0.985 and extinction mean-free-path-length ~16 microns. We will also present the results for Io and Ganymede.

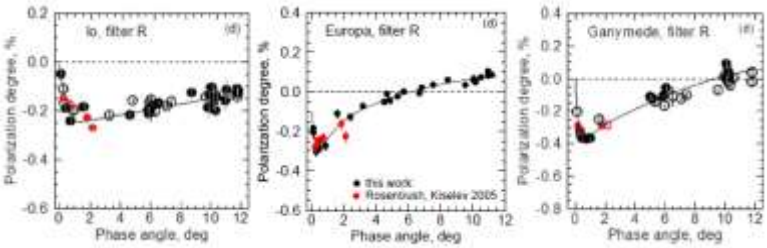

Fig. 1. Comparison of the NPB for Io, Europa, and Ganymede.

References

Muinonen K., Penttilä A., Videen. G. 2015. *Multiple scattering of light in particulate planetary media.* In: *Polarimetry of Stars and Planetary Systems*. (Eds. L. Kolokolova, J. Hough, A-Ch. Levasseur-Regourd), Cambridge University Press, Cambridge, 117–129.

Kiselev N., Rosenbush V., Muinonen K., Kolokolova L., Savushkin A., Karpov N. 2022. New polarimetric data for the Galilean satellites: Europa observations and modeling. PSJ 3, 134 (13pp).

Quasi-simultaneous photometric, polarimetric, and spectral observations of centaur 174P/Echeclus

O. Ivanova[1,2,3], J. Markkanen[4,5] and I. Luk'yanyk[3]

[1]Astronomical Institute of the Slovak Academy of Sciences, Tatranská Lomnica, Slovak Republic
[2]Main Astronomical Observatory of National Academy of Sciences of Ukraine, Kyiv, Ukraine
[3]Astronomical Observatory of Taras Shevchenko National University, Kyiv, Ukraine
[4]Institut für Geophysik und Extraterrestrische Physik, Braunschweig, Germany
[5]Max Planck Institute for Solar System Research, Göttingen, Germany

Centaurs are small body in the Solar system that represent transitional objects from the population of Kuiper belt objects. Many of these objects are scattered inward on unstable orbits, with dynamical lifetimes of around 10^6–10^7 years. Some become Jupiter family comets (JFCs), and over 13 percent of them exhibit comet-like activity. Therefore, studying active centaurs is important for better understanding the origin of JFCs. The outbursts of active centaurs are often unpredictable and not necessarily correlated with the Centaur's perihelion distance.

One well-known example is 174P/Echeclus, which experienced four major outbursts in 2005, 2011, 2016, and 2017, as well as one detected in Spacewatch images taken in January 2000. Its period is 35.06 years, and its heliocentric distance varies from 5.81 to 15.61 AU. In this study, we present new results of linear polarization measurements for Echeclus during its non-active period. Obtained linear polarization measurements for this object at phase angles near 3 degrees. We supplemented our polarimetric research by analysis spectral and photometric observation the centaur in active period in 2016 and 2017. Using our photometric and polarimetric observations of this centaur, we attempted to model the physical characteristics of its dust environment.

Photometric investigation of (493) Griseldis and (6478) Gault in their last apparitions

M. Husárik[1], O. Ivanova[1, 2, 3]

[1]Astronomical Institute of the Slovak Academy of Sciences, Tatranská Lomnica, Slovak Republic
[2]Main Astronomical Observatory of the National Academy of Sciences of Ukraine, Kyiv, Ukraine
[3]Taras Shevchenko National University of Kyiv, Astronomical Observatory, Kyiv, Ukraine

In this presentation, we show some photometric results for two candidates known as active asteroids. We have been studying and observing this type of interesting solar system objects at the Skalnaté Pleso Observatory for a long time interval.

The first object is (493) Griseldis. It was observed to have an activity or a broad tail in March 2015. Archival images as well as new observations have shown that the asteroid shows no activity. The aim of our observations in 2019 and 2020 was to spot possible activity, but also to determine the rotation period, the amplitude of the changes, or to try to define the coordinates of the rotation pole.

The second object is the well-known (6478) Gault, for which activity has been observed in multiple apparitions. No activity has been shown in 2020 and also now, in 2023. Observations of Gault are still ongoing in 2023, but it appears that the effective diameter and absolute magnitude are slightly different from the values in 2020.

The observations of both active asteroids were carried out with the 0.61-m *f*/4.3 Newton reflector at the Skalnaté Pleso Observatory (Slovakia, IAU code 056) and CCD camera SBIG ST-10XME and with the 1.3-m *f*/8.1 Cassegrain-Nasmyth reflector at the Skalnaté Pleso Observatory also and CCD camera FLI Proline 230. We obtained photometric data using broad-band Johnson-Cousins *B, V,* and *R* filters.

Activity of asteroid (248370) 2005 QN_{173}

O. Ivanova[1,2,3], J. Licandro[4,5], F. Moreno[6], I. Luk'yanyk[3], J. Markkanen[7,8], D. Tomko[2], M. Husárik[1], A. Cabrera-Lavers[9,4,5], M. Popescu[10,11], E. Shablovinskaya[12], O. Shubina[1,2]

[1]Astronomical Institute of the Slovak Academy of Sciences, Tatranská Lomnica, Slovak Republic
[2]Main Astronomical Observatory of National Academy of Sciences of Ukraine, Kyiv, Ukraine
[3]Astronomical Observatory of Taras Shevchenko National University, Kyiv, Ukraine
[4]Instituto de Astrofisica de Canarias, Research, La Laguna, Tenerife, Spain
[5]Departamento de Astrofísica, Universidad de La Laguna – ULL, Tenerife, Spain
[6]Instituto de Astrofísica de Andalucía, Granada, Spain
[7]Institut für Geophysik und Extraterrestrische Physik, Braunschweig, Germany
[8]Max Planck Institute for Solar System Research, Göttingen, Germany
[9]GRANTECAN, Cuesta de San José s/n, La Palma, Spain.
[10]Astronomical Institute of the Romanian Academy, Bucharest, Romania
[11]A Faculty of Physics, University of Bucharest, Ilfov, Romania
[12]Núcleo de Astronomá de la Facultad de Ingenierá, Universidad Diego Portales, Santiago, Chile

We present the results of observations of asteroid (248370) QN_{173} obtained during July 2021 – January 2022 with three telescopes. Our analysis revealed the presence of the dust tail for about half of a year. The direct images of the asteroid were obtained with broad-band filters. No emissions were revealed in the spectra, and the spectrum of the asteroid closely matched that of a C-type asteroid. Created color and linear polarization variations along the tail were analyzed. The asteroid demonstrated a redder color compared to the Sun. Dramatic changes in dust productivity obtained in different filters were not detected. The $g - r$ color changes from 0.2^m to 0.7^m over the coma, and the linear polarization degree varies from about 1.2% to 0.2% and from −0.2% to −1.5% at the phase angle of 23.2° and 8.16°. The total dust mass ejected until the latest observation on October 10 is 4.2×10^7

kg, with a maximum rate of 2.6 kg s−1 based on the Monte Carlo modeling of the dust tail. The estimated asteroid size is 1.3 km. It is shown that large particles are concentrated around the nucleus, whereas smaller ones dominate in the tail. The evolution of (248370) QN_{173} orbit and the orbits of the sample of the 464 short-periodic comets were followed. Ten of them approached the asteroid's orbit. These objects are not genetically related, despite the very close distance of their orbits for a relatively long time.

Rotation parameters of the nucleus of comet C/2013X1 (PanSTARRS) according to the morphological analysis of the coma

V. Kleshchonok[1,2], O. Ivanova[1,3,4], O. Shubina[3,4]

[1]Astronomical Observatory of Taras Shevchenko National University, Kyiv, Ukraine
[2]Max Planck Institute for Solar System Research, Göttingen, Germany
[3]Astronomical Institute of Slovak Academy of Sciences, Tatranská Lomnica, Slovak Republic
[4]Main Astronomical Observatory of National Academy of Sciences of Ukraine, Kyiv, Ukraine

The non-periodic comet C/2013X1 (PanSTARRS) was observed from December 6, 2015 to January 8, 2016 using 61cm (f/4.2) automated Newtonian telescope of the Astronomical Observatory at Skalnate Pleso (Slovakia). The comet had a sharply asymmetric shape. For some observation dates, the comet's tail began away from the optocenter of the coma. This indicates a strong jet activity of the comet's nucleus. The images of the comet were processed using a rotational gradient for morphological studies of the structures in the coma. The simple geometric model was used to interpret digitally processed images. As a result, the existing structures and their evolution were explained by the presence of two active regions on the nucleus, which form two jets. One jet (J1) is formed by the near-polar active region of the nucleus at a latitude of +85±5°, and the other (J2) is formed by an active region at a latitude of +40±5°. The shape of the J2 jet indicated a particle velocity of 0.44±0.07 km/s. The north pole of the nucleus rotation axis has the following coordinates: right ascension 260±6° and declination +40±4°. The nucleus rotation period was 24.02±0.02h. The article by Manzini et al, 2016 (Planet. Space Sci., 129, 108) reported a similar right ascension of 240°±10° for the north pole of the rotation axis of this comet.

They also estimated a rotation period of 0.498±0.015 days for the nucleus from photometric data. This value is exactly half the period according to our data. We discuss how photometric analysis can sometimes yield a rotation period that is half of the actual value.

Activity of Comet 29P/Schwassmann-Wachmann 1 in November 2020

A.Voitko[1], Ya. Ryzhko[2], O. Ivanova[1,3,4], M. Husárik[1]

[1]Astronomical Institute of the Slovak Academy of Sciences, Tatranská Lomnica, Slovak Republic
[2]Anatoliy Lygun Scientifical Lyceum, Kamianske, Ukraine
[3]Main Astronomical Observatory of National Academy of Sciences, Kyiv, Ukraine
[4]Astronomical Observatory, Taras Shevchenko National University of Kyiv, Kyiv, Ukraine

Our research is aimed at studying the properties of cometary dust through variations of its color. The activity of distant comets at heliocentric distances larger than 3 au has different nature. So far from the Sun activity of comets is driven by sublimation of more volatile species than water or crystallization of water ice. Moreover, cometary spectra in visible part are mostly free of gaseous emissions at such distances.

Comet 29P/Schwassmann-Wachmann 1 is famous for its activity outbursts and continuous activity beyond Jupiter's orbit. Also, this comet was the first one for which dust color variations were reported. During the previous study of the comet, it was obtained that activity outburst provoked a change in the chemical composition of dust particles from mostly Fe-Mg silicate and organic to mostly water-ice and Mg-rich.

Here we present results obtained from photometric observations of 29P/Schwassmann-Wachmann 1 taken using the 0.61-m Newtonian telescope of Skalnaté Pleso observatory (AI SAS) on November 18-26, 2020, when the comet possessed the activity outburst. From our observations, we have obtained absolute magnitude, photometric dust color, and the Afρ parameter as the measure of dust productivity. We have found the blue V-R color of the comet during the outburst maximum. We have also analyzed the coma morphology. During the outburst on November 21, two jets were formed, later it was visible how they evolved and widened.

Simulation the coma of comet 67P with the rotation of the nuclear

V. Reshetnyk[1,2], R. Marschall[3], O. Ivanova[2,4]

[1] Taras Shevchenko National University of Kyiv, Ukraine
[2] Main astronomical Observatory of National Academy of Sciences of Ukraine
[3] Observatoire de la Côte d'Azur in Nice, France
[4] Astronomical Institute of Slovak Academy of Science

A characteristic feature of comets is a coma. A coma is formed during the sublimation of the iced nuclear and dragging of dust particles. The sizes of cometary nuclei are much smaller than the gas-dust coma. The studies of comets with the spacecraft in-situ help us to establish the geometric and physical parameters of cometary nuclei. The most part of the background observations do not allow obtaining such a spatial resolution. The most detailed studies of the comet 67P/Churyumov-Gerasimenko were carried out by the Rosetta spacecraft. It was revealed the shape of the nucleus and the direction of the axis of rotation. This investigation helps to build more realistic models of sublimation of the iced components and acceleration of dust particles. We developed a model of dust coma formation taking into account the shape of the nuclear. An important improvement of our model was the consideration of the rotation of the nucleus. The gas productivity in the model was taken to be proportional to the solar illumination at each point of the nucleus. But even such a simplified model showed the presence of jet-like structures in the coma which were smoothed out with rotation of the nuclear. The simulated coma shows large-scale quasi-constant structures. These structures are formed by the shape of the nucleus and the location of the axis of rotation.

The preliminary results of observations with the upgraded AZT-8 Telescope at Lisnyky observation station: focus on small solar system bodies

V. Karbovsky[1], M. Buromsky[2], M. Lashko[1], I. Kulyk[1]

[1]Main Astronomical Observatory of the National Academy of Sciences of Ukraine
[2] Astronomical Observatory of Taras Shevchenko National University of Kyiv

The AZT-8 Telescope (D=0.7 m, F=2.8 m) of the observation station at Lisnyky village was upgraded with the new CMOS camera Moravian C4-16000EC and external filter wheel with UBVRI filters of Johnson-Cousins photometric system. The CMOS detector has resolution 4096×4096 pixels with pixel size of 9×9 μm, which leads to almost 37×37 mm light sensitive area. The camera was located at a prime focus providing the pixel scale of 0.66 ″ per pixel and field of view of 45×45'. Such telescope mode is suitable to solve a number of scientific tasks covering different area of the modern astronomy and specifically the investigations of small solar system bodies. The latter includes the precise measurements of positions, photometric monitoring of cometary activity, observation of occultations and mutual eclipses, searching for new comets and asteroids, etc.

Several runs of observations have been conducted so far to test the camera parameters and clarify the observation and data processing methods. The star fields, comet C/2017 K2 (PanSTARRS) and comet C/2022 E3 ZTF were observed in UBVRI band passes. In this report we present some preliminary results of the processing of this first limited data sample.

Creation of an acoustic Interferometer for determining the spatial position of natural and man-made sound sources in the Earth's atmosphere

O. Shulga[1], M. Kalyuzhny[1], Yu. Protsyuk.[1], F. Bushuev[1], V. Khramtsov[1,2], M. Kulichenko[1], D. Motorkin[1]

[1] Research Institute "Mykolaiv Astronomical Observatory", Mykolaiv, Ukraine
[2]Institute of Astronomy Kharkiv National University, Kharkiv, Ukraine

The report presents a working model of an acoustic interferometer for automatic acoustic monitoring of the surrounding space. The acoustic interferometer can be used to determine the exact positions of natural and man-made events, which are accompanied by the simultaneous generation of acoustic pulse signals. Among natural events, special attention is given to infrasound acoustic signals from meteor phenomena in the atmosphere.

To ensure the creation of a full-fledged sound-metric hardware and software complex (SMC), the following was carried out:

- Modeling of the spatial placement of sound measuring devices (SMDs) with an estimate of the error in determining the spatial coordinates of sources of sound impulse events (SIEs) in a hemisphere with a radius of 100 km;
- Study of methods for increasing the sensitivity of the SMD, linking the SIE to a unified time scale, accurately determining the coordinates of the SMD;
- Development and production of electronic circuits and devices;
- Development of software for preliminary processing, filtration and analysis;
- Development of software for determining the spatial coordinates of the SIE;
- Development of software management system for monitoring and processing.

The SMC for determining of the spatial positions of the SIEs will be built according to an open cluster scheme, which can include sound-metric hardware and software stations (SMSs) spaced at a distance of up to 1000 m. Communication between the SMSs will be mobile or satellite Internet, or relay lines. A separate SMS has a cross-shaped scheme and consists of 5 SMDs at distances of up to 100 m from the center and at heights of up to 20 m. The SMD consists of: a microphone, an acoustic amplifier (acoustic horn),

a sound card, a GPS with a built-in antenna and a PPS (Pulse - Per -Second) signal, cable connection module to the control computer.

The current working SMS model has the SMDs placement at distances of 80 m from the center. It provides an accurate binding of SIEs to a unified time scale using PPS. The SMDs was linked to the WGS84 coordinate system using GPS RTK technology. Determination of rectangular XYZ SIE coordinates is performed by the method of multilateration based on measured TDOA (Time Difference of Arrival) values.

A database of frequency images of sound signals of various origins is also being created and researched. A technique for analyzing information on SMS using machine learning techniques is being developed. Signals from the SMDs are processed by the SMS computer in real time. Data from SMS are transferred to a central server for database filling, possible additional analysis and visualization of coordinate information in real time.

Influence of timers synchronization accuracy of video cameras onto the error of trajectory parameters calculation of meteors and other moving objects in the Earth's atmosphere

P. Kozak

Astronomical Observatory of Taras Shevchenko National University of Kyiv, Kyiv, Ukraine

In classical observations of meteors in the upper layers of the Earth's atmosphere - the range of 130-80 km - it is considered that the meteor moves along a straight trajectory. Since for most meteors, the time of their existence before complete evaporation does not exceed one second, so there is no gravitational distortion of the trajectory. This approach makes it possible to avoid high-precision time synchronization of observation video cameras - actual synchronization is not required in this case - and knowledge of the time corresponding to the moment of flight is used only for further calculation of the elements of the heliocentric orbit of a meteor, since this requires knowledge of the position of Earth on the orbit. Another advantage of this approach is the ability to study the meteor, even if the observation cameras record its movement in different parts of the trajectory, which may not overlap - for example, one camera sees the beginning of the meteor, and the other - the end of its trajectory.

However, in some cases this approach does not work. This applies to the arrivals of relatively large space bodies that can fall to the Earth's surface in the form of meteorites, and before that they decelerated quite significantly in the lower dense layers of the atmosphere, distorting their trajectory due to the influence of Earth's gravity. Another variant that is implemented, although it is quite rare [1], is a situation when the meteoroid flies along the base line that passes through both observation points. In this case, the error of calculating the radiant (and therefore other parameters) will go to infinity. As for flights of artificial formations in the Earth's atmosphere - both ballistic and controlled - obviously strict time synchronization is required.

Obviously, for real-time processing of observations of artificial controlled objects – where fast decision-making is required – the timers must be synchronized in advance. However, in some cases, when you can be satisfied with post-processing, the question arises whether it is possible to somehow correct the situation if there is a suspicion that there is a slight shift in the indicators of the camera timers. Such a problem arose during the processing of a unique bolide observed by amateurs of meteor astronomy over Kyiv in 2020 [1], when, due to relatively large calculation errors, a suspicion of inaccuracy of synchronization arose. For verification, numerical simulations of the direct problem were carried out for different meteor trajectories, different meteor velocities, camera placements, and a shift in time synchronization. It was shown that inaccurate synchronization leads to a meteor shift on the Earth's surface (shift in latitude and longitude) when calculating sequentially from different observation points (another point serves only to determine the distance to the meteor). A shift in heights was also observed. To solve this problem, a sequential variable shift of the time zero-point of one camera relative to another was proposed in order to minimize the displacement of geodetic coordinates and heights - this approach allows specifying the displacement in the synchronization of cameras and taking into account the systematic error in the calculations - however, for this it is important that the range of observed points of one of the cameras lay in a wider range of points of the other camera.

[1] Kozak P.M., Zlochevskyi Y.E., Kozak L.V., Stariy S.V. Problems of processing of videorecords of bright bolides and falling cosmic vehicle remnants detected with the low-sensitive home video cameras in bad observational conditions. – 27, 6. – 2021. – P. 84-97.

Thermal desorption of the dust particles matter near the Sun. Data analysis of meteor observations and their interpretation

O. Golubaev[1], A. Mozgova[2]

[1] Institute of Astronomy, V.N. Karazin KhNU, Kharkiv, Ukraine
[2]Astronomical Observatory of Taras Shevchenko KNU, Kyiv, Ukraine

The FIELDS instrument of the Parker Solar Probe spacecraft provided the first observations of interplanetary dust at a distance of less than 0.3 AU from the Sun. Parker Solar Probe found a sharp decrease in dust at the distances of less than 0.08 AU from the Sun.

The researches of meteors makes it possible to study the physical properties of the space near the Sun and to compare them with the results obtained by spacecrafts. For this purpose, we study the peculiarities of the Sun's influence on the physical and chemical properties of the meteoroids matter with perihelion distances less than 0.1 AU.

Using the methods of statistical analysis of the meteor observations database and model calculations, we checked the assumption that the decrease of the dust near the Sun is associated with their partial or full evaporation.

As a result of the analysis of terrestrial observations of meteors, the effect of sublimation of dust particles at the close distances from the Sun was found. The mass distribution of meteoroids reveals a relative decrease in the mass of dust particles near the Sun in the post-perihelion part of their orbits. The distribution of meteor particles by perihelion distances shows a sharp decrease in the number of observed meteor particles with $q < 0.08$ AU. This fact is consistent with the results of observations by Parker Solar Probe spacecraft. It was concluded that there is an area with a radius of 0.1 AU around the Sun where the significant evaporation of meteoroid matter occurs.

On the Twin Comets

Guliyev A.S, Guliyev R.A, Kasumov A.

Shamakhy Astrophysical Observatory, Baku, Azerbaijan

We have carried out the comparative analysis of the long-period comet orbits observed in different epochs. The purpose of this analysis is to identify the comet pairs and attempt to explain the similarity of their orbital elements. At the first stage we compare the orbital angular elements. If they are very similar, we compare perihelion distances. If there is also similarity, we compare the perihelion ages of each cometary pair. If they are similar and differ by only a few years, then we can talk about the origin of the pair by the decay of a common nucleus. Otherwise, there are other interpretations of the elements similarity, including the assumption that the pairs are different appearances of the same comets. There are pairs of extreme interest; (C/1968 N1 and C/1468 S1); (C/1907 G1 and C/1742 C1); (C/1914 J1 and C/1790 H1) (C/1863 Y1 and C/1810 Q1); (C/2019 Y4 and C/1844 Y1); (C/1994 T1 and C/1877 R1); (C/1898 U1 and C/1881 N1); (C/2016 R3 and C/1915 R1); (C/1846 O1 and C/1973 D1); (C/1988 A1 and C/2015 F3); (C/1932 Y1 and C/2020 M3).

Possible source and mechanism for the origin of the dwarf planets in the Kuiper belt

A. Kazantsev

Astronomical observatory Taras Shevchenko National University of Kyiv

It is proposed a mechanism that is different from the existing ones for the origin of the Kuiper belt (KB) bodies. The distributions of the orbits of the most of bodies of the “hot” component in the KB were analyzed. The shapes of the distributions indicate that all those bodies could have arisen as a result of the destruction of one massive body (the Kuiper belt planet, KBP).

The separation velocities of the fragments were determined mainly by the linear velocities of the parts of the KBP at different depths and latitudes. The

maximum separation velocity corresponded to the linear velocity on the surface of the KBP near the equator and could be 2.4 km/s

The size of the KBP could be slightly smaller or larger than the size of the Earth. The spin period could be about 4 hours. The spin axis of the KBP was tilted at a little angle to the ecliptic plane and at the moment of the destruction it was directed towards the Sun.

The performed model calculations of the KBP destruction show that the resulting distributions of the model fragment orbits in the coordinates of semimajor axis – eccentricity ($a - e$) and semimajor axis – inclination ($a - i$) almost completely correspond to the distributions of the real orbits of the KB bodies.

This mechanism agrees well with existing observational data. It can explain a noticeable number of bodies in the SD with satellites, as well as the existing dependence of the bulk density of the bodies on the size.

According to this mechanism, the spin axes of the fragments (primarily large ones) should be tilted at little angles to the ecliptic plane. The spin axes of the dwarf planets Pluto and Haumea are inclined to the ecliptic plane at angles of 23^o and 10^o respectively. If the proposed mechanism is correct, then the spin axes of other large bodies of the KB should also be inclined to the ecliptic plane at relatively little angles.

Astrometric observations of comets with new CCD camera at Kyiv Comet Station (MPC 585)

A. Baransky[1], D. Prowolowska[2]

[1]Astronomical Observatory of Taras Shevchenko National University of Kyiv, Kyiv, Ukraine
[2]National Technical University of Ukraine "Igor Sikorsky Kyiv Polytechnic Institute"

We present the results of astrometric observations of comets on AZT-8 with new Moravian-C4 16000 CCD camera, in Johnson-Cousins R, V and I filter at Kyiv Comet Station (Code MPC 585) of Taras Shevchenko National University of Kyiv. The 470 precise positions observations of 16 comets were obtained from Aug. 2022 to Mart 2023, among them 218 observations of 8 short periodic comets (*22P/Kopff, 29P/Schwassmann-Wachmann, 44P/Reinmuth, 61P/Shajn-Schaldach, 118P/Shoemaker-Levy, 408P/Novichonok-Gerke, P/2022 L3 (ZTF), P/2022 P2 (ZTF)*) and 252

observations of 7 long periodic comets (*C/2019 U5 (PANSTARRS), C/2020 K1 (PANSTARRS), C/2020 V2 (ZTF), C/2021 T4 (Lemmon), C/2021 Y1 (ATLAS), C/2022 A3 (Lemmon-ATLAS)*). All observations were published in Minor Planet Electronic Circulars and Minor Planet Circulars (pdf – format).

For astrometric measurements, the Astrometrica software was used with the Gaia DR2 and UCAC-4 star catalogues. The orbits of comets and (O–C) residuals – differences between the observed coordinates and the coordinates calculated from the bigger number of observations – for both RA and Dec were determined using the Find_Orb software, combining our own observations with data from the Minor Planet Center database. The (O–C) RA residual varies from −0.450 to 0 .959, ±σ″ RA – from 0.012 to 0.614. The (O–C) Dec residual varies from −0.309 to 0.905, ±σ″ Dec – from 0.080 to 0.642. The results of astrometric measurements showed that the images, obtained with the new CCD camera, despite the optical aberration in the form of a coma, are suitable for precise astrometry of comets.

Astrometry and photometry of the DART space mission object asteroid (65803) Didymos in Lisnyky

A. Kasianchuk[1], A. Baransky[2], S. Borysenko[3]

[1]Faculty of Physics Taras Shevchenko National University of Kyiv, Ukraine
[2]Astronomical Observatory of Taras Shevchenko National University of Kyiv, Ukraine
[3]Main Astronomical Observatory of the NAS of Ukraine, Kyiv, Ukraine

(65803) Didymos is a binary asteroid of spectral class S with a primary diameter of 0.78 km and a secondary diameter of 0.15 km. (65803) Didymos was the target of NASA's DART mission (2022), the Italian Space Agency's LICIA mission (2022), and is the target of the European Space Agency's upcoming Hera mission (2026).

In this work, we present the results of our observations (65803) Didymos on 16 and 1 Nowember 2022, when the object had a pronounced tail of particles after the DART impact on 26 September 2022. Our observations were obtained using a 0.7-meter (f/4) reflector AZT-8 and Moravian-C4 16000 CCD camera, in Johnson-Cousins V, R and I filters at the Lisnyky observatory station (Code MPC – 585). For measurements, the Astrometrica 4 software was used with the Gaia DR2 star catalog. During the two nights,

80 images were taken, of which 73 were used for astrometric measurements, 60 for photometric measurements.

For 2022 10 16.06 (UT) 24 astrometric observations were published in circular MPS 1816756; mean RA residual -0.270±0.299 dec -0.069±0.184. For 2022 11 01.02 (UT) 49 observations were published in MPS 1729252; mean RA residual -0.131±0.161 dec 0.023±0.180

The photometric part is to estimate the length of the visible tail formed after the impact with the DART. Results as of 2022 10 16: for V (2′10″±5″, PA 277,3±0,586°). Accordingly, for 2022 10 01: for V (2′12″±2″, PA 277,9±0,170°), R (4′14±2,5″, PA 277,3±0,164°), I (2′28″±6″, PA 276,6±0,690°). The values of the visible tail in km 2022 10 16: for V (10274±414 km). Accordingly, for 2022 10 01: for V (10359±161 km), R (20092±202 km), I (11668± 495 km).

OBSERVATIONAL ASTRONOMY

Discovery and period analysis of 7 new TESS variables

O. Pyshna[1] and D. Tvardovskyi[2]

[1]The British School of Brussels, Tervuren, Belgium
[2]Centennial Centre for Interdisciplinary Science, Department of Physics, Edmonton, Alberta, Canada

In this work we present the results of analysis of 7 eclipsing binaries: TIC 455732776, TIC 65106309, TIC 202601061, TIC 198555959, TIC 150783753, TIC 392536805 and TIC 207504663. Among them only TIC 150783753 and TIC 392536805 were previously known as variables and TIC 207504663 was known as X-ray source 1RXS J163228.4+585104. Moreover, none of them had the classification before. Thus, we report the discovery of variability of 5 stellar systems and classification of all 7 objects. Some of them have additional interesting effects such as long-term pulsations which were detected and described in this study. In addition, we calculated the period, initial epoch, plotted and analyzed O-C curves (for minima and maxima) for each stellar system.

For our study we used open-access data from TESS space telescope, provided by Mikulski Archive for Space Telescopes (MAST). We used photometric observations from sectors 14-22, 25, 26, 40, 41 and 47-59. For separating maxima and minima extrema and determining approximate period

we used a code called "splitter" developed by Dmytro Tvardovskyi. When the types of extrema were separated, we used MAVKA software for approximations of photometric data and recording the moments of minima and maxima. For symmetrical extrema we implied WSAP and Mikulashek methods of data approximation, and for asymmetric and general cases we used Polynomial approximation.

As the result of our study, we concluded that TIC 150783753 (period = 0.59055±0.00007 days) and TIC 65106309 (period = 10.9478±0.0005 days) are EW/W Ursae Majoris type eclipsing binaries. Interestingly, remaining stars, classified by us as EA/Algol type eclipsing binaries, have additional effects: TIC 392536805 (period = 8.40971±0.00004 days) have pulsating component in a system and it is also likely that TIC 202601061 (period = 0.66095 ±0.00001 days) and TIC 455732776 (period = 1.3850 ±0.00013 days) have this property as well. TIC 198555959 (period = 4.19185±0.00005 days) has pulsating component and elliptical orbit and TIC 207504663 (period = 0.588254±0.000003 days) has reflection effect and unperiodic flares. However, the shape of O-C diagrams of particular stars is quite unusual, which could lead to further investigation of their properties.

Period analysis of 3 eclipsing binary stars with TESS data

A. Dzygunenko[1], D. Tvardovskyi[2]

[1] Private institution of general secondary education “Lyceum «Kvinta Hromadska School” Gatne village, Fastiv district, Kyiv region, Ukraine
[2] Centennial Centre for Interdisciplinary Science, University of Alberta, Department of Physics, Edmonton, Alberta, Canada

We present our research based on the processing of photometric data from the TESS space telescope for three eclipsing binary systems: TIC 199716496, TIC 414764074 and TIC 435447013. Based on this data, we determined the types of these binary stars. Among them there are two unclassified variable stars and one with previous incorrect classification. We discovered variability of TIC 414764074 and TIC 435447013 and classified them as EW and EA types correspondingly. Classification of TIC 199716496 was corrected from EB to EA type. Moreover, we completed period analysis for each star. This type of analysis includes calculation the period and initial epoch, plotting and studying of O-C curves & periodograms.

The main part of our research was the calculation and plotting of O-C curves. The observations of each star were divided into separate minima and maxima using a Python program called "splitter" version 2.6. Then the separated data sets were processed using MAVKA software. MAVKA is the software used for calculation the moments of extrema and their magnitude with various methods. For minima, we used a symmetric polynomial approximation. Simple polynomial approximation was used for maxima. By analyzing the shape and behavior of the O-C curve, we can gain insight into the dynamics and evolution of binary star systems, and the processes that govern their behavior.

As the result of plotting O-C curves separately for minima and maxima, we were able to detect some effects. For example, based on the O-C of TIC 199716496 for maxima, we assume that one of its components has pulsations. In addition, on the light curve of TIC 199716496 we recorded irregular flares. For TIC 435447013 we noticed quite strong reflection effect. For TIC 199716496 the reflection effect is also present, however it is noticeably weaker. Finally, we plotted and analyzed periodograms for three binary systems.

We calculated periods, initial epochs and error of periods. For easier representation we unified the T0's (initial epoch) to make them as close to JD=2475000 as possible.

TIC 199716496: P = (1.045837±0.000002) days, T0 = 2457000.05538 JD
TIC 414764074: P = (2.5467±0.0006) days, T0 = 2456999.6716 JD
TIC 435447013: P = (0.8325±0.0001) days, T0 = 2457000.192 JD

Observations and study of GRB 221009A afterglow at the Kyiv comet station

O. Pyshna[1], A. Baransky[1]

[1]Astronomical Observatory of Taras Shevchenko National University of Kyiv, Kyiv, Ukraine

GRB 221009A — hyper-luminous, long-duration gamma-ray burst (GRB) detected by Neil Gehrels Swift Observatory on October 9, 2022 and classified as the brightest GRB ever detected. In this work, we are presenting the results of our observations and photometric analysis of GRB221009A at the Kyiv comet station, as a part of international GRANDMA network (Global Rapid Advanced Network Devoted to the Multi-messenger Addicts).

Additionally, our study includes estimation of physical parameters based on empirical correlations and best-fit approximation for a light curve.

We observed the optical afterglow of GRB 221009A on AZT-8 with Moravian-C4 16000 CCD camera, in Johnson-Cousins R and I filter. For photometry of our data, we used and investigated methods of transient object photometry in the following software: MaxIm DL, STDpipe (simple transient detection pipeline code) and Astrometrica, using Pan-STARRS1, Gaia DR2 and USNO-B1 catalogs. Our first observation was obtained on 2022-10-10: 1.223 days after the trigger of Gamma Ray Burst Monitor and the Large Area Telescope of the Fermi observatory. We continued observations for the next five days, overall, we obtained 371 images in R filter and 165 images in I filter with 30 s or 60 s exposure. In GRANDMA database we uploaded stacked images: 14 in R and 2 in I filters, with exposure from 300 s to 6660 s, for better object visibility. During this time, the brightness of GRB 221009A decreased from 18.31^{m} to 20.48^{m} in the R filter and from 18.14^{m} to 20.13^{m} in the I filter. The photometric error varies from 0.03^{m} to 0.46^{m} (R filter) and from 0.01^{m} to 0.98^{m} (I filter).

We estimated physical parameters of GRB 221009A based on empirical correlations for long-durational gamma-ray bursts, using peak energy value: E_p = 1060 keV, reported by GCN CIRCULAR 32668 and based on obtaining best fit parameters for the light curve approximations in X-ray and optical band using *afterglowpy* top-hat, gaussian core and smooth power law jet models. As the result, we estimated on-axis isotropic equivalent energy and isotropic bolometric peak luminosity to be: $E_0 \approx 10^{54}$ erg and $L_{\gamma,\,p,\,iso} \approx 3.97 \cdot 10^{53}$ erg/s, which place it among the most luminous gamma-ray bursts ever detected, and more probably makes GRB 221009A the most luminous GRB ever detected.

Periodogram analysis of the semiregular variable star RX Leporis

A. Dzygunenko[1], A. Baransky[2]

[1] Private institution of general secondary education “Lyceum «Kvinta Hromadska School” Gatne village, Fastiv district, Kyiv region, Ukraine
[2] Astronomical Observatory of Taras Shevchenko National University of Kyiv, Kyiv, Ukraine

In this work, we present the periodogram analysis of the semiregular variable star RX Leporis based on AAVSO database, photometry data

analysis from TESS space telescope and our own observations. The object of our research, RX Lep, is an oxygen-rich semiregular pulsating variable star of the SRB type, spectral class M6III, in the early phase of the asymptotic giant branch.

In the first part of the work, we performed a Periodogram analysis from the data of the AAVSO database. In total, we analyzed 75 years of observations of RX Lep from the AAVSO database using the VStar program. Utilizing the Fourier series method, we managed to find different periods of RX Lep oscillations.

In past studies of RX Lep shorter period was previously determined. A period of 79.54 days is specified in the AAVSO database, and two additional periods of 90.1 and 101.7 days are mentioned in the article "Long-term photometry and periods for 261 nearby pulsating M giants". However, based on periodogram analysis, we found that there is one common period that can vary from ~80 to 100 days. Moreover, according to processing and analysis data from the AAVSO database, we detected a longer period that was unknown in earlier studies. We also determined that this period varies from ~500 to 780 days. In addition, we constructed phase curves and calculated an error for each of the periods.

In the second part of the study, we analyzed the photometric data of RX Lep from the observations of the TESS space observatory. Using the Makulsky archive for space telescopes, we downloaded data from sectors 5 and 32. Due to the fact that TESS has quite accurate data, we discovered chaotic pulsations with a small amplitude. In addition, we found periodic flashes with a period of 3 days based on the photometric data of the TESS telescope.

Additionally, RX Lep observations were made on December 27, 2022. Aperture photometry was performed using the Maxim DL program. MaxIm DL is a software designed for astronomical image processing and data analysis. According to the results of aperture photometry, it was found that the brightness of RX Lep change from 5.5 to 5.8 magnitude in 8 minutes of observation.

ФІЗИКА СОНЦЯ ТА СОНЯЧНА АКТИВНІСТЬ

SOLAR PHYSICS AND SOLAR ACTIVITY

The north-south asymmetry of solar activity during cycles 23–24

O.A. Baran[1], A.I. Prysiazhnyi[1]

[1]Astronomical Observatory of Ivan Franko National University of Lviv

We monitored the occurrence of ARs of different magnetic complexity and flares associated with them during the solar cycles 23–24. The basis of the study of their latitudinal distribution was the SolarMonitor data, supplemented by the information about solar flares obtained with the XRS instrument of the GOES satellite.

The asymmetric character of the ARs latitudinal distribution was more noticeable during the descending phase of solar activity: at the end of cycle 23 more ARs and flares occurred in the southern hemisphere, and at the end of cycle 24 they prevailed in the northern hemisphere.

We studied cyclic changes in the total values of the ARs area and peak soft X-ray flux from flares separately in the two solar hemispheres. For both cycles, the maximum values of these parameters were observed earlier in the northern hemisphere than in the southern hemisphere.

The general behaviour in the north-south asymmetry of solar activity was changed during the transition from cycle 23 to cycle 24. In cycle 23, the northern hemisphere was more active at the beginning of the ascending phase whereas the southern hemisphere was more active in the maximum and descending phases. In cycle 24, the northern hemisphere activity dominated throughout.

Forecast of the amplitude of the 25th cycle of solar activity based on a comparison of the rates of changes in the number of sunspots during the growth and decline phases of the cycles

V.M. Efimenko[1], V.G. Lozitsky[1]

[1]Astronomical Observatory of the Taras Shevchenko National University of Kyiv, Ukraine

We propose a prediction of the amplitude of the 25th cycle of solar activity based on the analysis of data on 24 previous solar cycles, which relate to the statistical relationship between the rate of changes in the sunspot

numbers in the phases of the growth and decline phases of 11-years cycles versus the amplitudes of the cycles. It turned out that the forecasting result depends on several initial assumptions, in particular, which section of the growth curve is taken into account for forecasting, as well as whether all 24 cycles are considered, or only the odd ones. The assumption of a monotonic or non-monotonic growth curve also plays an important role. Regarding the latter, the cluster analysis showed that until the 35th month of the cycle, there are no visible signs of non-monotonicity of the growth curve, similar to the one that was in the 24th cycle. We conclude that the maximum smoothed number of sunspots in the 25th cycle Wmax (25), most likely, should be equal to 152 units in the new system, This estimation well agrees with other forecast which based on correlation between the rate of changes of sunspot number in the decline phase of a given cycle versus the amplitude of the next cycle. From this correlation it follows that the probable amplitude of the 25th cycle is expected on level of 148 units. From these two very close estimations we have middle value Wmax (25) = 150 units, which corresponds to the average power of the solar cycle, with good implementation of the Hnievyshev-Ohl rule. With such parameters of this cycle, there are no signs of approaching the deep minimum of the age cycle in the middle 21st century. This does not exclude the fact that this deep age minimum can occur suddenly and sharply immediately after the 25th cycle, as was the case, for example, in the Dalton minimum. A possible sign of the upcoming age cycle may be the abnormally long decline phase of the current 25th cycle, about 10 years, as it was in the 4th cycle.

It is interesting to note that the point for the 20th cycle deviates essentially from the correlation dependence "average rate of activity decline in the current cycle versus amplitude of the next cycle" indicated above. If it fell perfectly on this dependence, then the 20th cycle would be the strongest in the age cycle. But this would violate one of the signs of the 44-year cycle found by the authors in: Adv. in Space Research, 2018, 61, Iss. 11, 2820-2826 (https://doi.org/10.1016/j.asr.2018.03.012). From this we can conclude that the 44-year cycle (Hale's double cycle) is a more fundamental regularity than the above-mentioned correlation dependence.

Evidence of strong magnetic fields in the active prominence on July 24, 1999 observed at 07:00:10 UT

M.A. Gromov[1], I.I. Yakovkin[2], V.G. Lozitsky[2]

[1]Faculty of Physics of the Taras Shevchenko National University of Kyiv, Ukraine
[2]Astronomical Observatory of the Taras Shevchenko National University of Kyiv, Ukraine

The active prominence on July 24, 1999 was already studied by the two authors of this report in a paper published in Advances in Space Research, 2022. Vol. 69, Iss. 12, P. 4408-4418 (DOI: https://doi.org/10.1016/j.asr.2022.04.012). In the mentioned paper, the 6:49 UT moment was considered. It was shown that at the indicated moment the $I \pm V$ and V profiles of the H-alpha line does not reveal clear signs of the presence of particularly strong magnetic fields of the 10^4 G level. Since observational data were also obtained for this prominence at a later time, 07:00:10 UT, here we examined these observational data to test the above conclusion. The observation material for our work was obtained on the Echelle spectrograph of the horizontal solar telescope of the Astronomical Observatory of Taras Shevchenko Kyiv National University.

The prominence spectrum at 07:00:10 UT was slightly different from that at 6:49 UT. At this later time, the H-alpha line was stratified, it contained both a narrow component at a height of 11-13 Mm, and a wide and asymmetric component at a height of 15-20 Mm (Fig. 1).

Fig. 1. General appearance of the H-alpha line in the studied spectrogram in two polarizations corresponding to combinations of Stokes parameters I+V and I-V.

The spectrogram under study was scanned using the Epson Perfection V 550 scanner. The blackening was converted into intensity taking into account the characteristic curve of the photomaterial of the spectrogram and the nonlinearity of the scanner itself. To measure the Zeeman splittings, the $I + V$ and $I - V$ spectra were "tied" by wavelengths using telluric lines.

It was found that the bisectors of the $I \pm V$ profiles are non-parallel to each other in those places of the prominence that correspond to broad emission in the H-alpha line (Fig. 2). This indicates the inhomogeneity of the magnetic field: with a uniform magnetic field, the bisectors should be parallel. Moreover, the maximum splitting of bisectors is observed not only in the core of the line (which was noted earlier by other authors), but also in the far wings, at distances from the center of the line in the range of 1.5-2.0 angstroms.

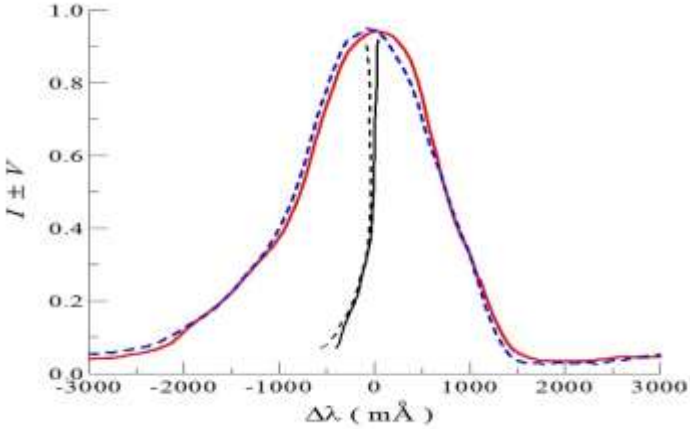

Fig. 2. $I \pm V$ profiles of the H-alpha line in the prominence, which correspond to a height of 15 Mm. It can be seen that the splitting of the bisectors is maximal not only in the core of the line, but also in its far wings. The latter may indicate particularly strong magnetic fields with an intensity of almost 10^5 G.

The specified maximum splitting of the bisectors corresponds to stresses of about 3000 G, but this value should be considered only as a lower estimate of the local magnetic fields. In particular, the second maximum of bisector splitting may indicate that the actual value of Zeeman splitting in small-scale structures with a small filling factor reaches the above value of 1.5-2.0 A. This corresponds to the field value of almost 100 kG, that is, close to those

found in the above-cited article. The results of the conducted research are another argument in favor of the reality of such extremely strong fields and indicate that the phenomenon of such fields may not actually be a rare phenomenon, but a rather common one, which, however, can be recorded only under certain favorable observational conditions.

Analysis of the array of discovered exoplanets on the subject of the possibility of the existence of earth-type life

A.O. Ivanov[1], V.O. Ponomarenko[2]

[1]Zhytomyr Ivan Franko State University, Zhytomyr, Ukraine
[2]Taras Shevchenko National University of Kyiv, Kyiv, Ukraine

The analysis of the necessary basic conditions for the origin and development of terrestrial life on exoplanets was presented. Based on information from the open database https://exoplanet.eu, with the help of specially developed software in the Python programming language, the selection from all confirmed exoplanets, as well as from all candidates for exoplanets was made. In the research, the influence of parameters of the exoplanet and external factors on the evolution of exoplanet were analyzed, that is parameters of the star: spectral class of central star and its metallicity; parameters of the exoplanet: temperature of surface, mass, radius and its density; and also orbital parameters of the exoplanet: semi-major axes and its eccentricity. According to our ideas, fulfillment of all these restrictions makes possible the origin of terrestrial life on an exoplanet.

Using the program in Python language, we sifted out unsuitable exoplanets and got the most curious candidates where Earth-like life is possible. These exoplanets deserve more detailed study using, for example, modern telescopes (JWST and others) to analyze their atmosphere.

Wave motions in the solar facular region: observations and simulations

R.I. Kostik

Main Astronomical Observatory, National Academy of Sciences, Kyiv

The results of spectropolarimetric and filter observations of the facular region in the lines Fe I 1564.3, Fe I 1565.8 nm, Ba II 455.4 nm, and Ca II H 396.8 nm obtained near the center of the solar disk at the German Vacuum Tower Telescope (Tenerife, Spain) are discussed. It is shown that the facular contrast at the center of the Ca II H line increases more slowly as the magnetic field strength increases and, then it begins to decrease if the field increases further. It is concluded that the reason for such behavior is the nonlinear height dependence of the line source function due to the deviation from the local thermodynamic equilibrium. It is found that waves propagating both upward and downward can be observed in any area of the facula, regardless of its brightness. In bright areas with a strong magnetic field, upward waves predominate, while downward waves are more often observed in less bright areas with a weak field. It is shown that the facular contrast measured at the center of the Ca II H line correlates with the power of wave velocity oscillations. In bright areas, it increases with the power regardless of the direction in which the waves propagate. In facular regions with decreased brightness, the opposite dependence is observed for both types of waves. In turn, the power of wave velocity oscillations is sensitive to the field strength magnitude. In the magnetic elements of the facula with increased brightness, the stronger the field, the higher the power of oscillations of both upward and downward waves. In areas with decreased brightness, the inverse dependence is observed. It is concluded that the contrast increase with the increase in the power of wave velocity oscillations observed in bright areas of the facula can be considered as evidence that these areas look bright not only because of the Wilson depression but also because of the heating of the solar plasma by the waves. The results of observations are compared with the 3d-dynamical model of the atmosphere of the Sun.

Magneto-active longitudes in the Sun and stars

V.N. Krivodubskij

Astronomical Observatory of Taras Shevchenko National University of Kyiv, Kyiv, Ukraine

An overview of studies of long-term increased magnetic activity in selected longitudinal sectors, which are observed on the Sun and on the surface of certain types of stars, is made. Today, as a result of statistical analysis of data observed for more than a century, it has been established that there are two active longitudinal sectors on the solar surface, shifted by approximately 180° relative to each other, which can stably maintain the phase coherence of activity for a long time. At each given moment of time, one of the two longitude intervals is more active (dominant) one.

Research of selected active longitudes on the surface of stars began at the end of the 80s of the last century. Active sectors of the stars are revealed on the basis of studying the spottedness of the stellar surface. Star spots are colder than the surrounding photosphere (by 100 1500 K). The temperature difference between the spotted areas and the photosphere leads to a change in the apparent brightness of the star during its rotation. Therefore, the spotting of stars is determined by photometric measurements (based on the Doppler effect), as a rotational modulation of their brightness. Star spots are significantly larger in size than spots on the Sun and have magnetic fields with an induction value of 3 to 5 kG.

The observed "flip-flop" phenomenon is highlighted, the essence of which is a sudden rapid switching of the increased level of activity between two longitude sectors on opposite sides of the star. The detected phenomenon is regularly repeated, which indicates the existence of stellar magnetic flip-flop cycles. At the same time, solar-type cycles are also characteristic of young analogues of the Sun. On the other hand, based on the evolution of the spot area, a magnetic flip-flop cycle with a duration of about 3.7 years was also detected on the Sun. It is relevant that the ratio of the periods of both types of cycles for young dwarfs and the Sun is the same: the flip-flop cycle is approximately 3-4 times shorter than the cycle of the solar type. Therefore, it is believed that the dynamo mechanisms of excitation of magnetism and the phenomenon of flip flop cycles on the Sun and in these stars are similar. This makes it possible to compare the results of a detailed study of the evolution

and reconstruction of magnetism on the Sun with the phenomena of stellar magnetic activity.

Mechanisms of excitation of magnetoactive longitudes proposed by the researchers were analyzed. Dynamo-excitation models of axially asymmetric magnetic harmonics look promising. Our calculations showed that the $\alpha\Omega$-dynamo models with the involvement of helioseismological data on the internal rotation of the Sun ensure the coexistence of dipole and quadrupole harmonics of the global magnetic field, which are necessary for the reproduction of selected longitudinal sectors of increased magnetic activity.

Theoretical and observed signs of excitation of small-scale magnetic fluctuations in the depth of the Sun

V.N. Krivodubskij[1], N.M. Kondrashova[2]

[1]Astronomical Observatory, Taras Shevchenko National University of Kyiv, Kyiv, Ukraine
[2]Main Astronomical Observatory, National Academy of Sciences of Ukraine, Kyiv, Ukraine

An actual problem today is the search for observed evidence of the existence of deep small-scale magnetic fields of the Sun. In this regard, we analyzed the proposed by the authors [Brandenburg A. at al.Current status of turbulent dynamo theory. From large-scale to small-scale dynamos// Space Sci. Rev. 2012. V.169. P.123-159] a theoretical criterion for separating the contributions to the solar surface magnetism of two qualitatively different mechanisms of a small-scale dynamo, the action of which is hidden in the depths of the solar convection zone (SCZ).The first mechanism ensures the generation of small-scale magnetic fields due to the interaction of turbulent motions with the mean magnetic field (small-scale dynamo 1 of macroscopic MHD), while the second mechanism causes self-excitation of magnetic fluctuations due to turbulent pulsations of highly conductive plasma (small-scale dynamo 2 of classical MHD).

The essence of the proposed criterion is that deep small-scale magnetic fields under certain conditions can lead to violations of Hale's and Joy's laws of observed magnetism on the surface of the Sun. Statistical analysis of these disturbances allows us to identify the differences in the evolution of the observed manifestations of two sources of small-scale fields, since the contribution of two deep dynamo mechanisms to surface magnetism varies

with the phase of the solar cycle in different ways. Such an important feature is the behavior of the percentage of anti-Hail groups of sunspots (in relation to the total number of sunspots) during the cycles. In the case of small-scale dynamo 1, the percentage of anti-Hale groups is independent of cycle phase, whereas the percentage of anti-Hale groups associated with small-scale dynamo 2 should reach its maximum value at solar minima. Therefore, the variations of magnetic anomalies make it possible to separate the tiny contributions of two small-scale dynamo mechanisms to surface magnetism. In this connection, the task of identifying the harbingers of a small-scale dynamo in the solar depths from observations is gaining relevance.

With this in mind, we conducted an analysis of literature data of statistical studies of long series of observed violations of Hale's and Joy's laws, which can be caused by the presence of deep small-scale magnetic fluctuations of various origins. In particular, in the work [Sokoloff D. et al.Solar small-scale dynamo and polarity of sunspot groups// MNRAS.2015. V.451. P.1522] on the basis of processing the data of different catalogs for the period 1917 - 2004, it was demonstrated that the percentage of anti-Hale groups of spots increases during the minima of solar cycles. This testifies to the operation of a random small-scale turbulent dynamo 2 within the SCZ, the efficiency of which becomes noticeable near the minima of the cycles, when the global toroidal magnetic field weakens.

We have analyzed anti-Hale sunspots over the past 20 years since 2004. It was revealed that the active regions NOAA 10715, 10875, 10930, 12752, 12826, 13088 observed near the minima of the 23th and 24th solar cycles were the clear examples of violation of Hale’s and Joy’s laws. We have previously studied in detail anti-Hale active region NOAA 13088/13102, which was observed in August-September 2022 (shortly after the minimum of the 24th cycle). As a result of our analysis of the development of this area, it was established that the orientation of the magnetic polarities of the spots in it is very different from the location of the polarities of other groups of spots in this solar hemisphere. Therefore, we assume that the detected deviations from the laws of Hale and Joy may indicate the influence of the fluctuating small-scale mechanism of dynamo 2 on the evolution of the studied region, since this source gives the most noticeable contribution to the surface magnetism near the cycle minima.

Understanding the Complexity of Photospheric Flux Emergence with Machine Learning Techniques

Matthew Lennard[1], Suzana S. A. Silva[1], Benoit Tremblay[2], Andrés Asensio Ramos[3], Hideyuki Hotta[4], Haruhisa Iijima [5], Sung-Hong Park[6], Gary Verth[1],Viktor Fedun[1]

[1]University of Sheffield, United Kingdom
[2]High Altitude Observatory, University Corporation for Atmospheric Research
[3]Instituto de Astrofísica de Canarias, Spain
[4]ISEE, Nagoya University, Japan
[5]HEPL, Stanford University, USA
[6]Stanford University, Stanford, California, USA

Advances in modelling magnetic flux inside the Sun's convective region (see, e.g. Hotta & Iijima, 2020; Chen et al., 2021) have provided high-resolution data, which allow the study of the influence of photospheric flows on emerging magnetic flux. In the literature, photospheric velocity fields have been inferred by employing optical feature tracking, e.g., local correlation tracking (LCT), which typically displays poor performance at smaller scales. Neural network approaches, such as DeepVel (DV, Asensio Ramos et al., 2017), have been developed for deriving transverse flows from time-consecutive images of the photosphere by learning from numerical simulations. DV works for photospheric observations at a wide range of spatial resolutions and cadences, only limited by the training data thereby averting the limitations of feature tracking. The combination of speed and accuracy of recovery from a trained version of DV provides opportunity to study structures in solar images, which have previously been inaccessible. These highly detailed velocity fields can be used to analyse the evolution of complex flow topology in the photosphere, hence giving insight to the constant restructuring of the magnetic field and subsurface flows e.g., with methodologies utilising the Finite-Time Lyapunov Exponent (FTLE) proposed by Chian et al., 2020. In this work, we have tested the ability of DV to recover velocities from a simulated emerging active region using the R2D2 code (Hotta and Iijima, 2020). We have found that the FTLE fields obtained from the velocity fields recovered by DV are able to better capture the complexity of photospheric flows before, during and after emergence in comparison to those obtained using recovery via FLCT. In particular, our

results identify signatures in emerging active regions compared with quiet regions; i.e., before any visible indicators of strong flux emergence through the presence of pores or sunspots.

Observations of high-speed downflows in the region of the seismic source in a large solar flare according to spectro-polarimetry in the D3 line

N.I. Lozitska[1], I.I. Yakovkin[1], V.G. Lozitsky[1]

[1]Astronomical Observatory of the Taras Shevchenko National University of Kyiv
Kyiv, Ukraine

We present the results of a study on the extremely powerful X17.2 / 4B solar flare on October 28, 2003, which occurred in the NOAA super-active region 0486. Based on the criterion of peak X-ray power recorded by the GOES detectors since 1976, this flare is one of the most powerful - it holds the third position in the list of such flares. This flare was observed by Natalia Lozitska and Vsesolod Lozitsky with the Echelle spectrograph of the Horizontal Solar Telescope of the Astronomical Observatory of Taras Shevchenko National University of Kyiv. Some results obtained on a base of this observations were published, in particular, in MNRAS, 2018, 477, Iss. 2, 2796-2803 (see link: https://academic.oup.com/mnras/article/477/2/2796/4950618). An interesting feature of this flare is that it had three seismic sources (https://doi.org/10.1007/s11207-006-0190-6; https://doi.org/10.1086/518731). It should be noted that seismic sources are the least studied phenomena accompanying the energy release of solar flares. They are observed on the dopplerograms of the Sun's photosphere as disturbances that spread concentrically from some source. Such waves were observed in ≈ 50% of solar flares, and some flares had multiple seismic sources. Physically, these are acoustic waves moving not on the surface, but within the Sun's interior (hence the name - seismic). They are reflected through the temperature gradient and reach the surface at a higher speed. Possible sources of energy are magnetic fields and beams of electrons and protons. Given these circumstances, it is important to obtain new observational data on magnetic fields and plasma velocities in the region of seismic sources of flares.

We analyzed the $I \pm V$ and V profiles of the D3 line in the mentioned flare for moment 11:15 UT when the entrance slit of the Echelle spectrograph was projected onto the region of the seismic source S2 / S3 according to the sources cited above. In this location, the emission in the D3 line was very intense, exceeding the level of the spectral continuum level up to 5-6 times. The splitting of the $I \pm V$ profiles of this emission corresponded to fairly strong magnetic fields, about 1.5 kG. However, this is apparently only a lower estimate of the local fields, since the pattern of splitting of the bisectors of the $I \pm V$ profiles is atypical for a uniform magnetic field: it was maximal both in the core of the emission and in its far wings. With a uniform field, this splitting should be the same everywhere.

The most interesting results were obtained when studying the Stokes V at large distances from the center of intense emission, ± 15 angstroms (Å). Two main effects were found: (1) a change in the sign of this parameter when passing through the center of the line, and (2) local and narrow areas of a sharp change in the sign of the parameter V in the "red" wing of the line at distances of 4.0, 6.5, and 8.5 Å from the center of the undisturbed line. These effects likely indicate a combination of two essential factors in the area of the seismic source: very strong magnetic fields and significant descending velocities. In particular, effect (1) is similar to that described in the paper in Advances in Space Research, 2022, 69, Iss. 12, P. 4408-4418 (DOI: https://doi.org/10.1016/j.asr.2022.04.012), where it is detected by the H-alpha line. This effect is possible with extremely strong magnetic fields of the level of 10^5 G. As for effect (2), it reflects discrete plasma descent velocities with the following average values: 200, 330, and 435 km/s. The latter can be considered as confirmation of the hypothesis that hydrodynamic shocks are the source of seismic waves in solar flares.

Methodical approaches in the search for extremely strong magnetic fields in active regions on the Sun

V.G. Lozitsky [1], S.M. Osipov [2]

[1] Astronomical Observatory of the Taras Shevchenko National University of Kyiv, Ukraine
[2] Main Astronomical Observatory of National Academy of Science, Kyiv, Ukraine

We plan to discuss in our report the main points related to the search for extremely strong magnetic fields in active regions on the Sun. Some of these points are highlighted, in particular, in such publications: 10.1016/j.asr.2014.09.028 ; 10.30970/jps.26.4902. We draw attention to the fact that another approach may be promising, which is based on obtaining detailed spectro-polarimetric information at long distances (several angstroms) from the centers of strong Balmer lines (see reference: https://doi.org/10.1016/j.asr.2022.04.012). It is planned to briefly present the experience gained in this direction, as well as preliminary results.

Comparison of the Liège and Hamburg atlases of the spectra of the center of the solar disk

S.M. Osipov

Main Astronomical Observatory of NAS of Ukraine, Kyiv, Ukraine

Currently, the best atlases of the spectra of the center of the Sun are Liège and Hamburg. Registration of spectra in them was carried out in the 70s and 80s of the last century, but these atlases are still an example of the high technical standards that were used in the work. Atlases have a very high spectral resolution, but are obtained by fundamentally different methods. The Liege atlas is based on data obtained on the double-pass diffraction spectrometer of the Jungfraujoch observatory, located at an altitude of 3600 m. The Hamburg atlas is based on data from observations made on the Fourier spectrometer of the McMath-Pierce Solar Telescope at the Kitt Peak Observatory (height 2100m). The profiles of the spectral lines of these atlases have been repeatedly compared by many authors in various studies. In the

presented work, the following parameters are compared for 29 lines of the solar spectrum for both atlases: line strength, half-width, and equivalent width. The equivalent widths are also compared with the data obtained by us at the Holosiiv telescope of Ernest Gurtovenko. It is shown that the method of determining zero levels in spectra based on binding the equivalent width to the standard atlas value has low accuracy.

Spectral study of active region site with Ellerman bomb and ejections. Photosphere. Ellerman bomb

M.M. Pasechnik[1]

[1]Main Astronomical Observatory, NAS of Ukraine, 27, Zabolotnoho Str., 03143 Kyiv,
Ukraine

The results of spectral observation analysis of Ellerman bomb and its immediate vicinity, which was formed and developed in the emerging magnetic flux area of the active region NOAA 11024, are presented. Spectral data with high spatial (below 1 arcsec) and temporal resolution (about 3 seconds) were obtained with the French-Italian solar telescope THEMIS on July 4, 2009. The observation time was 20 minutes (from $9^h52^m35^s$ to $10^h11^m26^s$). The spectral region of $\lambda \approx 630$ nm was used to study the changes of physical conditions at different photospheric levels in the process of EB evolution. This region contains lines forming in a wide altitude range: two strong Fraunhofer neutral iron lines FeI λ 630.15 and 630.25 nm and two weak lines FeI λ 630.35 nm and Ti I λ 630.38 nm. Stokes I profiles were obtained, with an interval corresponding to 160 km on the surface of the Sun.

The results of the spectral observations analysis in the the Hα line, obtained in the previous work, showed that two periods can be distinguished in EB evolution: the preheating phase and the flaring phase, during which the gradual and pulse energy releases occurred. The changes in the shape of the Fraunhofer line profiles in the spectra obtained at different stages of the EB development are studied. It was found that the profiles of metal lines were asymmetric. In most cases, feature red asymmetry in their wings was present. The asymmetry was more pronounced in weak lines, in the profiles of which there were several distinguishable components. This suggests that the material flows in the lower photospheric layer consisted of several jets. The variation of central intensities (I/Ic) of Fraunhofer lines in the EB spectra and

their vicinity at different photospheric levels (from the continuum formation region to the upper layers) was analyzed. It was found that the Ellerman bombs formed in intergranular lanes. A sharp change in the intensity and half-width ($\Delta\lambda_{1/2}$) of the lines occurred during the transition from the preheating phase to the flare phase. At this time, I/I_c and $\Delta\lambda_{1/2}$ for the Fe I λ 630.15 and 630.25 nm lines increased by 19, 13% and 8, 6 %, respectively.

An increase the core intensity of all the studied photospheric lines was correlated in time with an increase of the intensity in the Ha line wings.

Changes in the line-of-sight velocity (V_{los}) magnitudes and direction of motion of matter in the Ellerman bomb area and in its immediate vicinity were determined and analyzed too. Since EB developed in the area of the new magnetic flux emergence, mostly upward mass motions were observed in all the photospheric layers. At the same time, a noticeable decrease of the line-of-sight velocity magnitudes was observed at the location of the EB. Possibly, this indicates that small-scale downward movements were superimposed on the large-scale upward motion of the new magnetic flux. Such a distribution of V_{los} could cause magnetic reconnections that occurred in the layer between the upper photosphere and the lower chromosphere. In the central part of the EB in the upper layer of the photosphere, the V_{los} varied between -0.5 ÷ 0.2 km/s, in the lower layer of the photosphere - -1.1 ÷ -0.1 km/s, respectively. The largest changes of Vlos occurred during the formation Hα ejection, which formed near the Ellerman bomb and had signs of plasma vortex motions. Downward flows of matter were observed in the upper photosphere with V_{los} of 0.2 km/s, at that time.

The results obtained in our work can be used to test existing and create new theoretical models of Ellerman bombs.

Influence of space weather conditions on the planetary and regional level by radio astronomical and magnetometric observations

M.I. Ryabov [1], A.L. Sukharev [1], L.I. Sobitnyak [1], V.G.Komendant [1,4] , V. Bezrukovs [2], J. Šteinbergs [2] , K. Skirmante [2], M.I. Orlyuk [3], A.O. Romenets [3]

[1]Odessa observatory URAN-4 Radio Astronomical Institute NAS, Ukraine
[2]Engineering Research Institute Ventspils International Radio Astronomy Centre (ERI VIRAC) of Ventspils University of Applied Sciences (VUAS), Latvia
[3] Institute of Geophysics NAS Ukraine by S.I.Subbotin name, NAS Ukraine
[4] Space Research and Technologies Institute, Sofia, Bulgaria

The development of solar activity in 25-cycle began in December 2019. An interesting feature of it is that in 2023 it shows growth rates that are significantly different from those predicted. Suffice it to say that the number of the most powerful X-ray flares only in the first quarter of this year turned out to be more than in the entire previous year 2022. Unusual is the synchronicity in the manifestation of the activity of the northern and southern hemispheres of the Sun. In previous cycles, the presence of double maxima was noted, formed in turn by different hemispheres of the Sun. In this regard, it is assumed that the time of the maximum, instead of 2025, will be at the end of 2023 or at the beginning of 2024. Thus, our proposed research has the prospect of interesting and unusual results. When the solar activity reaches its maximum, it is especially important to study the planetary and regional response of the magnetosphere-ionosphere system to the entire complex of manifestations of solar activity. Active phenomena occurring on the Sun such as flares, coronal mass ejections (CMEs), particle flows from solar coronal holes further create disturbances in the solar wind. In this case, recurrent and sporadic plasma flows and shock waves propagate in interplanetary space, forming a spectrum of electron density inhomogeneities. The impact of ionizing emission from solar flares and the flow of energetic particles on the Earth's magnetosphere and ionosphere create global magnetic storms with different regional responses depending on the electrical conductivity of the Earth's surface and the presence of magnetic anomalies. The initiators of this project are from Latvia (Ventspils International Radio Astronomy Center

(VIRAC) of Ventspils University of Applied Sciences (VUAS)), Ukraine (Radio Astronomy of the National Academy of Sciences of Ukraine (IRA NASU), Institute of Geophysics of the National Academy of Sciences of Ukraine (IGP)) and Finland (Sodankyla Geophysical Observatory of OULU University). These organizations have all the necessary equipment (low-frequency antenna arrays, full-rotation decimeter-centimeter radio telescopes, a network of sensitive magnetometers, a cosmic ray detector) to study space weather manifestations in the solar wind and ionosphere. Such coordinated studies are of the greatest interest at different latitudes and within close longitude ranges represent periods of extreme states of solar and geomagnetic activity under conditions of an unusual 25th cycle of activity.

Oscillatory reconnection and waves in merging flux ropes

L. A. C. A. Schiavo[1], James Stewart[1], P. K. Browning[1]

[1]University of Manchester, Manchester, UK

This talk will present results from 2D magnetohydrodynamic (MHD) simulations of merging flux ropes driving magnetic reconnection. The numerical simulations show oscillatory reconnection triggered by merging twisted flux magnetic ropes. The oscillatory reconnection generates slowly propagating waves from the reconnection site. This phenomenon is known as quasi-periodic pulsations (QPPs), which are often observed in flare emissions. While these may reveal much about the time-dependent reconnection involved in flare energy release, the underlying mechanisms are still poorly understood. The wave propagation pattern is carefully investigated by modal decomposition tools such as spectral proper orthogonal decomposition (SPOD) and Fourier decomposition. The impact of the poloidal magnetic component and resistivity is analysed in the emitted waves and reconnection rate. Modal decomposition is used to correlate the generated waves with the oscillatory magnetic reconnection and to develop a better understanding of the dynamical phenomena behind QPPs.

EUV coronal lines: from atomic modelling to measuring the magnetic field

N.G. Shchukina[1,2,3]

[1]Main Astronomical Observatory of NAS of Ukraine, Kyiv, Ukraine
[2]Taras Shevchenko National University of Kyiv, Kyiv, Ukraine
[3]Instituto de Astrofísica de Canarias, E-38205, La Laguna, Tenerife, Spain

The scientific goal of the talk is to present advancements in coronal spectropolarimetry based on using permitted EUV lines. Among them are the key polarized spectral lines of highly ionized Fe X, Fe XI, Fe XIII, Fe XIV, Si IX, and Si X atoms. We show that the atomic polarization generated in the lower levels of these ions by scattering in the forbidden M1 visible, red or IR lines can be transferred by isotropic collisions to the high lying upper levels of the permitted E1 EUV lines. As a result, the measurable linear polarization signals in these E1 lines caused by the ensuing selective emission processes would be sensitive to the electronic density and the magnetic field orientation.

To this end, we present the new code for polarized coronal line synthesis based on the interactive data language IDL (Interactive Data Language). We propose also several types of the Fe X, Fe XI, Fe XIII, Fe XIV, Si IX, and Si X model atoms of different degree of complexity which allows to calculate the radiation polarization of diagnostically important coronal lines in the IR and EUV range of the solar spectrum.

Addressing non-local relations in differently digitized spectra using machine learning

I.I. Yakovkin[1], A. O. Bartenev[2], and N. V. Petrova[3]

[1]Astronomical Observatory, Taras Shevchenko National University of Kyiv, Kyiv, Ukraine
[2]Department of Physics, University of Puerto Rico, Mayaguez, Puerto Rico 00681, USA
[3]Institute of Physics of National Academy of Sciences of Ukraine, Kyiv, Ukraine

The study explores the potential of machine learning in the processing of spectra, specifically with regard to its ability to transform between differently digitized spectra and fill the gaps in unique experimental data. When dealing with sets of data that have been digitized differently (for example, using various scanning techniques), it is crucial not only to consider the difference in characteristic curves but also the potential non-local differences due to the impact of different transmission/reflection curves, additional reflections, etc. By utilizing machine learning, we can transform between differently digitized spectra, effectively removing nonlocal effects if present in one of the sets.

In this study, a convolutional neural network was developed to transform between reflective and transmissive scans of a solar flare spectrogram. The performed analyses demonstrated that the transformation results closely matched the target data (Figure 1). These findings contribute to the development of novel techniques in spectra processing and underscore the potential of modern machine learning methods in the field.

The techniques established in this study can be applied to a broad range of spectroscopic measurements, encompassing those obtained using older technologies such as photoplates. This makes them a valuable tool for researchers working in the field of spectroscopy.

The authors would like to express their gratitude to V.G. Lozitsky for generously providing the spectra used in this study.

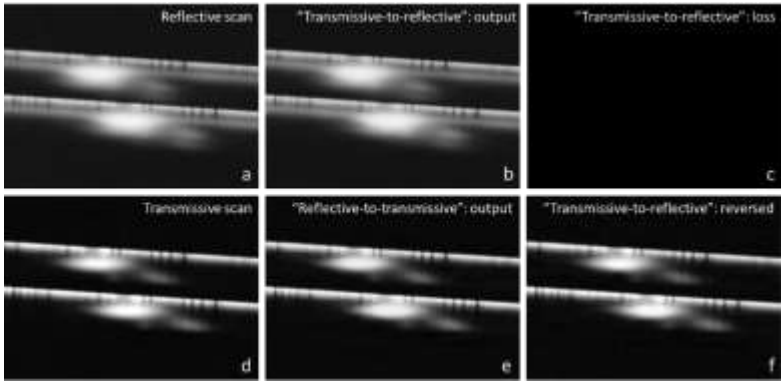

Figure 1. Training results for the Hγ spectral line of the limb solar flare on July 17th, 1981: (a) target reflective scan for the "transmissive-to-reflective" model, (b) model output, (c) loss function, (d) target transmissive scan for the "reflective-to-transmissive" model, (e) model output, and (f) output from the reversed "transmissive-to-reflective" model.

Detecting and addressing spectral contamination through machine learning

I. I. Yakovkin[1], A. O. Bartenev[2], and N. V. Petrova[3]

[1]Astronomical Observatory, Taras Shevchenko National University of Kyiv, Kyiv, Ukraine
[2]Department of Physics, University of Puerto Rico, Mayaguez, Puerto Rico 00681, USA
[3]Institute of Physics of National Academy of Sciences of Ukraine, Kyiv, Ukraine

The study introduces a technique for detecting and excluding impurities from final spectral images using a Convolutional Neural Network (CNN). The CNN transforms spectra between reflective and transmissive scans, effectively learning the relationship between both types of scans. CNNs excel in image processing tasks and minimize the risk of overfitting.

When applied to spectra with impurities, the models adeptly reproduce the true darkness of the photoemulsion while exhibiting high loss for scratches and impurities. Figure 1 illustrates the models' performance on contaminated spectra, revealing that areas of high loss correspond to the

presence of impurities. This approach enables automatic identification and exclusion of scratches, dust particles, and other impurities from the final spectrogram scans, ensuring data integrity.

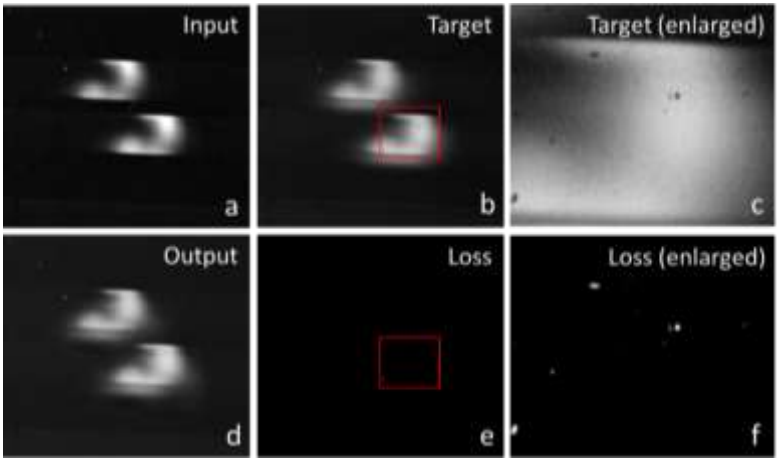

Figure 1. Visualization of the models' performance on contaminated spectra. The figure displays the model's input (a), target (b), enlarged fragment (c), output (d), intensity-normalized loss (e), and an enlarged view of the loss area (f). Comparing panels (c) and (f) reveals high loss areas corresponding to spectral impurities, enabling their reliable detection and exclusion during post-processing.

Compared to other post-processing defect detection methods, this algorithm offers a reliable and user-friendly solution without assumptions about impurity characteristics. The use of reflective scans further aids in detecting impurities that may be challenging to identify using transmissive scans alone. In conclusion, employing a convolutional neural network for transforming spectral images demonstrates promising potential in improving the accuracy of spectral measurements in solar physics and related fields.

The authors would like to express their gratitude to V.G. Lozitsky for generously providing the spectra used in this study.

Search for superstrong magnetic fields in active processes on the Sun using spectro-polarimetry within 15 angstroms around the D3 line

I.I. Yakovkin[1], V.G. Lozitsky[1]

[1]Astronomical Observatory of the Taras Shevchenko National University of Kyiv
Kyiv, Ukraine

We critically review our prior study on this topic (see refer: https://doi.org/10.1016/j.asr.2022.04.012) with a focus on two key points: (i) we extended the wavelength range around the D3 line examined, up to ±15 Å, a significant increase from the previous ±2.5 Å, and (ii) a larger volume of observational data was analyzed, including an additional *X* limb flare. Specifically, our study concerns the 2004 July 12 active prominence and the 2014 June 10 limb flare of X1.5 class. Observational data were obtained with the Echelle spectrograph of the horizontal solar telescope of the Astronomical Observatory of Taras Shevchenko National University of Kyiv. For the mentioned limb flare, we found reliable and oppositely polarized peaks of the *V* parameter located at distances of -4.5 Å and +2.7 Å from the line center. If these features are interpreted as manifestations of the magnetic splitting of the line together with its Doppler shift, than corresponding magnetic field is $\approx 2.2 \times 10^5$ G, and radial velocity -46 km s^{-1}. Similar spectral peaks were found in the active prominence too, but these are situated more symmetrically relative to the line center. For comparison with the theory, the spectral features of the Paschen-Back effect at magnetic fields up to 100 kG were also studied. It turned out that the theoretical width of the splitting components is relatively small, 0.3 Å, while the width of the observed peaks can be significantly larger. This may indicate a considerable dispersion of magnetic strengths and Doppler velocities in regions with particularly strong magnetic fields. On the basis of model calculations, it is shown that alternative explanations for the observational data could be available, which incorporate much weaker magnetic fields (5.5-7.1 kG) and significant macroscopic velocities of varying directions, at the level of 50-60 km s^{-1}.

Links of eigen vectors of solar magnetic field with the indices of solar activity in sunspots and flares

Zharkova V.V. [1,2], Shepherd S.J. [3] and Zharkov S.I. [2,4]

[1]MPEE, Northumbria University, Newcastle upon Tyne, UK
[2]ZVS Research Enterprise Ltd., London, UK
[3]PRIMAL Research Group, Sorbonne University, Paris, France
[4]Centre for Astrophysics, Hull University, Kingston upon Hull, UK

The eigen vectors of magnetic oscillations obtained with Principal Component Analysis from full disk synoptic maps of solar background magnetic field (SBMF) from the Wilcox Solar Observatory are shown to come in pairs assigned to magnetic waves produced by dipole, quadruple, sextuple and octuple magnetic sources. The first pair is linked to dipole magnetic waves with their summary curve revealing a reasonable fit to the averaged sunspot numbers in cycles 21-24. This verifies the previous results and confirms the summary curve as additional proxy of solar activity decreasing towards grand solar minimum in cycles 25-27, or grand solar minimum. There is also a noticeable asymmetry in latitudinal distributions of these PCs showing an increased activity in northern hemisphere in odd cycles and in south- ern hemisphere in even ones similar to the N-S asymmetries observed in sunspots. The second pair of PCs linked to quadruple magnetic sources, has 50% smaller amplitudes than the first, while their summary curve correlate closely with SXR fluxes in solar flares. Flare occurrences are also linked to variations of the next two pairs of eigen vectors, quadruple and sextuple components, revealing additional periodicity of about 2.75-3.1 years similar to observed oscillations in flares. Strong latitudinal asymmetries in quadruple and sextuple components are correlating with the N-S asymmetries of flare occurrences skewed to southern hemisphere in even cycles and to northern hemisphere in odd ones. PCA of solar magnetic field raises perspectives for simultaneous prediction of general and flaring solar activity.

Reference:

Zharkova and Shepherd, 2022, *MNRAS*, Vol. 512, Issue 4, June 2022, Pages 5085–5099 https://solargsm.com/wp-content/uploads/2022/04/zharkova_shepherd_mnras22.pdf

ДОСЛІДЖЕННЯ АТМОСФЕРИ ТА ІОНОСФЕРИ

ATMOSPHERE AND IONOSPHERE RESEARCH

Profiles of the vertical ozone distribution describing the ozone hole over the Faraday/Vernadsky station 1975-2009

Y. Andrienko[1], G. Milinevsky[1,2,3], J. Shanklin[4], A. Grytsai[1], O. Evtushevsky[1], Y. Shi[3], O. Ivaniha[2]

[1]Physics Faculty, Taras Shevchenko National University of Kyiv, Kyiv 01601, Ukraine
[2]State Institution National Antarctic Scientific Center, Kyiv 01601, Ukraine
[3]College of Physics, ICFS, Jilin University, Changchun 130012, China
[4]British Antarctic Survey, Cambridge CB3 0ET, United Kingdom
andrienko.j@gmail.com

The total ozone column and the vertical ozone distribution have been measured at the Antarctic Station 232 (this is the number in WOUDC classification) Faraday/Vernadsky. Ozone observations have been provided using Dobson spectrophotometer. During the analyzed period, three spectrophotometers measured ozone parameters at the station. Dobson 073, Dobson 031 were used at Faraday station. After the transfer of the station to Ukraine in 1996 Dobson 031 and Dobson 123 were used. We have processed the results of a unique series of ozone observations since 1973. During the processing of observations for each of the spectrophotometers, the corresponding calibration tables were used, which gave us the opportunity to build profiles of the vertical distribution of ozone over the Faraday/Vernadsky station precisely in the years of the formation of the ozone hole over the South Pole. After processing, 263 profiles of the vertical distribution of ozone over the station were obtained. We investigated variations in the vertical ozone distribution in September–October when the ozone hole is observed by dropping the total ozone column to less than 220 DU values. The shape of the profiles and ozone column are different before and after the occurrence of the ozone hole. In 1975-1979, the profiles of the vertical ozone distribution had a narrow maximum with values of partial ozone column in the range of 56-134 DU/layer. During this period, according to our results, the ozone hole was not recorded. The first vertical profile of the ozone distribution, which describes the "ozone hole", was constructed by us using data from September 23, 1989. Profiles in ozone hole conditions have two maxima and an area of significant drop in ozone partial column. The maximum concentration of ozone in the layer does not exceed 45

DU/layer. For the vast majority of profiles, the zone of ozone depletion is located at an altitude of 15-17 km. Most of the profiles have a decrease in concentration in the lower layers. The deeper the ozone hole, the deeper the zone of ozone depletion in maximum concentration. The assimilated plots of the ozone distribution from the TEMIS website (https://www.temis.nl/protocols/O3global.php) confirm the presence of an ozone hole over the station for the dates with "double maxima" observed.

This work was partly supported by the project BF/30-2021 of Taras Shevchenko National University of Kyiv. Part of this research was performed at the International Center of Future Science, Jilin University (JLU), under the contract with the JLU.

Observations of the mid-latitude ionosphere during the solar eclipse of October 25, 2022

L.Ya. Emelyanov, O.V. Bogomaz

Institute of Ionosphere, Kharkiv, Ukraine
leonid.ya.emelyanov@gmail.com

The results of observations of the critical frequency (f_oF2), ionospheric F2 peak electron density (N_mF2) and peak height (h_mF2) of the ionosphere over Kharkiv (Ukraine, 49.6° N, 36.3° E) during a partial solar eclipse (SE) on 25 October 2022 are presented. The data were obtained using the digital ionosonde of Institute of Ionosphere of NAS and MES of Ukraine.

On the day of the SE, the geomagnetic state was quiet (the value of the geomagnetic index $K_p \leq 2$), while the days before the SE (from October 22 to the beginning of October 24) a geomagnetic storm was observed, and the consequences of its influence could remain. Therefore, October 21 was chosen as the main reference day ($K_p \leq 1+$, D_{st} index was within 5...12 nT). A comparison was also made with adjacent days.

The SE started at 09:29 (time in UT here and further), ended at 11:59, and the maximum phase of the SE was at 10:45 (the obscuration of the Sun's disk area was 57.2%, and the magnitude was 0.66). The analysis showed a clear effect in the variations of f_oF2 (and, accordingly, N_mF2): during the SE, f_oF2 decreased by 36%, and after the moment of the SE maximum phase, increased to its usual level. From the beginning of the SE, h_mF2 decreased from 285 to 255 km, and then it began to grow with a maximum near the moment of the greatest Sun’s obscuration. Such effects were not observed on

October 21 and 24. After noon until the end of the day on October 25, f_oF2 fluctuations with a quasi-period of 4.5 to 3 hours were observed, and h_mF2 wave-like variations with a gradual decrease in amplitude and period of oscillations were present, while on October 21 and 24 such fluctuations were absent.

To identify longitude effects and refine the factors of influence on the temporal variations of the ionospheric parameters, the results of observations of the ionosphere over Kharkiv were compared with the data obtained by the ionosonde in Pruhonice (Czech Republic, 50.0° N, 14.6° E, https://lgdc.uml.edu/common/DIDBYearListForStation?ursiCode=PQ052). In Pruhonice, the start of the SE was at 09:13, the maximum phase was at 10:17, and the end was at 11:23. The obscuration was 30.2%, and the magnitude was 0.42. The comparison was carried out for the universal coordinated time (UT) to take into account the global factors influencing the ionospheric parameters, for the local time (LT) to take into account diurnal variations, and when the moments of the maximum phase of the SE in Kharkiv and Pruhonice were superposed to highlight the direct effect of the SE. Analysis of parameter variations showed the following.

Comparison of ionospheric data by LT time gave f_oF2 and h_mF2 diurnal variations similar in nature and values for Kharkiv and Pruhonice, except for the time intervals accompanied by a solar eclipse. Since the SE intervals in Kharkiv and Pruhonice did not coincide in LT, the variations in the ionospheric parameters during these intervals are related precisely to the SE, and not to the factors causing their diurnal changes. Comparison of data by UT time showed a coincidence in the nature and time of oscillations in both f_oF2 and h_mF2 observed in Kharkiv and Pruhonice on October 25. Comparison of the ionospheric data by superimposing the time moments of the SE maxima showed that at the beginning of the SE, the effect of a decrease in f_oF2 in Pruhonice was the same as in Kharkiv, but its growth occurred earlier than the maximum phase, while the f_oF2 minimum in Kharkiv coincided with the time of the SE maximum. Variations in h_mF2 caused by SE in Kharkiv and Pruhonice are identical.

The behavior of HF radio waves under the action of typhoon-induced atmospheric gravity and infrasound waves

L.F. Chernogor[1,2,3], K.P. Garmash[2], Q. Guo[3], V. T. Rozumenko[2], Y. Zheng[1]

[1]Qingdao University, Qingdao, China
[2]V. N. Karazin Kharkiv National University, Kharkiv, Ukraine
[3]Harbin Engineering University, Harbin, China
vtrozumenko45@gmail.com

The purpose of this study is to present the observations of the changes that HF radio waves underwent in response to the atmospheric gravity and infrasound waves related to super typhoon Kong-rey from 30 September to 6 October 2018. The measurements have been made with the Harbin Engineering University, the People's Republic of China (PRC), multi-frequency multiple path radio system involving the software-defined technology. The receiver and signal processing system has been developed by researchers from the V. N. Karazin Kharkiv National University (Ukraine) and the Harbin Engineering University. As the transmitters in this study, the system utilized radio transmissions of broadcast stations located in the PRC, the Republic of Korea, Japan, and Mongolia, whose signals travelled along eight propagation paths and were received and processed at the Harbin Engineering University campus (45.78° N, 126.68° E). The temporal variations in the Doppler spectra, the Doppler shift in the main ray, and the signal amplitude are usually subjected to the systems spectral analysis. The radio system delivers the 0.02-Hz Doppler shift resolution and the 7.5-s temporal resolution. The amplitude Doppler shift variations usually have a few local maxima, which are distinguishable in the 5% of power in the maximum component steps. These maxima in the Doppler spectrum are considered to be separate radio wave rays either traveling along different propagation paths or having different states of polarization. The system sounds the ionosphere at the propagation path midpoints of order of 1,000 km apart horizontally and randomly distributed in the bottom side ionosphere altitude range. The disturbances arising at the oceanic surface and traveling to ionospheric heights undergo a chain of nonlinear transformations. In the ionosphere, they are usually superimposed on the background perturbations originating at the Sun or induced by the sunset or sunrise terminator. Therefore, the state of space weather plays a key role in the examination of

HF radio waves. To distinguish the manifestation of disturbances originating from different sources, one of the co-authors, Chernogor, L. F., has developed a general methodology for revealing perturbations launched in the ionosphere by various significant inputs of energy into the lithosphere–atmosphere–ionosphere–magnetosphere system. In this event, the analysis showed that solar activity and the state of space weather were favorable to observing the ionospheric effects from typhoon Kong-Rey.

The Doppler spectra and the Doppler shift observed during sunlit hours exhibited insignificant temporal variability through the course of the typhoon action, since the radio waves in the ~6–10 MHz band were reflected either from the ionospheric *E* region or from the sporadic *E*. At night, the radio waves were reflected from the ionospheric *F* region, and the Doppler shift was observed to reach maximum values of up to 0.5–1 Hz. The super typhoon action on the ionosphere was accompanied by the generation or amplification of quasi-sinusoidal variations in the Doppler shift by a factor of 2–3 with amplitudes of ~0.1–0.5 Hz and periods of 2–5 min and 10–100 min. The Doppler spectra showed diffuseness and up to ±1 Hz broadening due to an increase in the number of rays. The solar terminator also generated temporal variations in the Doppler shift. The Doppler measurements have shown that dusk terminators and the super typhoon acted synergistically to amplify the ionospheric response to these sources of energy. The diurnal variations in the signal amplitude $A(t)$ were observed to attain 30 dBV, while $A(t)$ values at night were three orders of magnitude greater than during the daytime, which is due to the disappearance of the absorbing *D* region.

The ionospheric response to the April 11, 2019, submarine earthquake near Japan captured by the Harbin Engineering University HF software-defined radio system

L.F. Chernogor[1,2,3], K.P. Garmash[2], Q. Guo[3], V. T. Rozumenko[2], Y. Zheng[1]

[1]Qingdao University, Qingdao, China
[2]V. N. Karazin Kharkiv National University, Kharkiv, Ukraine
[3]Harbin Engineering University, Harbin, China
vtrozumenko45@gmail.com

The Harbin Engineering University, the People's Republic of China (PRC), multifrequency multiple path software-defined radio system for

probing the ionosphere at oblique incidence continuously monitors dynamic processes acting in the ionosphere over the PRC and beyond its borders since 2018. The receiver and signal processing hardware are located at the Harbin Engineering University campus (45.78°N, 126.78°E). The Doppler spectra are estimated over 20-s intervals with a 7.5-s temporal resolution and 0.02-Hz Doppler resolution. The transmissions in the 5.00–9.83 MHz band of fourteen broadcast stations located in five countries are used as probing signals. In the present study, the measurements were subjected to a retrospective analysis to reveal the ionospheric disturbances that occurred at 845–2,260-km great-circle distances from the earthquake epicenter to the propagation path midpoints, and were associated with the April 11, 2019, earthquake near Japan.

The temporal dependences of the Doppler spectra show an additional Doppler spectrum broadening and the Doppler shift exhibits quasi-sinusoidal variations. The Doppler shift oscillations with 2- to 5-min periods are due to infrasound, whereas the oscillations with 8–20-min periods are caused by atmospheric gravity waves. The relative amplitude of the disturbances in the electron density is estimated by invoking the relation between the Doppler shift and electron density disturbances. However, the ionosphere can be affected by disturbed space weather, and therefore the isolation of earthquake related disturbances require a comprehensive analysis of the state of space weather. The main characteristics of the state of space weather were as follows. On April 8 and 9, 2019, the proton number density n_{sw} in the solar wind exhibited increases of up to 11×10^6 m^{-3} against the 2×10^6 m^{-3} background value; the plasma flow speed V_{sw} showed enhancements from 400 km/s to 450–460 km/s, whereas temperature T_{sw} displayed a rise from 10^4 K to 18×10^4 K. As a result, the dynamic pressure exhibited an increase from 0.5–1 nPa to 3–3.2 nPa. The B_y component of the interplanetary magnetic field showed fluctuations within the –6.3 nT to 3.1 nT limits, while the B_z component exhibited variations from –5.1 nT to –6.4 nT. The energy input from the solar wind into the Earth's magnetosphere ε_A showed an increase of up to 4–10 GJ/s. The planetary K_p index exhibited an increase of up to 3–4, whereas the equatorial D_{st} index showed a minimum of down to –(25–27) nT. Thus, during April 8, 9, and the first half of 10, 2019, a very weak magnetic storm was observed to occur. Three hours prior to and eighteen hours after the earthquake, the K_p index ≤ 2, while the D_{st} value was greater than –12 nT, and therefore, the ionospheric perturbations due to space drivers were insignificant. As a whole, the situation was favorable for observing the ionospheric effects from the April 11, 2019, earthquake that occurred near Japan.

The response of the ionosphere to the moderate submarine earthquake (magnitude M ≈ 6) was detected in the ~(1–2)×10^3 km range from the epicenter in the 5–9.8 MHz range of operating frequencies. The atmospheric gravity waves with ~0.5–0.8 km/s horizontal speeds and ~8–20 min periods were observed to travel after the earthquake, and they acted to modulate the electron density with an ~2–19% amplitude. The generation of infrasound with 2–5 min periods and about 0.3–0.4 km/s horizontal speeds was observed to accompany the earthquake, which acted to modulate the electron density with 0.6–1.2% amplitude. The seismic waves (apparent horizontal speeds of about 2–3 km/s) displayed only uncertain response along some propagation paths.

Physical Effects of the Kyiv Meteoroid

L. F. Chernogor

V. N. Karazin Kharkiv National University, Kharkiv, Ukraine
leonid.f.chernogor@gmail.com

The fall of each new sufficiently large celestial body undoubtedly is an interdisciplinary problem. It is well known that the flight and explosion of a meteoroid cause a whole complex of physical processes to act in all geospheres, i.e., in the lithosphere–atmosphere–ionosphere–magnetosphere system, as well as in geophysical fields.

The purpose of this report is to evaluate the main physical effects and to comprehensively simulate the processes that operated in all geospheres due to the fall and explosion of the April 19, 2023, meteoroid. According to the International Meteor Organization (Event 2223-2023), the absolute magnitude reached –18 or slightly more, the initial velocity of the meteoroid was 29 km/s, and the explosion took place at the point whose geographic coordinates were (49.9°N, 29.9°E) at 18:57:20 UTC. The total radiated power of the bolide was approximately 21 GW, and the total radiated energy was 25 ± 2.5 GJ. The initial kinetic energy was calculated to be 375 ± 35 GJ, while the initial meteoroid mass was estimated to be (0.9 ± 0.1) × 10^3 kg, volume 0.26 ± 0.026 m^3 (assuming a typical density of 3.5 × 10^3 kg/m^3), and an equivalent diameter to be 0.79 ± 0.03 m. The initial angle of the trajectory inclination with respect to the horizon has been estimated to be 32°. The explosion occurred 38 km over the city of Kyiv, and consequently the celestial body has been termed the Kyiv meteoroid by the author.

The main investigation and simulation results are described. The evaluation and simulation of mechanical, optical, gas-dynamic, thermodynamic, plasma, plume, turbulence, magnetic, electric, electromagnetic, acoustic, and seismic effects are performed.

The passage and explosion of the Kyiv meteoroid created noticeable disturbances in all geospheres, and exhibited magnetic, electric, and electromagnetic effects, partially filling the gaps in the theory of the physical effects of meteoroids on the lithosphere–atmosphere–ionosphere–magnetosphere system. Celestial bodies similar to the Kyiv meteoroid fall to Earth every 10–12 days on average.

The work has been partially supported by the National Research Foundation of Ukraine (grant No. 2020.02/0015; "Theoretical and experimental studies of global disturbances from natural and technogenic sources in the Earth–atmosphere–ionosphere system"). The work also has been partially supported by Ukraine state-funded research projects (grant Nos. 0121U109881, 0122U001476).

PERUN project for research, diagnostic and analysis climate changes

I. Dvoretska[1, 2], R. Tolasz[1], V. Sustkova[1], A. Valik[1], R. Brožková[1]

[1] Czech Hydrometeorological Institute (CHMI), Ostrava, Czech Republic
[2] Ukrainian Hydrometeorological Institute (UHMI), Kyiv, Ukraine
iryna.dvoretska@chmi.cz

As one of the largest projects in terms of number of participants and duration (6.5 years), the PERUN project (Prediction, Evaluation and Research for Understanding National sensitivity and impacts of drought and climate change for Czech Republic) started in July 2020. The PERUN focuses on research on climate extremes, drought and climate change impacts in the Czech Republic (CR). It is the first step towards a new long-term climate change research in the CR. The project is under the supervision of the Czech Ministry of the Environment and has eight participants (https://www.perun-klima.cz/), with CHMI being the principal investigator and contractor.

The preparation of the climate scenario and its validation is the aim of the first step of the PERUN project. As ground observational data, a dataset based

on CHMI observations for the period from 1990 to 2014 is used, together with the data exchanged with the NMHs in the surrounding countries (Poland, Germany, Austria and Slovakia). This data set is referred to as GriSt. The modelling data is presented as ALADIN-CLIMAT/CZ data set for the same base period and has the prediction period from 2021 to 2100 years with the resolution of 2.3 km (29154 grid points).

Aire Limitée Adaptation dynamique Développement InterNational (ALADIN) developed in CNRM/Meteo-France in 2000s as regional climate bispectral model with name CNRM-ALADIN or ALADIN-CLIMAT. The second climatological version prepared in CHMI has name ALADIN-CLIMAT/CZ and uses in PERUN project. Now ALADIN modelling data has a very high resolution - 2.3 km and it is important to compare ALADIN data with ground observations to understand, validate and use all ALADIN data sets not only for the base period but also for prediction data sets in the future for the objectives of the PERUN project and to diagnose climate changes in the CR for the next part of the century.

The calculating yearly and seasonal spatial distributions of the daily means temperature (T), minimum (T min) and maximum (T max) temperature and precipitation for base period from two datasets (ALADIN dataset and ground observation dataset) was the first step in validation modelling data. Comparison of mean temperature data shows less than 0.5 C° average difference for base period data and consist with the results of previous researches (Lucas-Picher et al., 2023). High differences of extremal temperature could be explained by orography of CR, influence mountain climate to the modelling and a small number of observation stations in mountains. ALADIN precipitation data for territory of CR is high (1014 mm. as average value for base period, that overestimate ground observed value by 46 %), but not higher than in previous validation researches for this domain (Giot at al., 2016), where indicated overestimated precipitation amounts by the ALADIN model. So far we have used only DELTA correction, BIAS procedures (Räty, et al. 2014) will follow.

The next step of our research will be to continue validation of ground observational and modelled datasets with the aim of reducing of overestimated ALADIN data for T min and precipitation amounts and using the resulting method to obtain the most representative data.

Lucas-Picher, P., Brisson, E., Caillaud, C. et al., 2023. Evaluation of the convection-permitting regional climate model CNRM-AROME41t1 over Northwestern Europe. *Clim Dyn*. DOI: https://doi.org/10.1007/s00382-022-06637-y

Giot, O., Termonia, P., Degrauwe, D., De Troch, R., Caluwaerts, S., Smet, G., Berckmans, J., Deckmyn, A., De Cruz, L., De Meutter, P., Duerinckx, A., Gerard, L., Hamdi, R., Van den Bergh, J., Van Ginderachter, M., and Van Schaeybroeck, B., 2016. Validation of the ALARO-0 model within the EURO-CORDEX framework, Geosci. Model Dev., 9, 1143–1152. DOI: https://doi.org/10.5194/gmd-9-1143-2016

Räty, O., Räisänen, J., Ylhäisi, J. S., 2014. Evaluation of delta change and bias correction methods for future daily precipitation: intermodel cross-validation using ENSEMBLES simulations. Clim Dyn, 42, pp.2287—2303. DOI: https://doi.org/10.1007/S00382-014-2130-8

Pattern Identification in AERONET Data through Machine Learning Techniques

I.V. Fesianov

Taras Shevchenko National University of Kyiv, Kyiv, Ukraine
fesianov.i@gmail.com

The Aerosol Robotic Network (AERONET) data is crucial for studying the impact of atmospheric aerosols on the environment and human health. The AERONET provides aerosol optical depth measurements, a critical parameter for understanding aerosol concentration, size distribution, and composition. These measurements can help identify aerosol types and their sources and monitor changes in atmospheric aerosols over time. AERONET data has multiple variables and high dimensionality, making it challenging to analyze using traditional statistical methods. So this research presents approaches to data analysis using machine learning techniques, namely clustering and dimensionality reduction. Clustering algorithms group data points into clusters based on their similarity, allowing for the identification of different aerosol types and their sources. Dimensionality reduction techniques are used to compress the data by reducing the number of variables, which can help visualize the data and identify significant predictors of aerosol optical depth. This study explores the practical application of several algorithms, including DBSCAN, hierarchical clustering, principal component analysis (PCA), and UMAP, using observational data from the site of Kyiv as an example. In addition, various technical features of data preparation, application of algorithms, analysis, and visualization are considered.

This work was partly supported by the project BF/30-2021 of the Taras Shevchenko National University of Kyiv.

Bay-shaped variations in the geomagnetic field that accompanied the catastrophic explosion of the Tonga volcano on January 15, 2022

L. F. Chernogor[1], M. Yu. Holub[1]

[1]V. N. Karazin Kharkiv National University, Kharkiv, Ukraine
leonid.f.chernogor@gmail.com

Tonga Volcano is one of the five most powerful volcanoes in the world. The explosion of the Tonga volcano on January 15, 2022 was unique. It led to disturbances in the lithosphere, World Ocean, atmosphere, ionosphere, magnetosphere and all geophysical fields. A number of works have been devoted to the disturbance of the Earth's magnetic field. The transport of magnetic field disturbances by atmospheric gravity waves and tsunamis, disturbances in magnetically conjugated regions due to acoustic resonance, the effect on the equatorial electrojet, etc., have been studied. The list of the variety of magnetic effects of the Tonga volcano does not end there.

The purpose of this work is to describe the results of the analysis of global bay-disturbances in the geomagnetic field observed after the Tonga volcano explosion on January 15, 2022.

The results of measurements of temporal variations in the level of the *X*-, *Y*-, and *Z*-components carried out by the INTERMAGNET world network of stations were used as initial data. The analysis of magnetic data was preceded by an analysis of the state of space weather. A preliminary analysis of temporal variations in the level of the *X*-, *Y*-, and *Z*-components indicates that on the reference days these variations were smoother than on January 15, 2022. An analysis of time variations in the level of the *X*-, *Y*-, and *Z*-components of the geomagnetic field and a statistical analysis of the disturbance parameters showed the following. With the time delay, which varied depending on the distance to the volcano from several tens to 100–200 min, bay-disturbances of all components of the geomagnetic field were observed. The magnitude of the effect varied from ~10 to ~60 nT. The greatest disturbances occurred in the *Y* component. The delay time and duration of disturbances increased with increasing distance from the volcano, while their amplitude, on the contrary, decreased. The propagation speed of bay-disturbances was close to the speed of the blast wave. Bay-disturbances

were weakly expressed or completely absent on the night side of the planet. It is substantiated that bay-disturbances are closely related to the occurrence of an ionospheric «hole» under the action of a blast wave from the volcano. The results of estimates of the bay-disturbance are in good agreement with the observation results.

Work by L. F. Chernogor was supported by the National Research Foundation of Ukraine for financial support (project 2020.02/0015, "Theoretical and experimental studies of global perturbations of natural and man-made origin in the Earth–Atmosphere–Ionosphere system"). Work by L. F. Chernogor also was supported by Ukraine state research project #0121U109881 and #0122U001476.

Influence of sudden stratospheric warming in the Arctic on total ozone over Ukraine

A.V. Grytsai, A.O. Burmai

Taras Shevchenko National University of Kyiv, Ukraine
a.grytsai@gmail.com

The total column ozone (TCO) changes over Ukraine are typical for the mid-latitudes of the northern hemisphere. The annual maximum is observed in spring (March–April), and the minimum occurs in autumn (October–November). The typical maximum values are close to 400 Dobson Units (DU) and minimum values fall to 250 DU. In general, TCO over Europe is relatively low in comparison with its zonal mean. The summer and autumn values are more stable, but significant variations happen near the maximum, with changes exceeding 100 DU during several days. This phenomenon occurs under the influence of planetary waves, which increase zonal asymmetry in the ozone distribution.

The strong activity of planetary waves can weaken the stratospheric polar vortex and even lead to its destruction. These events are known as sudden stratospheric warmings, and they result in an increase in the stratospheric temperature and total ozone in the polar region. Impact of the stratospheric warmings on conditions in the middle latitudes is not so simple. Cold air from the core of the stratospheric vortex moves equatorward, and it is probable that this movement will be directed toward the location of the zonal minimum. Accordingly, a sudden stratospheric warming can decrease TCO in some regions.

We have processed TCO data of Multi-Sensor Reanalysis for the 1979–2022-time range, presented as overpasses for the Kyiv-Goloseyev observational station (https://temis.nl/protocols/o3field/overpass_msr2.php). OMI model data from 2005 were also considered (https://temis.nl/protocols/o3field/overpass_omi.php). The method of superimposed epochs was used, where the day of sudden stratospheric warming was chosen as an initial point. The seasonal variation was taken into account by comparison with multi-year climatology. The obtained results indicate a TCO decrease by several tens of DU, which is observed within a week after the event. The phenomenon requires a more detailed study with an analysis of the spatial pattern and time features, but our preliminary results confirm the idea on the total ozone decrease over Ukraine after sudden stratospheric warmings.

About one property of the dispersion equation for latitudinal acoustic-gravitational waves

O.N. Kryshtal, A.D. Voitsekhovska, O.K. Cheremnykh, S.O. Cheremnykh

Space Research Institute of the NASU and the SSAU, Kyiv, Ukraine
kryshtal@mao.kiev.ua

Acoustic-gravity waves are an example of processes that largely determine the dynamics of the Earth's atmosphere. This is due to the fact that the sources of these waves are located throughout the height of the atmosphere, from the very "bottom", where earthquakes, volcanic emissions, tsunamis, tornadoes, etc. and to the very "top", where perturbations of the solar wind, magnetic storms, and precipitation of particles in high latitudes are active. All this phenomena leads to the active exchange of energy between all layers of the Earth's atmosphere and the interaction of wave disturbances of significantly different scales - from several thousand kilometers to several hundred meters, and this - to the appearance and development of processes of convection and turbulence in the environment. It seems that only nonlinear processes should dominate under such conditions. For a large extent, it is true, but at the same time, observations indicate that in the process of propagation of acoustic-gravity waves (AGW) in many cases, the effects can be comprehensively described within the framework of the linear approximation of perturbation theory and well developed theory of oscillations. At the same

time, under creating models of process it turned out to be appropriate to use sufficiently justified physical approximations, such as isothermality of the atmosphere, its unlimitedness in the horizontal direction and compressibility in the vertical direction. At the same time, taking into account the real scales of the AGW, it is possible to neglect the curvature of the Earth's surface and consider it locally flat at any point of the surface, and use the Cartesian coordinate system X, Y, Z in the calculations. To describe the environment, it makes sense to use non-dissipative hydrodynamics, and in an equilibrium state the hydrostatic equilibrium equation and barometric equation. The above-mentioned approximations and the mathematical apparatus of the theory of oscillations and the theory of differential equations allow, when studying the initial system of equations describing the dynamics of AGW, to obtain a dispersion equation in the form of a polynomial of the fourth degree relative to the angular frequency of rotation ω as a function of the normalized wave vector of disturbance $\vec{k}$ (AGW). AGW spectrum is a spectrum of the atmosphere's own oscillations in the form $\omega = \omega\left(\vec{k}\right)$ and its obtaining can be considered as final solution of the initial problem, if we ignore the obvious influence on the AGW spectrum of the angular frequency of rotation of the atmosphere Ω, which must necessarily be present in the dispersion equation due to the influence of the Coriolis force. The formal reason for the absence of the components of the vector Ω in the dispersion equation (DE) is the fact that the $\left|\vec{\Omega}\right|$ is minimum of two orders of magnitude smaller than the characteristic rotation frequency of the atmosphere ω_0, which is equal to the acoustic cutoff frequency. At the same time, the improvement of modern atmospheric observation equipment places increases the requires for the accuracy of DE model solutions.

We study in detail the dispersion equation for latitudinal AGW. The need for such consideration, as will be shown, is a consequence of the structure of this equation, namely, the presence of a linear frequency term in it. Preliminary analysis showed that existing mathematical methods do not provide an unambiguous solution to this equation. This suggests the need to study possible solutions of the equation in terms of their coincidence with previously obtained ones for some partial cases. Such research allows us to choose the right decision. In the proposed study, we have shown that the Euler-Lagrange method allows, under certain additional conditions, to obtain an exact solution of the modified equation for AGW in closed analytical form.

Second-Order Fractals in the Geospace Researches

L.F. Chernogor[1], O.V. Lazorenko[1], A.A. Onishchenko[2]

[1]V.N. Karazin Kharkiv National University, Kharkiv, Ukraine
[2]Kharkiv National University of Radioelectronics, Kharkiv, Ukraine
oleg.v.lazorenko@karazin.ua

According to the non-linear and the system paradigms, many processes generated in open, non-linear, dynamical systems under influence of a powerful source of energy release are appeared to be short-time, ultra-wideband, non-linear and fractal. The geospace was shown to be a good example of such systems. Many processes caused in geospace by the non-stationary powerful sources of energy release have significant fractal properties. Therefore, the investigations of such properties seems to be actual and interesting.

The purpose of this work is to find so called 'second-order fractals' in the signals and processes registered in geospace during impact of different non-stationary powerful sources of energy release, such as geospace storms, earthquakes, meteoroid falls and other.

The concept of the second-order fractals has been introduced by the authors of this paper in early 2023. Let's consider the main idea of this concept. Well known that to describe a mono-fractal signal, it is necessary to use only one value of the fractal dimension chosen for its analysis. Namely for this reason, such signal was called as 'mono-fractal'. In such case, its fractal dimension D will be constant and not a function of time t, that is $D \neq D(t)$. But in many practical investigations, being locally mono-fractal (or almost mono-fractal), the real natural signal is appeared to be non-stationary (of course, in sense of fractal properties) and has the fractal dimension $D(t)$, which varies in a time. Strictly speaking, as well as fractal dimension of the signal analyzed has been changed in time, then such signal is a multi-fractal one, and for its investigation, the multi-fractal methods should be used. Nevertheless, we shall consider only the mono-fractal analysis methods used with application of a sliding window in time domain. Such approach was shown to be quietly correct in this case. For a one-dimensional fractal signal $s(t)$, there is only one strict requirement to $D(t)$ function, namely, $1 < D(t) < 2$. If $D(t) = 1$, then a signal is appeared to be non-fractal one. It means that function $D(t)$ can be as smooth as non-differentiable, as deterministic as

stochastic. Briefly speaking, it can be a fractal function too. Basing on these reasons, we have proposed a new class of fractals called as 'the second-order fractals'. By the definition, second-order fractal is a fractal, fractal dimension of which is appeared to be a fractal function of time or space variable. A fractal signal with such property is called as second-order fractal signal. Moreover, in such way, the fractals of higher (third, fourth and other) orders can be introduced.

A simple theoretical deterministic model of the second-order fractal signal can be created with application, for example, of well-known non-stationary Weierstrass function, in which the time-dependent Holder exponent ($0 < H(t) < 1$) is present. In turn, to be a fractal function, the Holder exponent $H(t)$ can be modeled with application, for example, the ordinary Weierstrass function. Using such simple models, the fractal and time-frequency properties of the second-order fractal signals were investigated in detail. Moreover, the second-order fractal structures were discovered in temporal variations of the Earth's electromagnetic field detected during the geospace storms, earthquakes and other. The fractal and time-frequency properties of these structures were investigated, the set of corresponding numerical characteristics was estimated.

Work by L. F. Chernogor was supported by the National Research Foundation of Ukraine for financial support (project 2020.02/0015, "Theoretical and experimental studies of global perturbations of natural and man-made origin in the Earth–Atmosphere–Ionosphere system"). Work by L. F. Chernogor also was supported by Ukraine state research project #0121U109881 and #0122U001476.

Estimation of the Geomagnetic Response to the X-class Solar Flares of September 2017

Y. Luo[1,2], L.F. Chernogor[1], K.P. Garmash[1]

[1]V.N. Karazin Kharkiv National University, Kharkiv, Ukraine
[2]Ghent University, Ghent, Belgium
leonid.f.chernogor@gmail.com

The impact of solar flares on the near-Earth environment has been extensively studied over the years. In this research, we analyzed the geomagnetic response to X-class solar flares that occurred in September 2017, using data obtained from the Low-Frequency Observatory of the

Institute of Radio Astronomy of NASU and the Magnetometric Observatory of V. N. Karazin Kharkiv National University (KhNU). Our study compared observations with estimates to understand the effects of solar flares on the near-Earth environment.

The analysis of time variations in the Earth's magnetic field was conducted using data obtained from two observatories: the Low-Frequency Observatory of the Institute of Radio Astronomy of NASU (located at 49.93°N, 36.95°E) and the Magnetometric Observatory of KhNU (located at 49.64°N, 36.93°E). The Low-Frequency Observatory employs a magnetometer with a high temporal resolution of 1 second and a sensitivity of 10 pT to measure the *H*-, *D*-, and *Z*-components of the magnetic field. The Magnetometric Observatory utilizes a magnetometer-fluxmeter to measure fluctuations in the horizontal *H*- and *D*-components of the geomagnetic field in the period range of 1–1000 s, with a time resolution of 0.5 s. The sensitivity of the magnetometer is at least 1 pT–1 nT for periods 1– 1000 s.

The main effects of solar flares were estimated by determining the magnitude of X-ray radiation with a wavelength that penetrates up to a minimum height. The minimum height was estimated to be between 80-110 km using the ionization cross-section and the concentration of neutral particles at a certain altitude. The heating of atmospheric gases due to X-ray radiation was estimated using the mass of heated air, specific heat capacity of the gas at constant pressure, and gas temperature. Our estimated results showed good agreement with the observed results, including: (1) The estimated atmospheric heating caused by X-ray emissions was approximately 1-10 K. (2) X-ray radiation with a wavelength of 0.1-1 nm and an energy flux of around 0.001W/sq.m increased the electron concentration in the dynamo region's heights by approximately 10-100%. When the energy flux was reduced to around 0.0001 W/sq.m, the disturbances were an order of magnitude smaller. (3) The increase in electron concentration resulted in a decrease of all components of the main geomagnetic field by tens of nanotesla. However, the reduction in the level of fluctuations in the horizontal components of the geomagnetic field, in the period range of approximately 100-1000 s, was only one order of magnitude smaller.

Our study provides estimates of the geomagnetic response to X-class solar flares of September 2017. The estimates suggest that solar flares have minimal impact on the heating of the Earth's atmosphere, but can significantly impact the ionization of the atmosphere. The estimated magnitude of X-ray radiation and heating of atmospheric gases due to solar flares will aid in the prediction and understanding of geospace storms, which have significant

scientific and practical importance. Further studies are needed to understand the long-term effects of solar flares on the Earth's environment.

Work was supported by the National Research Foundation of Ukraine for financial support (project 2020.02/0015). Work by L. F. Chernogor was supported by the Ukraine state research project #0121U109881 and #0122U001476, work by K. P. Garmash was supported by the Ukraine state research project #0121U109882, and work by Y. Luo was supported by the Special Research Fund of Ghent University of Belgium (project #BOF22/CDV/061).

October 25, 2022, Solar Eclipse Manifestations in the Ionospheric Effects over Northern Eurasia

L.F. Chernogor[1], Y.B. Mylovanov[1], V.L. Dorohov[1]

[1]V. N. Karazin Kharkiv National University, Kharkiv, Ukraine
hobit1957@gmail.com

The purpose of this study is to describe the features of the ionospheric effects observed during the October 25, 2022, partial solar eclipse that occurred early in the morning at subauroral latitudes. The temporal variations were studied in the total electron content (TEC) derived from measurements made between 15 ground-based receivers and the Global Positioning System satellites (G03, G04, G06, G09, G11, G12, G16, G19, G20, G22, G25, G26, G29, G31). During the solar eclipse, the state of space weather was determined to be quiet, which was favorable for observing the effects that the solar eclipse had on the ionosphere.

The solar eclipse first contact occurred at 08:58 UTC to the north of Ireland, and the fourth contact took place at 13:02 UTC within the Arabian Sea. The partial eclipse became a total eclipse only outside the planet. From 09:00 UTC to 11:00 UTC, the Moon’s shadow moved eastward along the Arctic Circle, and the maximum phase of the eclipse took place near the city of Nizhnevartovsk (61.6°N 77.4°E) where the eclipse magnitude reached 0.86 at 11:00:09 UTC. Further, the trajectory of the Moon’s shadow traversed the dusk terminator, which complicated the display of the eclipse effects. Nevertheless, the ionospheric effects of the solar eclipse were confidently detected despite a significant complication created by the twilight zone.

To study the effects that the solar eclipse had on the ionosphere, the Besselian elements has been used to estimate the phase of the eclipse, the

fraction of the sun's area occulted, and the fraction of the absorbed solar energy in the places where the TEC measurements were taken. A noticeable decrease in TEC has been determined to arise upon a 0.1 increase in the eclipse phase. The ionospheric response persisted over a time interval of 100–120 min, which virtually equals the time length of the solar eclipse. The maximum TEC reductions were estimated to reach values of about 2 TECU to 15 TECU, with an average of 5.8 TECU. The relative reduction varied from –20% to –40%, with an average of –27%.

The reduction in TEC exhibited maximum in 30–40 min after the moment the solar eclipse attained the maximum phase. The time lag between the ionospheric response and the solar eclipse maximum indicates the inertia of the chemical processes in the ionospheric *F* region. This time lag is determined by oxygen ion–nitrogen molecule and oxygen ion–oxygen molecule reaction rates.

A characteristic feature of this eclipse is that it occurred before the polar night. For instance, the receiver at the city of Kiruna is located to the north of the Arctic Circle, and the polar night there lasts from December 11 to January 2. Thus, the insufficient amount of solar energy in the subauroral ionosphere during this particular solar eclipse made it possible to more accurately estimate the relation between the eclipse phase and the subsequent reduction in TEC. The local time dependence of the magnitude of the TEC reduction due to the solar eclipse has been revealed, viz., the TEC reduction increased during the daytime, while wave disturbances in TEC were not observed.

The work was partially supported by the National Research Foundation of Ukraine for financial support (project 2020.02/0015, "Theoretical and experimental studies of global disturbances from natural and technogenic sources in the Earth-atmosphere-ionosphere system"). The work was also partially supported by the Ukraine Ministry of Education and Science research projects (#0121U109881, #0121U109882, and #0122U001476).

Investigation of ionospheric wave processes at midlatitudes during magnetic storm period using incoherent scatter and GNSS data

S.V. Panasenko[1], K.D. Aksonova[1,2], V.V. Skipa[3], I.F. Domnin[1]

[1]Institute of ionosphere, Kharkiv, Ukraine
[2]Institute of Atmospheric Physics of the Czech Academy of Science, Prague, Czech Republic
[3]Institute of Radio Astronomy of the National Academy of Sciences of Ukraine
sergii.v.panasenko@gmail.com

The energy that comes to the Earth from the Sun during geomagnetic storm periods assists a significant enhancement of the total electron content and plasma redistribution processes. Such processes induce atmospheric gravity waves that are manifested as traveling ionospheric disturbances (TIDs) at ionospheric heights. TIDs classified into two types: medium-scale and large-scale disturbances. Evidence for the presence of LS structures occurrence in the ionosphere has been available from the 1950s onwards. It has been confirmed that the large scale TIDs (LSTIDs) have periods of 30 min to 3 h, speeds of 300 to 1000 m/s, horizontal wavelengths exceeding 1000 km and predominantly equatorward propagating for thousands of kilometers without significant attenuation. Despite the fact that a large number of studies devoted to the study of such structures by now, a complete understanding of the sources and mechanisms of their generation, strengthening and direction of movement are still an open question. This is due to the different reaction of the ionosphere even to storms with a similar intensity. In general, the parameters of ionosphere, and hence TIDs parameters, depend on the local time of the storm onset, the intensity of the storm, geomagnetic conditions preceding the event under study, the geomagnetic / geographical observation site, the season, the phase of the solar cycle, etc. These questions can be solved using complex research methods. Therefore, it is necessary to study the ionosphere state at the local, regional and global level for each specific storm which will provide additional information about all processes that occur in it.

In this study we focused our attention on analyzing TIDs induced during the moderate magnetic storm of 22 – 24 September 2020 at midlatitudes. For these purposes, we used the data obtained from the Kharkiv incoherent scatter radar (ISR) and GNSS receiver located in the Ionospheric observatory of

Institute of ionosphere. We also used the unified methodology for a joint analysis of the GNSS- and ISR-derived time series. This method incorporates the estimation of long-term variations (trends), removal of these trends to yield the perturbation quantities (absolute variations) and division by the trends to yield the fractional perturbations (relative variations) as well as a spectral analysis and bandwidth filtration. Additionally, the new developed methodology based on the fuzzy logic algorithms was applied to clearly identify a number of wave patterns in the altitude-time incoherent scatter power relative variations.

During the magnetic storm period, the numerous TIDs in wide period range were detected over Kharkiv. They are likely associated with the substorm activity and solar terminator passage. Analysis of the ISR data enabled characterization of TIDs having the dominant periods from 41 to 168 min and the maximum relative amplitudes of 0.10 – 0.43. The enhanced TID activity in the nighttime of 24 September 2020 and near the sunrise and sunset periods was documented. The altitudes where these TIDs reach the maximum amplitudes were of 190 – 235 km. TID horizontal phase velocities and wavelengths estimated from ISR data evidenced that LSTIDs mainly occurred during the observation period. The GNSS derived results confirmed the propagation of LSTIDs in the same time intervals where they were revealed using ISR data.

Energy conversion rate spectra in the Earth's magnetotail

B. Petrenko[1,2], L. Kozak[1,2], E. Kronberg[3], I. Ballai[4], V. Fedun[4]

[1]Taras Shevchenko National University of Kyiv, Kyiv, Ukraine
[2]Institute of Space Research, Kyiv, Ukraine
[3]Geophysics Department of Earth and Environmental Sciences University of Munich, Munich, Germany
[4]Plasma Dynamics Group, School of Mathematics & Statistics, University of Sheffield, Sheffield, UK
gutovska@ukr.net

Turbulence is a fundamental plasma process occurring in the Universe ubiquitously. It controls the transfer of energy, mass, and momentum in space plasmas. Dissipation is an important process of destruction of turbulent energy cascade rate at kinetic scales. In our work, we have considered multiple current sheet crossings to investigate scale features of turbulence

dissipation in the Earth's magnetotail. In the magnetotail, the energy at the largest scales comes from the solar wind-magnetosphere interaction and dissipates at the smallest scales due to wave-particle interactions and viscous heating. For high-beta plasma, the non-local energy transfer is present, so the conversion of bulk kinetic energy into heat occurs even in the inertial range. Therefore, the goal of our study was to observationally quantify such dissipation effects in plasma sheet turbulence using multi-spacecraft measurements and methods.

Measurements of electromagnetic fields and plasma parameters from the MMS mission were used for the research. We have applied multi-spacecraft techniques to derive current density, and then build energy conversion rate spectra using continuous wavelet transforms of electric field and current density. It allowed us to uncover dissipative scale features, and how dissipation converts eddies' energy into the plasma population. Non-constant energy transfer rate indicates not fully developed intermittent turbulence, such that cannot be described by Kraichnan and Kolmogorov phenomenology.

This work was supported by grant No. 97742 of the Volkswagen Foundation (VW-Stiftung), the Royal Society International Exchanges Scheme 2021 (211177) and BF/30-2021.

Large-scale MHD ionospheric disturbances of the planetary electromagnetic waves type

Y. Rapoport[1], V. Grimalsky[2], S. Petrishchevskii[3]

[1]University of Warmia and Mazury in Olsztyn, Poland
[2]CIICAp, Autonomous University of State Morelos (UAEM), Cuernavaca, Mor., Mexico
[3]Taras Shevchenko National University of Kyiv, Ukraine
msergiyp@gmail.com

An extended theory of large-scale magnetohydrodynamic (MHD) ionospheric disturbances of the planetary electromagnetic waves (PEMW) type is considered. The present research on the theory of large-scale MHD nonlinear waves in the inhomogeneous ionosphere is a farther extension of the approach [1], but out of the frameworks of the standard "β-plane" approximation. The theory includes the system of nonlinear MHD equations

of motion of the ionospheric plasma medium, taking into account the rotation of the Earth and the presence of the geomagnetic field.

The origin of the large-scale PEMW type disturbances is associated with ultralow frequency (ULF)-emission from the side of the solar wind and magnetosphere and also from powerful sources in the lower atmosphere. Nonlinearity, inhomogeneity and diffusion losses determine the conditions for the existence of structures.

Numerical calculations of the evolution of initial mechanical, magnetic and combined vortex disturbances for different heights of the F-layer of the ionosphere have been performed. The calculations were carried out for different sets of ionospheric parameters that differ by season and time of day. It is shown that in comparison with the calculations obtained in the beta approximation, such disturbances have a longer characteristic time of live (about tens of minutes) and a greater spatial concentration. The characteristic magnetic fields of these structures are ~(1-100) nT.

1. Rapoport Yu.G. Exitation of planetary electromagnetic waves in the inhomogeneous ionosphere / Yu. Rapoport, Yu. Selivanov, V. Ivchenko, V. Grimalsky, E. Tkachenko, V. Fedun // Ann. Geophys. – 2014. – Vol. 32. – P. 1-15.

Baseline air pollution for assessment the consequences of Russian invasion of Ukraine

M.V. Savenets, T.V. Kozlenko, K.M. Komisar, A.P. Umanets, N.S. Zhemera

Ukrainian Hydrometeorological Institute, Kyiv, Ukraine
savenetsm@gmail.com

The full-scale Russian invasion of Ukraine is having a tremendous negative impact on the environment. Among environmental components, atmospheric air faced continuous pressure because of pollutants' emissions. At the same time, assessing the consequences for air quality remains challenging due to the changeable atmospheric dynamics and chemistry. All the tasks connected with the assessment of air quality changes, estimation of risks and losses due to air pollution, cost calculations, etc., require not only the accurate fixation and monitoring of observed accidents but also the necessity of a pre-war baseline for comparison.

In this study, we analyzed ground-level concentrations of air pollutants (dust, sulfur dioxide (SO_2), carbon monoxide (CO), nitrogen dioxide (NO_2) and formaldehyde (CH_2O)) and remote sensing data of atmospheric composition (column number densities of NO_2, CO, SO_2 and CH_2O) collected for a period of 2019-2022, which can be used as a baseline air pollution before the war.

Normally, air quality in Ukrainian cities was affected by elevated concentrations of one or two main pollutants, most commonly dust and NO_2. The frequency of threshold levels reached 33% for NO_2, 50% for dust, 35% for CO and 60% for CH_2O. In the most polluted industrial cities, average content was ca. 5-10 times higher depending on pollutant in comparison to smaller regional centers. By combining ground-level and remote sensing observations and analyzing meteorological conditions, we examined the reasons for data inconsistencies and similarities among spatial air pollution hotspots. Six polluted areas were identified: 1) Donestk region; 2) the line of cities Kamianske – Dnipro – Zaporizhzhia together with the surrounding cities of the Kakhovka Reservoir; 3) the line of cities Gorishni Plavni – Kremenchuk – Svitlovodsk; 4) Kharkiv together with the Zmiiv thermal power station (TPP); 5) the area from Kyiv to the Trypilliia TPP; 6) the area around the Burshtyn TPP and the Dobrotvir TPP.

Infrasonic effect of the Kyiv meteoroid

L.F. Chernogor[1], O.I. Liashchuk[2], M.B. Shevelev[1]

[1]V.N. Karazin Kharkiv National University, Kharkiv, Ukraine
[2]Main Center of Special Monitoring, Institute of Space Research, Kyiv, Ukraine
mykyta.b.shevelev@gmail.com

The fall of a sufficiently large meteoroid (superbolide effect) is accompanied by disturbances in the atmosphere, as well as in the lithosphere, ionosphere, and magnetosphere, and in all geophysical fields. The baric field is no exception.

The aim of this work is a preliminary description of the infrasonic effect of a meteoroid that swept over northern and central Ukraine on April 19, 2023 at 18:57:20 UT. When moving over Kiev, its height was about 80 km. It is reasonable to call this meteoroid the Kyiv meteoroid. The space body, which was moving from the northeast to the southwest, exploded at an altitude of

about 38 km. The magnitude of the flare was –18. The explosion was accompanied by the generation of a sufficiently powerful shock wave and infrasound. Infrasonic fluctuations are registered by the Ukrainian network of means of special control. As an example, let us consider temporal variations in pressure in an infrasonic wave recorded at Gorodok and Malin stations. At Gorodok station, the signal appeared at 19:01:31.8 UT and lasted approximately 4 s. In all signal channels, a positive pressure surge with a duration of 0.7 s was observed, followed by a negative surge with an amplitude almost two times smaller than the same duration. Oscillations with an average period of about 0.44 s were superimposed on the negative spike. A total of 9 oscillations were observed. This behavior of pressure variations is characteristic of a shock wave. Knowing the oscillation period allows us to estimate the energy of infrasound, which was about 1.4 GJ. At a distance of 92.4 km from the explosion height to Gorodok station, the speed of arrival of the infrasonic signal was close to 367 m/s. The behavior of the infrasonic signal at Malin station was somewhat different. The signal arrived at 19:02:19.5 UT and lasted 3.25 s. It consisted of three trains, each about 1 s long. At a distance from the explosion height to the station of 108.9 km, we have an infrasonic signal arrival velocity of 361 m/s. This value of velocities is characteristic of the shock wave velocity. The presence of atmospheric-stratospheric wind also affected the velocity value. The average period of 24 oscillations was about 0.135 s.

The work of Chernogor L.F. and Shevelev M.B. partially has been supported by the National Research Foundation of Ukraine (grant no. 2020.02/0015; “Theoretical and experimental studies of global disturbances from natural and technogenic sources in the Earth-atmosphere-ionosphere system”). The work Chernogor L.F. and Shevelev M.B. partially also has been supported by a Ukraine state-funded research projects (grant no. 0121U109881, 0122U001476).

Impact of the major sudden stratospheric warming on mid-latitude weather/climate

Y. Shi[1], G. Milinevsky[1,2,3], O. Evtushevsky[2], L. Wang[1]

[1]International Center of Future Science, Jilin University, Changchun, China
[2]Taras Shevchenko National University of Kyiv, Kyiv, Ukraine
[3]National Antarctic Scientific Center, Kyiv, Ukraine
shiyu18@mails.jlu.edu.cn

Major sudden stratospheric warming (SSW) events occurred in the Northern Hemisphere during the winter 2018. In mid-February 2018, the stratospheric polar vortex in the Arctic split into two sister vortices, the zonal wind reversed in the stratosphere–mesosphere from westerly to easterly, and warm air penetrated the polar cap regions. This process caused large-scale disturbances in the middle atmosphere of the polar and middle latitudes.

The impact of these dramatic changes extends both vertically, down into the troposphere and up into the mesosphere, and horizontally into mid- and low latitudes. On average, split events account for about 50% of SSWs, and a surface response can first appear within 2–3 days after their onset. It was shown that the stratospheric anomaly could lead the surface signal with a lag of around +3 days, and surface anomalies can persist for up to 60 days. Another critical factor in the connection between the troposphere and stratosphere is their coupled thermal state, usually realized through the tropopause. In general, the tropopause ascent/descent is related to a warming/cooling in the upper troposphere and a cooling/warming in the lower stratosphere, as well as to anticyclonic/cyclonic systems in the troposphere.

The impact of the Arctic major sudden stratospheric warming in 2018 on regional cold weather in the northern midlatitudes is analyzed. Data from temperature observations in Changchun (Northern China) and Kharkiv (Northern Ukraine) and NCEP–NCAR reanalysis are used. The variability of the vertical profiles of temperature anomalies in latitude and longitude during two strong surface cooling events is compared. Weather anomalies in Changchun and Kharkiv appeared under strong vortex conditions with wave-1 dominance (the pre-SSW period in January) and during vortex perturbation and split due to intensification of wave-2 (major SSW in February), respectively.

The results show that in both cases, surface cooling looks like a response to rapid tropopause descent under the influence of heating in the lowermost stratosphere. The positive stratospheric temperature anomaly migrated both downward, penetrating the lowermost stratosphere at 200–300 hPa, and equatorward, reaching midlatitudes. The change in the lowermost stratosphere heating is associated with lowering the tropopause by 2–3 km in 5–7 days and the appearance of the negative surface anomaly of about –12°C. Maximum tropopause pressure increased to about 400 hPa (~7 km), while climatologically, it is usually ~9–10 km in mid-latitudes. Observations showed that the surface temperatures during these events dropped by 18°C in Changchun and by 14°C in Kharkiv. The results are generally consistent with the concepts of tropospheric column compression below the lowered tropopause and surface amplification of the stratospheric signal discussed in other works.

This work was partly supported by the project BF/30-2021 of Taras Shevchenko National University of Kyiv. Part of this research was performed at the International Center of Future Science, Jilin University (JLU), under the contract with the JLU.

A new microwave radiometer system for observing O_3 and CO in the atmosphere

L. Wang[1], Y. Shi[1], O. Pylypenko[1], X. Wang[1], G. Milinevsky[1,2]

[1]International Center of Future Science, Jilin University, Changchun, China
[2]National Antarctic Scientific Center, Kyiv, Ukraine
ldwang22@mails.jlu.edu.cn

More remote sensing techniques need to be expanded for measuring vertical profiles of several gases in the stratosphere and mesosphere. Because microwaves can penetrate clouds, light rain, and fog, radiometers are less affected by weather changes. The ground-based microwave radiometer is the only measurement method that continuously observes O3 and CO in the middle atmosphere for 24 hours. Due to radiation signals with frequencies higher than 150 GHz muted by water vapor in the troposphere, only molecules with emission lines lower than 150 GHz can be observed. However, microwave instruments placed at sites at high altitudes and in dry atmospheric conditions can avoid water vapor influence [1, 2]. The CO and

O3 gases have sufficiently strong emissions at frequencies below 150 GHz. Therefore, microwave technology can provide CO and O3 measurement information below 150 GHz. These measuring instruments only exist in relatively few places. More simple and reliable instrument solutions are needed to extend the measurement technology more widely. The need is acute today because the number of satellite sensors observing the middle atmosphere is about to shrink dramatically.

The report introduces the radiometer's overall framework, including the antenna, RF LNA, HPF, Mixer, and IF LNA. The receiver back-end module includes a double mixer module and a double local oscillator module. Radiometer also consists of the National Instrument QuickSyn frequency synthesizer that can switch output frequency 52.0768 or 52.1068 GHz and FFTS module. The main control board controls the synthesizer through the BIFROST program. Compared with the microwave radiometer RSO3CO-120-1 located at Jilin University, the receiver cooling back-end unit is integrated into a small module, making the receiver size smaller.

In the future, we are planning the following works: (1) complete the construction and testing of the radiometer RF receiver; (2) control panel design of National Instrument QuickSyn frequency synthesizer FSL-5067 was completed (3) complete the FFTS based on USRP (4) complete the construction of cold load and hot load (5) complete the acquisition and processing of radiometer measurement data, and perform inversion to determine the accuracy of measurement data.

This work was partly supported by the project BF/30-2021 of Taras Shevchenko National University of Kyiv. Part of this research was performed at the International Center of Future Science, Jilin University (JLU), under the contract with the JLU.

1. Nagahama, T.; Nakane, H.; Fujinuma, Y.; Ninomiya, M.; Ogawa, H.; Fukui, Y. Ground-based millimeter-wave observations of ozone in the upper stratosphere and mesosphere over Tsukuba. Earth Planets Space. 1999, 51, 1287–1296.

2. Shi Y.; Shulga V.; Ivaniha O.; Wang Y.; Evtushevsky O.; Milinevsky G.; Klekociuk A.; Patoka A.; Han W.; Shulga D. Comparison of major sudden stratospheric warming impacts on the mid-latitude mesosphere based on local microwave radiometer CO observations in 2018 and 2019. Remote Sens., 2020, 2(23), 3950.

3. Forkman, P.; Christensen, O.M.; Eriksson, P.; Billade, B.; Vassilev, V.; Shulga, V.M. A compact receiver system for simultaneous measurements of mesospheric CO and O3. Geosci. Instrum. Method. Data Syst. 2016, 5, 27–44.

The impact of the Russian-Ukrainian war on the characteristics of aerosols in the atmosphere over Kyiv and Ukraine

Yu. Yukhymchuk[1,2,3], G. Milinevsky[1,4,5], V. Danylevsky[1,4], I. Fesianov[4]

[1]Main Astronomical Observatory of National Academy of Sciences of Ukraine, Kyiv, Ukraine
[2]Laboratoire d'Optique Atmosphérique, University of Lille, Lille, France
[3]Institute of Physics of National Academy of Sciences of Ukraine, Kyiv, Ukraine
[4]Taras Shevchenko National University of Kyiv, Kyiv, Ukraine
[5]College of Physics, International Center of Future Science, Jilin University, Changchun, China
yuliia.yukhymchuk@mao.kiev.ua

According to AERONET observations, changes in the annual dynamics of the Angstrom exponent in 2022 were detected. The AE values decreased, and there was an increase in the influence of the coarse mode. Analysis of changes in the complex refractive index of aerosols in the atmosphere over Kyiv found an increase in both the real and imaginary parts of it, indicating a shift in the dominant type of aerosols in the atmosphere in 2022. The results of the radiative forcing assessment showed more noticeable changes in the upper atmospheric boundary in 2022. While no abnormal increases in $PM_{2.5}$ concentrations were detected by the AirVisual network during 2022 and early 2023, the AQI remained above the WHO recommended level and exceeded 50 during the cold season, particularly in March and April of 2022.

The average ground-level concentrations of $PM_{2.5}$, SO_2, SO_4, and NO_2 during February 16–23 and February 24 – March 2, 2022 were analyzed using MERRA-2 reanalysis. It was shown that prior to February 24, relatively low average concentrations of particulate matter were observed in Ukraine, but the situation drastically changed thereafter. $PM_{2.5}$ levels increased by at least two times. Moreover, it was found that the average mass concentration of sulfates in the atmosphere over Ukraine increased following the full-scale invasion.

This work was partly supported by the project BF/30-2021 of Taras Shevchenko National University of Kyiv. Part of this research was performed

at the International Center of Future Science, Jilin University (JLU), under the contract with the JLU.

Ionospheric effects of 5–6 January 2019 solar eclipse over the People's Republic of China

L.F. Chernogor[1, 2, 3], K.P. Garmash[1], Q. Guo[2], V.T. Rozumenko[1], Y. Zheng[3]

[1]V. N. Karazin Kharkiv National University, Kharkiv, Ukraine
[2]Harbin Engineering University, Harbin, China
[3]Qingdao University, Qingdao, China
k.p.garmash@gmail.com

The purpose of this work is to present the observations of variations in the Doppler spectra and in the amplitudes of radio waves that travelled along oblique propagation paths over the People's Republic of China (PRC) in the course of the partial solar eclipse of 5 – 6 January 2019 UT period and on the previous and next days.

In the PRC, the solar eclipse was observed to be partial. The eclipse magnitude at an altitude of 100 km under the propagation path midpoints varied from 0.356 to 0.614, whereas the eclipse obscuration varied from 23.5 % to 51.6 %. The eclipse duration changed from 133 min to 160 min. In a number of regions of the PRC, the solar eclipse began to occur prior to sunrise.

In general, the states of solar activity and space weather were favorable for the observations of ionospheric effects from the partial solar eclipse over the PRC: the magnetic field perturbation, $K_p \approx 3$, took place during 6 January 2019, when the value of the D_{st} index did exceed –10 nT.

The observations of the effects from the solar eclipse were made with the multi-frequency multiple path radio system designed to probe the ionosphere obliquely. This study makes use of signals that were transmitted by the broadcasting stations at Lintong/Pucheng, Hailar/Nanmen, Beijing, Shijiazhuang, and Hohhot (PRC), Hwaseong and Goyang (Republic of Korea), Chiba/Nagara and Yamata (Japan), Ulaanbaatar/Khonkhor (Mongolia), and Yakutsk (Russian Federation), 14 propagation paths altogether in the frequency range 5–10 MHz.

The response of the ionosphere to the solar eclipse have been inferred from temporal variations in the Doppler spectra, the Doppler shift, and in the

signal relative amplitude. The solar eclipse was accompanied by Doppler spectrum broadening, up to ±1.5 Hz, by alternating sign Doppler shift variations, up to ±0.5 Hz, in the main ray, and by quasi-periodic Doppler shift changes. Using alternating sign Doppler shift variations during the period of the maximum occultation of the Sun's surface area, the greatest decrease in the electron density has been estimated to be about –15 %, whereas the theoretical model has shown that it is –16 %, which may be considered as being in good agreement. The atmospheric gravity waves launched by the solar eclipse acted to excite quasi-periodic, 15 min period variations in the Doppler shift, while the amplitude of the perturbations in the electron density has been estimated to be 1.6–2.4 %. The infrasound waves launched by the solar eclipse acted to excite quasi-periodic, 4–5 min period variations in the Doppler shift, whereas the amplitude of the perturbations in the electron density has been estimated to be about 0.2–0.3 %.

Features of the magneto-ionospheric effects of the March 21–23, 2017 geospace storm

L.F. Chernogor, K.P. Garmash

V.N. Karazin Kharkiv National University, Kharkiv, Ukraine
k.p.garmash@gmail.com

The purpose of this report is to present the results of the analysis of the magneto-ionospheric effects that accompanied the geospace storm (GSS) of March 21 to 23, 2017. The following tools were used to observe effects in the ionosphere and in the magnetic field caused by the geospace storm of March 21 to 23, 2017: a custom-made digital ionosonde and a Doppler vertical sounding radar located at the V.N. Karazin Kharkiv National University Radiophysical Observatory (49°38′ N, 36°20′ E) and a fluxmeter-magnetometer at the Magnetometer Observatory of the Kharkiv National University (49°38′ N, 36°56′ E). As a rule, the Doppler vertical sounding radar makes measurements at two fixed frequencies, 3.2 and 4.2 MHz. The smaller of them is effective when studying dynamic processes in E and F1-layers and the larger one, in F1 and F2-layers. The fluxmeter-magnetometer is intended for monitoring the variations of horizontal H- and D-components of the geomagnetic field in the time range 1 – 1000 s. Ionospheric processes are analyzed using ionograms.

A geospace storm, the energy per unit time of which reached 20 GJ/s, was observed on March 21 to 23, 2017. The storm is classified as weak based on its intensity. The geospace storm was accompanied by a weak ionospheric disturbance in the daytime and a strong ionospheric storm at night. The electron density decreased by 1.3 and 4 – 5 times, respectively. The geospace storm was also accompanied by two moderate magnetic storms with energies of the order of 10^{15} J and a power of 70 GW. On March 21 to 23, 2017, K_p-index values increased from a background value of 0 – 0.3 to 4 – 5.3.

It can be found that the electron density N at 260 km decreased to $N \approx (2 – 2.5) \times 10^{10}$ m^{-3} on the nights of March 21 – 22 and March 22 – 23, 2017. At the same time, it was approximately 10^{11} m^{-3} on the adjacent nights of March 20/21 and March 23/24, 2017, which is four to five times higher. During the daytime around noon on March 21, 2017, $N_0 \approx 4.5 \times 10^{11}$ m^{-3}, while $N \approx 3.5 \times 10^{11}$ m^{-3} on March 22, 2017, at the same time. In this case, $N_0/N \approx 1.29$, and $\delta N = N/N_0 - 1 \approx –0.22$, or –22%. The behavior of N_0/N was qualitatively the same at altitudes of 200 and 230 km. At nighttime, it was impossible to reconstruct $N(z)$ profiles at altitudes less than 200 km.

Ionospheric storms had relatively little effect on the Doppler frequency shift (DSh) while the diurnal variations were more significant. A few hours before sunset at the Earth's level, DSh became negative, and it became positive after sunrise at the ionospheric heights. Quasi-periodic variations of DSh were superimposed on the slow diurnal variations . During the daytime period $T \approx 5 – 8$ min, $f_{da} \approx 0.1$ Hz and it increased to $T \approx 15 – 25$ min and $f_{da} \approx 0.15 – 0.30$ Hz at nighttime.

During the magnetic storms, the level of fluctuations of the horizontal components in the 100 − 1000 s period range increased from ±0.5 to ±5 nT. The results of the system spectral analysis shows that, in the first subrange with periods $T = 1 – 50$ s in a relatively quiet magnetic field, the prevailing period was approximately 35 – 45 s, while it decreased to 30 – 40 s during the GSS. This period is associated with oscillations of the magnetic flux tube at the observation site. The amplitude of these oscillations is the smallest. Decrease of the period during the storm is caused by deformation, more precisely, compression of magnetic field lines. In the second subrange (50 – 200 s), $T \approx 80 – 100$ s and $T \approx 150 – 200$ s predominate under quiet conditions. During the storm, $T \approx 140 – 190$ s. The oscillations with periods $T \approx 600 – 900$ s had the highest amplitude, while the amplitude of the oscillations with periods of 300 to 400 s was somewhat lower.

The work of L. F. Chernogor partially has been supported by the National Research Foundation of Ukraine (grant no. 2020.02/0015; "Theoretical and experimental studies of global disturbances from natural and technogenic

sources in the Earth-atmosphere-ionosphere system"). The work also has been supported by a Ukraine state-funded research projects (grant no. 0121U109881, 0122U001476).

Local and global effects of seismic activity in the atmosphere and ionosphere

I.G. Zakharov, L.F. Chernogor

V.N. Karazin Kharkiv National University, Kharkiv, Ukraine
izakhar@ukr.net

The patterns of seismic-atmospheric-ionospheric coupling on different spatial scales and for moderate to destructive earthquakes (EQs) were studied. Seismic effects in the atmosphere were estimated using surface air pressure and temperature data (https://psn.noaa.gov website). Ionospheric effects were estimated using data on the total electron content (TEC) of the ionosphere (http://www.aiub.unibe.ch/download/CODE/ website). Earthquake data are taken from https://earthquake.usgs.gov/earthquakes/search website. Daily data from 2012 to 2018 were used. The role of moderate and medium EQs is considered on the example of the Vranca seismically active zone, Romania. Atmospheric effects of strong EQs were considered mainly along the latitude of 40 °N, ionospheric – for the entire northern hemisphere, except for the polar region. Both local effects (above EQ hypocenter) and remote (global) effects at an arbitrary distance from EQ hypocenter were considered.

The following main results were obtained.

1. Moderate and medium EQs in the Vrancha zone lead to reliable atmospheric and ionospheric effects lasting several days. Since such EQs are an everyday phenomenon, we get that the lithospheric-atmospheric-ionospheric coupling is implemented continuously, regardless of the presence or absence of powerful disturbances in the Earth's crust and near-Earth space.

2. The seismic-atmospheric-ionospheric effect has a planetary character, which is superimposed by local effects over individual EQs. Average amplitudes of local effects: pressure 2.6 hPa, temperature 1.8 K, TEC 8%. The average amplitudes of distant EQs (global effect): pressure 2.2 hPa, temperature 0.5 K, TEC 4.6 %. The initial surge (decline) of the atmospheric or ionospheric indicator (locally and globally) is followed often by changes with the opposite sign for several days.

3. The amplitude of seismic-atmospheric and seismic-ionospheric effects

is determined by the properties of the Earth's crust at the observation point, the background value of atmospheric pressure and weakly depend on the EQ magnitude. Accordingly, EQs start the process of lithospheric-atmospheric-ionospheric coupling, but do not fully determine its characteristics.

4. The maximum amplitude zone of seismic-atmospheric and seicmic-ionospheric effects falls on middle latitudes, especially 35 - 40 ° N, and within this zone on longitudes near 30 ° W (Mid-Oceanic Ridge) and 140 - 150 ° E (Japanese Islands and adjacent the water area of the Pacific Ocean), as well as along lineaments marking weakened zones of the Earth's crust with an increased flow of deep gases. The latitudinal variations of the amplitude of the seismic-ionospheric effect coincide well with the latitudinal distribution of EQs in both geographic and geomagnetic coordinate systems.

5. The obtained temporal and spatial features of the seismic-atmospheric-ionospheric effect are consistent with the known features of radon emanation and other deep gases. This testifies to the important role of surface air ionization by radon in the initiation of a number of processes leading to the formation of atmospheric and ionospheric anomalies.

This work has been partially supported by the Ministry of Education of Ukraine (grants No. 0121U109881 and No. 0122U001476) and by the National Research Foundation of Ukraine (project 2020.02/0015, “Theoretical and experimental studies of global disturbances from natural and technogenic sources in the Earth-atmosphere-ionosphere system”).

Influence of 27-day solar cycles on the troposphere-stratosphere system

I.G. Zakharov, L.F. Chernogor

V.N. Karazin Kharkiv National University, Kharkiv, Ukraine
izakhar@ukr.net

The research objective is to reveal the regularities of the troposphere-stratosphere system (TSS) response to solar forcing, including the fluxes of galactic cosmic rays (GCRs) modulated by the solar wind. The solar activity (SA) influence on the TSS was considered for 27-day solar cycles, which ensured high uniformity of solar and atmospheric data and allowed us to consider the role of individual influencing factors: UV radiation, GCRs, interplanetary magnetic field, and geomagnetic activity. The study was conducted for the decline phase of the 23rd 11-year solar cycle (2001–2005)

with pronounced 27-day variations of the SA. The main attention is paid to high latitudes.

Statistical analysis revealed stable 27-day variations of TSS indicators with amplitudes of about 4 K for surface temperature, 2 K for the lower stratosphere, 7 hPa for sea level pressure. The tropopause height changes by about 1 km (9%). At the same time, the spatial gradients of surface air temperature and pressure change by 25–75 %. Fluctuation of air temperature occurs in antiphase at the diametrically opposite longitudes of the Eurasia and the North America, which can be considered as a result of periodic displacement and change in the shape of the polar vortex due to modes $m = 1$ and $m = 2$ of planetary waves. 27-day air temperature fluctuations in the troposphere and stratosphere also occur in antiphase, which indicates the important role of internal gravity waves and synoptic waves ($m = 4 – 8$) in the stratosphere-troposphere coupling, including under the influence of SA. In the lowest stratosphere, 13.5-day variations in temperature prevail as a result of the superimposition of 27-day fluctuations with the opposite sign at higher and lower altitudes.

The primary source of 27-day fluctuations in the TSS is most likely stratospheric temperature changes under the influence of solar UV radiation, which corresponds, in general, to the well-known "top-down" mechanism of SA influence on the weather. Features of the stratospheric-tropospheric coupling during 27-day solar cycles also show common features (with a smaller amplitude) with the stratospheric-tropospheric coupling during sudden stratospheric warming.

The influence of GCRs on the troposphere becomes noticeable only if the influence of electromagnetic radiation can be excluded, and is no more than 0.4 K and 4 hPa for surface air temperature and pressure, respectively, as well as changes of up to 4% relative humidity at the height of low cloudiness. These estimates are close to changes in the surface atmosphere that occur under the influence of additional ionization due to radon coming from the soil in seismically active regions. The physical mechanisms are apparently also similar: the newly formed ions become condensation centers for moisture, which leads to an increase in temperature (in the form of latent heat of evaporation), a decrease in pressure and changes in the electrical properties of the atmosphere.

This work has been partially supported by the Ministry of Education of Ukraine (grants No. 0121U109881 and No. 0122U001476) and by the National Research Foundation of Ukraine (project 2020.02/0015, “Theoretical and experimental studies of global disturbances from natural and technogenic sources in the Earth-atmosphere-ionosphere system”).

Features of ionospheric effects from the partial solar eclipse over the city of Kharkiv on 10 June 2021

L.F. Chernogor, K.P. Garmash, Y.H. Zhdanko

V.N. Karazin Kharkiv National University, Kharkiv, Ukraine
eugenezhd@gmail.com

Solar eclipses pertain to high-energy sources of disturbance in the subsystems of the Sun–interplanetary-medium–magnetosphere–ionosphere–atmosphere–Earth and the Earth–atmosphere–ionosphere–magnetosphere systems. During the solar eclipse, the coupling between the subsystems in these systems activates, and the parameters of the dynamic processes become disturbed. Investigation of these processes contributes to understanding of the structure and dynamics of the subsystems. The ionospheric response to the solar eclipse depends on the season, local time, magnitude of the solar eclipse, phase of the solar cycle, the observation site, the state of space weather, etc. Therefore, the study of the effects, which each new solar eclipse has on the ionosphere remains an urgent geophysics and radio physics problem.

The purpose of this paper is to describe the radio wave characteristics and ionospheric parameters, which accompanied the partial solar eclipse of 10 June 2021 over the City of Kharkiv.

To make observations, the means of the HF Doppler measurements at vertical and oblique incidence available at the V.N. Karazin National University Radiophysical Observatory were employed. The data obtained at the "Lviv" Magnetic Observatory were used for making intercomparison.

The radiophysical observations have been made of the dynamic processes acting in the ionosphere during the solar eclipse of 10 June 2021 and on the reference days. The temporal variations in the Doppler frequency shift observed at vertical and oblique radio paths have been found to be, as a whole, similar. Generally speaking, the Doppler spectra over these radio propagation paths were different. Over the oblique radio paths, the number of rays was greater. The solar eclipse was accompanied by wave activity enhancement in the atmosphere and ionosphere. No less than three wave trains were observed. The values of the periods (about 5–12 min) and the relative amplitudes of perturbations in the electron density ($\delta_N \approx 0.3$–0.6%) give evidence that the wave disturbances were caused by atmospheric gravity waves. The amplitude of the 6–8-min period geomagnetic variations has been estimated to be 0.5–

1 nT. Approximately the same value has been recorded in the X component of the geomagnetic field at the nearest Magnetic Observatory. The aperiodic effect of the solar eclipse has appeared to be too small (less than 0.01 Hz) to be observed confidently. The smallness of the effect was predetermined by an insignificant magnitude of the partial eclipse over the City of Kharkiv (no more than 0.11).

The main features of the solar eclipse of 10 June 2021 include an insignificant magnitude of the aperiodic effect and an enhancement in wave activity in the atmosphere, ionosphere and the geomagnetic field.

Work by L. F. Chernogor was supported by the National Research Foundation of Ukraine for financial support (project 2020.02/0015, "Theoretical and experimental studies of global perturbations of natural and man-made origin in the Earth–Atmosphere–Ionosphere system"). Work by L. F. Chernogor, K. P. Garmash and Y. H. Zhdanko also was supported by Ukraine state research project #0121U109881 and #0122U001476.

Ionospheric perturbations that accompanied rocket launches from the Baikonur cosmodrome during solar cycle 24

L.F. Chernogor, Y.H. Zhdanko

V.N. Karazin Kharkiv National University, Kharkiv, Ukraine
eugenezhd@gmail.com

The rocket engine burns release energy comparable to that, which is characteristic of the many natural processes. The energy released by large rockets attains 10–100 TJ, and the engine power 0.1–1 TW. The energy released per unit volume is much higher than the specific energy content and energy release of all natural processes. Disturbances arise in the underlying surface, the atmosphere, the ionosphere, and even in the magnetosphere in the course of the rocket booster stages burns and the orbital maneuvering subsystem engine firings. Effects from rocket engine burns have been studied for a period longer than 60 years, and the results have been published in hundreds of scientific papers, reference books, and monographs. As it turns down, the effects produced exhibit diverse geophysical phenomena. The effects near the rocket trajectory, namely, the area of electron number density depressed (ionospheric hole), as well as the generation of infrasound and atmospheric gravity waves (density waves) have been studied best. The study of the geomagnetic effect has played a prominent role. The Doppler, Faraday,

ionosonde, magnetometer, incoherent scatter, etc., techniques has been used in the study. The effects accompanying the rocket booster stages burns and the orbital maneuvering subsystem engine firings are still under study. Large-scale (~ 1–10 Mm) perturbations arising from rocket engine burns have been studied at the V. N. Karazin Kharkiv National University for many years. Their study has contributed enormously to understand better the mechanisms for transporting perturbations from rockets to global-scale distances, the subsystem coupling in the Earth–atmosphere–ionosphere–magnetosphere system, and ecological consequences of rocket engine burns. Perturbations arising in the atmosphere and geospace significantly depend on the state of atmospheric–space weather, local time, season, and solar cycle. The perturbations arising in the system mentioned above even during the launches of two identical rockets can significantly differ. In addition, the rockets are differing in power, trajectories, kind of fuel, and the cosmodrome location. Therefore, the study of the subsystems response to the rocket booster stages burns and the orbital maneuvering subsystem engine firings remain pressing scientific and technical issues.

The purpose of the present work is to analyze the ionospheric effects from the Soyuz and Proton rockets launched from the Baikonur cosmodrome during solar cycle 24. The ionospheric effects caused by the Soyuz and Proton rockets launches from the Baikonur cosmodrome were observed by the vertical incidence HF Doppler radar. The measurements are taken at two fixed frequencies, 3.2 and 4.2 MHz. The smaller frequency is effective in studying dynamic processes acting in the E and F_1 layers, and the greater frequency is effective in conducting observations of the F_1 and F_2 layers.

The parameters of ionospheric perturbations observed after 81 Soyuz rocket launches and 53 Proton rocket launches from the Baikonur cosmodrome in 2009–2021 have been analyzed. A few groups of time delays have been confirmed to exist between the rocket launch and the supposed ionospheric response to the rocket launch. The magnitudes of these time delays varied from ~ 10 to ~ 300 min. The groups of the time delays correspond to a few groups of the apparent horizontal speeds of disturbance propagation (~ 100–200 m/s; 390 ± 23 m/s; 0.97 ± 0.10 km/s; 1.28 ± 0.13 km/s; 1.68 ± 0.13 km/s; 2.07 ± 0.13 km/s, as well as ~ 8 km/s). The slow atmospheric gravity waves, atmospheric gravity waves of man-made origin, density shock waves, slow and ordinary MHD waves have such speeds. As a rule, the resulting perturbations, except for shock waves, exhibited a quasi-sinusoidal at ~ 5 to ~ 20-min period, and the Doppler shift amplitude was observed to be 0.1–0.3 Hz. The quasi-sinusoidal variations in

the electron density were observed to usually have a relative amplitude of ~ 1–10%, and sometimes to attain ~ 20%.

Work by L. F. Chernogor was supported by the National Research Foundation of Ukraine for financial support (project 2020.02/0015, "Theoretical and experimental studies of global perturbations of natural and man-made origin in the Earth–Atmosphere–Ionosphere system"). Work by L.F. Chernogor and Y.H. Zhdanko also was supported by Ukraine state research project #0121U109881 and #0122U001476.

ІСТОРІЯ АСТРОНОМІЇ

HISTORY OF ASTRONOMY

History of Apollonius Problem, Caustics of an Ellipsoid and possible applications in Astronomy

Ya. Aliyev

ADA University, Baku, Azerbaijan

In the talk we discuss history of Apollonius Problem on the number of normals of an ellipse passing through a given point. By following the footsteps of Apollonius, it is shown that the number is dependent on the position of the given point with respect to a certain astroida. The special case when the point is on the ellipse is studied using the intersection points of the astroida and the ellipse. The problem is then generalized for 3 dimensional space, namely for Ellipsoids. The number in this case is shown to be dependent on the position of the given point with respect to caustics of the ellipsoid. If the given point is on the ellipsoid, then the number of normals is dependent on position of the point with respect to the intersections of the ellipsoid with its caustics.

How many normals can one draw from a point to an ellipse? In the current talk we will try to show different approaches to this problem and its generalization to 3 dimensions, using the methods of calculus, which were not around when Apollonius of Perga (c. III-II centuries BC) first asked and answered this question in his famous work “Conics”. Their number is not the only interesting question about these normals.

The problem about the number of normals, which Apollonius called as the shortest and sometimes the longest line segments, appeared in the fifth book of Apollonius, which survived only in Arabic translation. Apollonius did not mention any practical uses for his results, except that these normals corresponding to minimal and maximal distances, are worth investigating for their own sake and that, in contrast to the tangents, the normals were not studied much by the earlier mathematicians. We also discuss 3 dimensional generalization of the problem which is answered using Caustics of an Ellipsoid. Because of this connection with the extremal distances, there can be applications in optics, wave fronts, mathematical billiards, etc. One of the applications of these results in astronomy can be a possible explanation for the presence of 4 images of a distant quasar, whose light is being bent around elliptical Einstein Ring formed by two galaxies 3.4 billion light-years away.

Astronomical research in Kharkiv at the end of the 19th and the first half of the 20th century

M. Balyshev

Central State Scientific and Technical Archive of Ukraine, Kharkiv, Ukraine

The importance of studying the development of astronomy in Kharkiv at the end of the 19th century – the first half of the 20th century, on the one hand, is caused by the fundamental changes that took place in the methods of astronomical research at that time which led to the development of a system of interdisciplinary astronomical knowledge. The creation of a permanent research base (1883) and the modernization of the arsenal of instruments allowed the astronomical observatory of the Kharkiv University to go beyond the purely educational functions of the auxiliary university institution and to introduce a system of astrometric research and soon expand the field of scientific study. The first stages of the institutional changes gave the opportunity to Kharkiv astronomers already in the 90s of the 19th century to join the implementation of international astronomical programs, in particular to participate in important projects: observation of the stars of the zodiac zone in order to provide the reference stars for planetary observations and to determine the positions and proper stellar motions in relation to which the position of the minor planet (433) Eros has changed; the definition of right ascension and declination of the circumpolar stars in the system of reference stars of the Catalogue of Fundamental Stars NFK and participation in the program of the Berlin Academy of Sciences (compilation of a complete catalogue of stars observed from the middle of the 18th century to 1900); organization of large-scale observations of the total solar eclipse in 1914.

On the other hand, the need to reconstruct facts on the history of astronomy of the period under scrutiny is due to the influence of social and political transformations that took place against the background of the development of astronomical science in Kharkiv caused by the events of the First World War and the Ukrainian Revolution (1917–1921), including the participation of representatives of Kharkiv astronomy in military operations during the Soviet-Ukrainian War; the post-revolutionary reorganization of the university education system in Soviet Ukraine, in particular, the Kharkiv University; structural changes in the organization of scientific institutions connected with the creation of the Department of Scientific Research in

astronomy in 1921 with its subsequent merger with the Astronomical Observatory (1927). As a result of the mentioned reorganization, an important institutional transformation took place during which the status of the Observatory was finally changed from an educational and subsidiary institution to a scientific and research institute.

The implementation of the mentioned organizational stage of institutionalization of astronomical research made it possible during the 1920s and 1930s to significantly modernize the instrumental base of the University Observatory, including the creation of new astrophysical instruments (in particular, the first coronagraph in the USSR), and to develop a system of scientific communications. As a result, there was a deepening of international relations, which was reflected in the Observatory's involvement in the programs of the International Astronomical Union, in particular regarding the observation of reference stars for the coming opposition of the minor planet (433) Eros (1930–1931); the observatory participation in the international project on the Kopf–Rentz observation of the positions of stars for inclusion in the Catalogue of Fundamental Stars FK3; the involvement of Kharkiv astronomers in the creation of a catalogue of faint reference stars which was created for differential meridian observations.

The culmination and logical stage of the development of astronomy in Kharkiv during the studied period should be the institutionalization of astronomical research in a new astronomical center of national importance – the Central Ukrainian Observatory which was supposed to be established in Kharkiv in the second half of the 1930s. But the promising project was never implemented: on the one hand, in connection with the transfer of the capital of Ukraine from Kharkiv to Kyiv in 1934, which caused the relocation of all state bodies that supervised scientific institutions, on the other hand, due to the events of the period of political repression in the USSR in 1937–1938.

Mathematical methods of analysis in astronomy

L. Bashtova

The State Polytechnic Museum named after Boris Paton at Kyiv Polytechnic Institute named after Igor Sikorskyi, Kyiv, Ukraine

The development of astronomy depends on the development of related sciences. First of all, it is physics and mathematics. The achievements of these sciences determine the methods and possibilities of research in astronomy.

Modern spacecraft allow us to plunge into the depths of space, electronic optical devices allow us to see the hidden places of space. The accelerated development of astronomy in the twentieth century was made possible by the rapid development of science and technology.

Mathematical methods of analyzing astronomical phenomena occupy a special place in modern research. The fact that the world around us is subject to certain laws makes it possible to model processes taking place in it - to build accurate mathematical models of the phenomena under study. The advantage of using mathematical models in astronomy is the ability to answer many questions about cosmic phenomena. And also the fact that the number of required astronomical observations is reduced. Today, the modeling is a very effective research method in all areas of science and technology. Mathematical modeling has gained such popularity because it is a tool for understanding the internal laws that describe the phenomena and processes under study.

This widespread use of mathematics is due to the fact that the descriptive method has become insufficient. Further success in the development of all sciences is possible only on the basis of the use of precise quantitative research methods. For this purpose, it is necessary to apply the mathematical apparatus. And another reason is that the high level of development of mathematics has made it possible to create powerful electronic computers. These computers are capable of performing large amounts of cumbersome calculations.

Mathematics is constantly evolving. Functional analysis as an independent discipline began to develop at the end of the 19th century and was formed in the 20s and 30s of the 20th century. This branch of mathematics is of practical interest. It makes it possible to generalize certain processes and understand their nature.

In astronomical research, such branches of mathematics as mathematical analysis, probability theory, mathematical statistics, and the theory of differential equations are widely used. In particular, differential equations are used to describe the motion of planets according to Kepler's laws. In physics, differential equations are used to describe the motion of particles in electromagnetic fields. Unfortunately, humans are not always able to solve complex mathematical problems on their own. With the development of computer technology, programming is also evolving. Today, special mathematical packages exist to solve complex mathematical problems and interpret the results. With their help, solving complex problems becomes easier and more accessible to every researcher. In mathematical packages,

results can be obtained in analytical and graphical form. You can also easily change the initial conditions and draw conclusions based on the results.

The scientists of the Kyiv Polytechnic Institute (KPI) have been involved in the development of modern mathematical methods for the analysis of practical problems. Professor of the Department of Mathematical Methods of System Analysis - Yuriy Daltsekiy made a significant contribution to the development of mathematical models. His research is focused on functional analysis, the theory of random processes and differential equations. He was the founder of a scientific school that was internationally recognized. The scientist took an active part in the creation of the Faculty of Applied Mathematics of KPI (in 1990), the Faculty of Physics and Technology of KPI (in 1995), where the main areas of research were applied mathematics and applied physics. He was the founder of the Institute of Applied Systems Analysis at KPI (in 1998). This ensured progressive development.

Automatic interplanetary station (AIS) "Venus-4" Descent vehicle (DV)

S. Grachev, G. Ivanova

Department of aviation and Cosmonautics of the Boris Paton State Polytechnic Museum National Technical University of Ukraine «Igor Sikorsky Kyiv Polytechnic Institute», Kyiv, Ukraine

The Borys Paton State Polytechnic Museum at Igor Sikorsky Kyiv Polytechnic Institute (SPM) has a technological model of the Venus-4 lander. It is completely similar in design to the spacecraft that descended into the atmosphere of the planet Venus and reached its surface for the first time in the world on October 18, 1967. Several such models were created, and it is currently known that one of them is on display at the Memorial Museum of Cosmonautics in Moscow, and another is on display at the DPM, the only one in Ukraine. Technological models were used for ground testing of the structure and onboard systems, which ensured high reliability of their operation during a long space flight and during descent in the atmosphere of Venus, the parameters of which were not known for certain.

This spacecraft can be classified as a scientific instrument, as it was the first in the world to measure the parameters of the Venusian atmosphere and transmit these data to Earth.

The spacecraft was created at the Lavochkin Machine-Building Plant under the leadership of Chief Designer Georgy Babakin (1965-1971).

The tasks assigned to the Venus-4 spacecraft are as follows:

- Penetration into the atmosphere of Venus to the maximum possible depth, which is determined by the heat resistance and strength of the spacecraft;
- Attempting to land on the planet's surface if the temperature and pressure limits are not reached;
- Transmitting telemetry information during the process of atmospheric immersion and after landing on Venus.

The composition of the scientific equipment of the lander:

The lander had a shape close to a ball with a diameter of 103 cm. Its weight was 377 kg. Structurally, the LSA consisted of two pressurized compartments: an instrument compartment and a parachute compartment. The instrument compartment contained

- MDDA-type pressure sensors for measuring atmospheric pressure in the range from 100 to 5200 mm Hg (0.13-6.8 atm);
- G-8 gas analyzers for determining the chemical composition of the atmosphere;
- MSW instruments for determining the density and temperature of the atmosphere by height.

The main result of the Venus-4 mission was the first direct measurements of temperature, density, pressure and chemical composition of the Venusian atmosphere. The lander failed at an altitude of 28 km from the surface of Venus, as its design was designed for a pressure of only 20 atmospheres. However, the data transmitted were later used to create more robust vehicles capable of operating on the surface of Venus at an atmospheric pressure 92 times higher than Earth's (corresponding to an ocean depth of 900 meters) and a temperature of +462 degrees Celsius.

This made it possible to take the world's first (and so far the only) color panoramic photos from the planet's surface on March 1, 1982 (Lander Venus-13) and March 5, 1982 (Lander Venus-14).

This made it possible to do the following:

- On December 15, 1970, the world's first soft landing of a working spacecraft on the planet's surface took place (the Venus-7 spacecraft);
- On June 8, 1975, the first black-and-white photographs of the surface of Venus were taken and transmitted to Earth ("Venus-9");
- On March 01, 1982 ("Venus-13") and March 05, 1982 ("Venus-14"), the world's first (and so far the only) color panoramic photographs were taken from the planet's surface.

The first gravimetric measurements in Kyiv in 1904

L. Kazantseva

Astronomical Museum of the Astronomical Observatory of Taras Shevchenko Kyiv National University

Gravimetry, as the science of measuring the acceleration of gravity and other components of the gravitational field on the Earth's surface or near it, although it started counting back in the 17th century, in practice developed rather slowly. This applies both to the development of an instrumental base for measurements, and to international cooperation in the creation of common gravimetric maps.

As experts note, in the 17th - 18th centuries, the formation of the theoretical foundations of gravimetry continued, in the 18th and 19th centuries - the improvement of pendulum devices and the beginning of their use in global tasks of geodesy and geophysics. In the first half of the 20th century, the development of variometers and static gravimeters began, and regional gravimetric surveys for geophysicists began. And in the second half of the 20th century, the development of ballistic gravimeters and the creation of precision gravimetric networks for solving the problems of geodesy, geophysics and geodynamics continues to this day.

The world reference gravimetric network was created by J. P. Woollard in 1948-1960 during the implementation of the program of the Woods Hall Institute and the University of Wisconsin (USA).

The first gravimetric observatory in Ukraine, Poltava, started working in 1926. And the gravimetric map of Ukraine was created in more than 500 points for almost 12 years. By the beginning of the 60s of the XX century. in Ukraine, there were only three pendulum points of the reference gravimetric network of the 1st class, which were determined by the Central Research Institute of Geodesy and Cartography of the country at that time. These points were located in the basements of fundamental buildings in the cities of Poltava, Kharkiv and Odesa. Later, in connection with the appearance of new, more accurate gravimeters, during the years 1965-1970, the Institute of Earth Physics of the Academy of Sciences of the USSR built a reference gravimetric network of the first class on the territory of the USSR, which, on the territory of Ukraine, covered the above-mentioned points plus a reference point at the airport "Zhulyani" in the city of Kyiv . The network consisted of

a system of closed polygons tied to pendulum points, and had direct connections with the point "Moscow" (class A) - the main stronghold of the USSR.

At the same time, we managed to find little-known materials about the fact that in 1904, high-precision gravimetric measurements at that time were carried out on the territory of the Kyiv University Observatory and a gravimetric reference to Kraków was made. They were organized by Mauritsius Pius Rudzky (1862-1916), director of the Kraków Observatory. The measurements were carried out together with him by the then director of the Kyiv Observatory, Roberta Vogel and Serhii Chornyi. It was the latter, becoming the director of the AO, who, together with Oleksandr Orlov, made sure that the publication about this work was published in 1927, even after the death of Rudzky and Vogel.

66 years since the beginning of meteor radar research in Kharkiv and Ukraine

S. Kolomiyets, S. Kundyukov, I. Kyrychenko, Y. Pryimachov

Kharkiv National University Radio Electronics (NURE), Kharkiv, Ukraine

Meteor radar research in the world began to develop intensively in the middle of the 20th century. As part of the "International Geophysical Year 1957" project in Ukraine, meteor radar surveys were planned and carried out in Kharkiv, Kyiv and Odesa. Later, such studies were extended in Kyiv and Kharkiv. The Kharkiv meteor radar research received the first highest marks at the world level in 1958 at the General Assembly of the International Astronomical Union. Since then, meteor radar research in Kharkiv has become a well-known global brand among the meteor scientific community. The observational base of Kharkiv researchers of meteors by radio method was established in 1956 under the guidance of scientists Kashcheyev B.L. and Fedynsky V.V. The place of deployment is the village of Olkhovatka near the town of Balakleya (90 km from Kharkiv).

The observing meteor radar systems installed there were modernized several times. In 1968-1970. Kharkov scientists participated in the Soviet equatorial expedition to Somalia with the development of the “Tropic” equipment. More than 5 original versions of meteor automated radar systems were developed for the Balakley field laboratory. These radar systems were

used to study the physical properties of meteors, the electrodynamics of radio wave scattering on meteor trails, the statistical characteristics of meteor reflections, the distribution of meteor radiation sources over the celestial sphere, and the distribution of elements of meteor orbits in the vicinity of the Earth's orbit.

Since 1971, these meteor radar studies have been associated with the Kharkiv National University of Radio Electronics (NURE). The modernized multi-purpose geophysical complex for the study of the atmosphere and the influx of meteor matter of NURE, located on the territory of the Balakleysky scientific test site, by order of the Cabinet of Ministers of February 11, 2004 No. 73-p, was included in the state register of scientific objects that constitute the national heritage of Ukraine.

In 2022, this object of national heritage was under the occupation of Russian troops and was significantly damaged. Negotiations are underway with scientists from Canada and other countries on the restoration and modernization of the Balakleysky geophysical complex for meteor radar research after the end of the Russian-Ukrainian war.

Space equipment for magnetic recording - reproduction (EMRR) information for unmanned objects

O. Provozin

Scientific-research Institute of the Elrctromechanical device, Kiyv, Ukraine

EMRR has found a fairly wide application for so-called unmanned space flights on board numerous artificial satellites of the Earth (ASE) as part of various systems, primarily special communication systems, radio technical intelligence systems and some others. The mentioned systems provided valuable information to the power structures and contributed to ensuring the security of the Soviet state. Let's consider the role and some features of the use of tape recorders as part of such systems.

To solve these tasks, the Cosmos and Molniya series rockets were used, which were intended for the study of near-Earth space, for work in satellite communication systems, in radio-technical intelligence systems and were launched into Earth orbit by rockets developed at the Pivdenne Design Bureau. managed by academician M.K. Yangel, which is located in the city of Dnipro (Dnipropetrovsk).

. The following products were developed and carried out at the Kyiv Research Institute of Electromechanical Devices in the period from 1960 to 1990 for the specified SHSZ: "AgatA" (chief designer I.V. Suprunovskyi); "Volna" (chief designer V.P. Tyshchenko); "Granit", "Granit-2", "Sigma-B" (chief designers O.I. Babich, E.G. Dunaev); Strob-M3 (chief designers O.I. Babich, E.G. Dunaev, P.E. Dzyuba); "Planer", "Strob", "Sigma", "Mimosa", "Beta" (chief designer Babich O.I.); "Magnolia", "Magnolia-M" (OB-11), "Planer-68", "Aelita" (chief designer E.G. Dunaev); "Regenerator" (chief designer V.O. Kutishchev), "Segment", "Kamin" (chief designer P.E. Dzyuba); and others, a total of more than 17 names.

The main feature of these products is the recording of information in digital form during the satellite's stay over the territory being surveyed, followed by its accelerated transmission to ground points during the satellite's stay in the radio visibility zone of ground receiving points.

The magnetic carrier in all products (except for the Sigma product, which used a magnetic drum) is a magnetic tape, first imported, and then domestic, developed and manufactured either at the Research Institute of EMF, or later at the Shostkin Research Institute of Magnetic Information Carriers of the Svema NPO.

With the exception of the Mimosa and Magnolia products, which were single-channel on a 6.25 mm wide magnetic tape, all other products created were multi-channel with the number of channels from 3 to 24 on a 6.25 mm wide magnetic tape. 12.7 mm to 25.4 mm.

The recording/playback time is mainly within 6 - 6600s / 0.4 - 150s, maximum up to 5.5 hours. ("Agate-A" product). The acceleration factor when reproducing recorded information when it was dropped to Earth was from 1.5 to 4. The maximum amount of information that was transmitted to Earth was up to 10 Mbit. A characteristic feature of the mentioned devices was a precision tape stretching mechanism (SPM) for stretching the magnetic tape (MS).

The vibration resistance of the products at a vibration frequency in the range of 10 - 1500 Hz was up to 10 -12g.

The technical resource (service life) ranged from 100 hours/year for "Mimosa" to several hundred hours/year for subsequent products - it practically fit into the service life in orbit of all the satellites on which they were used.

At one time, the team of the EMD Research Institute was practically the main creator and manufacturer in the USSR (as well as serial factories - the Kyiv Mayak Plant and the Yaroslavl Radio Plant, which produced the

products developed at the institute, described above) of space tape recorders for unmanned objects.

Astronomy and military topography. Devices used.

S. Salata

Research Department of War History and Martial Arts Educational and Scientific Center of Military History, the National Defence University of Ukraine named after Ivan Cherniakhovskyi, Kyiv, Ukraine

The history of all wars, starting with the hand-to-hand combat of ancient times and ending with the armed conflicts of recent years, including on the territory of Ukraine, testifies to the ability of both great commanders and commanders of the distant past and the present to skillfully use this or that terrain to achieve victory in battle.

The ability to use the favorable properties of the terrain and avoid its negative impact during hostilities allowed commanders to often win with a smaller number of troops. Without a detailed study and assessment of the terrain and skillful use of its favorable properties for your troops, it is impossible to get such a victory.

The experience of conducting hostilities gained in the wars of the past years and the armed conflicts of today, especially in the battles in the southeastern territory of Ukraine, convincingly confirms the need for commanders of all levels to be able to quickly and accurately determine the coordinates of enemy targets on the battlefield, work with maps and aerial photographs and space images on unfamiliar terrain, confidently navigate it with and without a map, as well as study and evaluate the tactical properties of the terrain in various types of combat. The aforementioned features of the commander's work are studied by one of the branches of military science – military topography.

The conduct of a modern battle is influenced by many components: the degree of arming of units with combat equipment, their material and technical support, individual training of personnel, their psychological stability and morale, and others.

Of particular importance to the success of the unit in battle is the terrain, its physical and geographical features, which depend on the type and direction of combat operations, the effectiveness of the use of combat and other equipment.

Modern dynamic combat requires the use of high-precision rangefinders and protractors. The artillery compass is a geodetic device for measuring magnetic azimuths on the terrain.

Artillery compasses ПАБ-2 and its modifications were produced in the Soviet Union. ПАБ-2 and its modifications were widely used in the Soviet Army in artillery units when firing from closed positions and during combat training, reconnaissance (including artillery reconnaissance) units. They were regularly included in the stacking of many types of military equipment (for example: 9П132, 1В14, 1В18, 1В19, 1В119, ПУ-12, ППРУ-1, ІРМ "Жук", РЛС "Рись", Т-64 tanks, prototypes of equipment). Artillery compasses ПАБ-2 are used in military units to this day.

Adrianov's compass, a regular military wrist compass, the design of which was created by the cartographer V. M. Adrianov in 1907, was widely used in the Ground Forces of the Armed Forces of Ukraine. Along with the artillery compass, the АК was the most widespread navigational tool in the armed forces of the USSR.

The North Star is often used for orientation and determining one's location. Observations of it determine the inclination of the magnetic needle, corrections to the readings of compasses, gyrocompasses, and gyrotheodolites.

Studying the history of the use of the mentioned devices in military affairs will provide an opportunity to more fully reveal their influence on achieving victory in battle.

Devices for magnetic recording of information from the Baikonur cosmodrome in the exposition of the Boris Paton State Polytechnic Museum

A. Seredin, S. Grachov, N. Pysarevska

The Boris Paton State Polytechnic Museum, Kyiv, Ukraine

The gathering, transmission, processing and recording of technical information are very important in aviation and aerospace for remote analysis of the flight characteristics of aircraft. As a rule, these data are received by radio channel, that is, by means of telemetry. Telemetry is a set of technologies that allows remote gathering and transmission of information to the operator. One of the important applications of telemetry in flight tests of a new model of an aircraft or a missile is the collection and transmission of a

number of important technical parameters of the systems. For this, specially designed radio telemetry stations are used.

The theses will present two unique devices for magnetic recording of information, given to the Polytechnic Museum from the Baikonur Cosmodrome by Lapidus Bronislav Henrikhovich. This is the magnetic recording equipment of the radio telemetry station MA-9 MKTM-4 and the special tube tape recorder M-64 "Zvuk-1" with a set of magnetic tapes on which the negotiations of the crew of the Soyuz-21 spacecraft were recorded (Boris Volinov, Vitaly Zholobov) with the launch control center in the process of pre-launch preparation and launch into orbit on July 6, 1976.

In the theses, a technical description of these devices will be made, photographs will be presented, the history of their transfer to the museum, the place and role of these devices in the exposition of the Department of Aviation and Cosmonautics of The Boris Paton State Polytechnic Museum will be described. A separate section will be devoted to the biography of the person who contributed to the transfer of these and other interesting and unique devices from the Baikonur cosmodrome - Lapidus Bronislav Henrikhovich. This person is an honored tester of the Baikonur cosmodrome, director of the Kyiv branch of the Makarov National Center for Aerospace Education of Youth.

So, the purpose of these theses is to systematize the available information about the unique devices for magnetic recording of telemetric and sound information, which are in the exposition of the Department of Aviation and Cosmonautics of the Boris Paton State Polytechnic Museum, and to present to society little-known facts from the life of the person who contributed to the transmission from the cosmodrome Baikonur to the museum of a significant number of unique objects of space technology.

The influence of Heinrich Wild on the formation of modern geodesy: to the 100th anniversary of the first instruments of the WILD Heerbrugg company

Yu. Shevela

Polis National University, Zhytomyr, Ukraine

In 1923, exactly 100 years ago, the Swiss company WILD Heerbrugg released two portable optical-mechanical devices: the NII level and the Th1 theodolite, marking the beginning of modern geodesy.

The chief developer of instruments, Heinrich Wild, was born in Switzerland in 1877, from the age of 15 he worked as an apprentice for the engineer Legler in Glarus, and from 1899 - at the Federal Topographical Bureau in Bern! Already in 1904, according to his drawing, the first level was made, and since 1905. based on his own experience, he began to improve theodolites. Since 1907 G. Wild works at the Carl Zeiss company, where he manages his department, and since 1911 he has received patents for his inventions, and in 1921 patented the first own theodolite Th1.

In the same year 1921 G.Wild returns to Switzerland, where he founded his own company WILD Heerbrugg with colonel Jakob Schmidtheiny and geologist Robert Geblint, which in 1923 his first devices were made - Th1 theodolite and NII level.

When developing the Th1 theodolite, H.Wild, using his own experience, took into account the following requirements: the smallest possible dimensions and weight; convenient manipulation; greater resistance to transportation, exposure to rain and dust; combination of images from two opposite parts of the circle on one thin dividing line for observation in one eyepiece; images of the opposite points of the circle, which should be reproduced through the empty axis, so that the circles can be completely closed; use of a highly sensitive micrometer to adjust coincidence for direct reading of the arithmetic mean; using glass circles to provide a symmetrical type of graduation.

His system is based entirely on glass components such as prisms and lenses (hence the name OPTICAL theodolite) and marked the beginning of a new era in theodolite design! Also, several revolutionary functions were added to the design, which were included not only in the Th1 and Th2 theodolites, but also in the first NII and NKII levelers - in particular, an anallactic telescope of constant length with internal focusing! The design and construction were so successful that they were unchanged in different companies in different countries for more than half a century!

Starting with Th2, all products already had WILD Heerbrugg marks, and by 1930. almost 1000 pieces were made. And already in 1964 the 100,000th theodolite has been calibrated by WILD! Levels NII (from the German Nivellier) and NKII, with a horizontal circle (from the German Kreis), were made, respectively, 100 pieces, and to this day it is known about one preserved level NII and one NKII in the Museum of Navigation and Geodesy devices of Nicolas de Hilster (Netherlands), and nine Th1 theodolites in various museums around the world (including one in Ukraine!).

In 1932 Heinrich Wild left the WILD company (which he himself founded) and, completely, until his death in 1951. engaged in the

development and improvement of various devices for the companies WILD Heerbrugg, Carl Zeiss, Kern&Co, Leica Camera.

Among other iconic devices of G. Wild and the WILD company were: the first phototheodolites for aviation of the Swiss Federal Topographical Office (1926-27), the stereometric camera WILD C12 for stereometric experiments (1932), the new self-monitoring tachometer with a double circle DK-RT (1947), which was used in the land cadastre of Switzerland for several decades(!), the first infrared range finder DISTOMAT D10 (together with the French computer Sercel) and others.

In 1968 WILD included Leitz Wetzlar and Leica Camera, and in 1988 - computer Kern&Co AG. In 1990 WILD-Leitz merges with comp. Cambridge Instruments, - there is a computer. Leica Group. In 1991 computer Introducing the world's FIRST digital level WILD NA2000! In 1997 the Leica group of companies was divided into Leica Microsystems and Leica Geosystems. In 2005, there was a merger of the companies with the Swedish comp. HEXAGON AB.

LATE ABSTRACTS

Long-period dynamical evolution of the meteoroid stream originating in comet 21P/Giacobini-Zinner

D. Tomko
Astronomical Institute of the Slovak Academy of Sciences, Tatranská Lomnica, Slovak Republic

We investigated the dynamical evolution of the meteoroid stream originating in the nucleus of comet 21P/Giacobini-Zinner. We created 20 partial models, in each assuming 10,000 test particles, and fixed values for the evolutionary time and the strength of the Poynting–Robertson effect. We confirmed that the orbit of the parent comet and the orbits of the test particles, representing the meteoroids, evolved rapidly. This fast evolution resulted in a relatively short duration (up to approx. 1000 years) of the orbital concentrations of the meteoroids that could be identified as the meteor showers. We confirmed the relationship between comet 21P and the October Draconid meteor shower, #9. In addition to this shower, we predicted another five showers related to the comet. Four of these showers were also identified with their real counterparts. Some identifications were multiple. Specifically, we further found an association, or indication of association of 21P, with the ι-Cygnids, #525, August β-Aquariids, #474, June ξ1-Sagittariids, #861, ξ2-Capricornids, #623, Northern σ-Sagittariids, #167, α-Capricornids, #1, Daytime Capricornids-Sagittariids, #115, and ν-Draconids, #220.

Наукове видання

Астрономія та фізика космосу в Київському університеті

Міжнародна конференція

м. Київ, 23 травня – 26 травня 2023 р.

Збірка тез доповідей